ISSN: 2376-2136 (Print)
ISSN: 2376-2144 (Online)

Trends in Renewable Energy

Volume 3, Issue 3, December 2017
Special Issue on Smart Grid (2)

ISSN 2376-2136 09
9 772376 213001

futureenergysp.com
thefutureenergy.org

Trends in Renewable Energy

ISSN: 2376-2136 (Print) ISSN: 2376-2144 (Online)

http://futureenergysp.com/

Trends in Renewable Energy is an open accessed, peer-reviewed semi-annual journal publishing reviews and research papers in the field of renewable energy technology and science.

The aim of this journal is to provide a communication platform that is run exclusively by scientists working in the renewable energy field. Scope of the journal covers: Bioenergy, Biofuel, Biomass, Bioprocessing, Biorefinery, Biological waste treatment, Catalysis for energy generation, Energy conservation, Energy delivery, Energy resources, Energy storage, Energy transformation, Environmental impact, Feedstock utilization, Future energy development, Green chemistry, Green energy, Microbial products, Physico-chemical process for Biomass, Policy, Pollution, Renewable energy, Smart grid, Thermo-chemical processes for biomass, etc.

The Trends in Renewable Energy publishes the following article types: peer-reviewed reviews, mini-reviews, technical notes, short-form research papers, and original research papers.

The article processing charge (APC), also known as a publication fee, is fully waived for the Trends in Renewable Energy.

Editorial Team of Trends in Renewable Energy

EDITORIAL BOARD

Table of Contents

Volume 3, Issue No. 3, December 2017

SPECIAL ISSUE ON SMART GRID (2)

Editorials

Articles

Trends in Renewable Energy
OPEN ACCESS ISSN: 2376-2144
EDITORIAL futureenergysp.com/index.php/tre

Smart Grid is the Key to Enhance the Penetration of Renewable Energy into Electric Power Systems

Dear researchers,

Due to the rapid development of renewable energy technologies because of environmental concerns, the electric power grid is experiencing a significant change. The electrical power structure is no longer a vertically integrated structure due to the large grid parity of renewables and as a result, smart grid is the key to enhance the penetration of renewable energy into electric power systems. However, due to the intermittent probabilistic nature of renewable energy sources, design and management of power are a great challenge to both power and computing industry. Furthermore, it has been anticipated that future energy structure will be "two-way streets", allowing every energy user to be not only a customer, but an energy provider as well. So, a smart grid structure is the need in the present scenario. This transition from classical power structure inevitably demands significant research for many rapidly rising issues.

This Special Issue focuses on smart grid that can accommodate renewable energy into electric utility systems. The Special Issue is interested but not limited to the following issues relevant to increased renewable energy penetration:

1) Prediction of sustainable energy resources.
2) Stability and control of sustainable energy in supporting grid frequency and voltage.
3) Steady-state and transient assessment of system, etc.
4) Extent to which dispatchable generation reserves required and under what circumstances.
5) Effect on reliability be compromised with increased sustainable energy penetration.
6) Cost considerations with renewable's variability
7) Effect on system operating strategies with sustainable energy generation
8) Effect on various measuring devices for effective monitoring and evaluation of electric power system operation, etc.

Dr. Neeraj Gupta
(Ph.D. IIT Roorkee, India), MIEEE
Faculty EED
NIT Hamirpur, H.P., India

*Corresponding author: neeraj5822@gmail.com

Tr Ren Energy, 2017, Vol.1, No.3, 1. doi:10.17737/tre.2017.1.3.040

Trends in Renewable Energy
OPEN ACCESS ISSN:2376-2144
Peer-Reviewed Article futureenergysp.com/index.php/tre

Main Line Fault Localization Methodology in Smart Grid – Part 1: Extended TM2 Method for the Overhead Medium-Voltage Broadband over Power Lines Networks Case

Athanasios G. Lazaropoulos[1]

1: School of Electrical and Computer Engineering / National Technical University of Athens / 9 Iroon Polytechniou Street / Zografou, GR 15780

Received June 13, 2017; Accepted September 2, 2017; Published September 27, 2017

These three papers cover the overall methodology for the identification and localization of faults that occur in main transmission and distribution lines when broadband over power lines (BPL) networks are deployed across the transmission and distribution power grids, respectively. In fact, this fault case is the only one that cannot be handled by the combined operation of Topology Identification Methodology (TIM) and Instability Identification Methodology (FIIM). After the phase of identification of main distribution line faults, which is presented in this paper, the main line fault localization methodology (MLFLM) is applied in order to localize the faults in overhead medium-voltage BPL (OV MV BPL) networks.
The main contribution of this paper, which is focused on the identification of the main distribution line faults, is the presentation of TM2 method extension through the adoption of coupling reflection coefficients. Extended TM2 method is analyzed in order to identify a main distribution line fault regardless of its nature (i.e., short- or open-circuit termination). The behavior of the extended TM2 method is assessed in terms of the main line fault nature and, then, its results are compared against the respective ones during the normal operation, which are given by the original TM2 method, when different main distribution line fault scenarios occur. Extended TM2 method acts as the introductory phase (fault identification) of MLFLM.

Keywords: Smart Grid; Intelligent Energy Systems; Broadband over Power Lines (BPL) Networks; Power Line Communications (PLC); Faults; Fault Analysis; Fault Localization; Distribution Power Grids

1. Introduction

During the past few years, a tremendous development in the deployment of broadband over power lines (BPL) networks for enhancing the intelligence, stability and autonomy of the vintage power grid infrastructure has been witnessed [1], [2]. Only considering the scale of transmission and distribution power grids in the countries of modern world, BPL technology can transform these traditional grids into an integrated intelligent IP-based communications network with a myriad of smart grid applications [3]-[5].

Apart from the size of today's power grids, the recent interest in smart grids stems from the significant increase in electricity needs of our societies, the need for a more

*Corresponding author: AGLazaropoulos@gmail.com

Tr Ren Energy, 2017, Vol.3, No.3, 2-25. doi: 10.17737/tre.2017.3.3.0036

interconnected power grid and a more dynamic manner of power management. Therefore, the demand for coordination, agility and feedback of a new global interconnected power grid implies the delivery of high-bandwidth smart grid applications with data rates that exceed 1Gbps due to the vast amount of information required across the grid. Since the transmission and distribution power grids were not originally intended for conveying high frequency signals, any communication across the grids would be exposed to severe adversarial factors, such as high and frequency-selective channel attenuation and noise [6]-[12].

As concerns the determination of the channel attenuation and reflection coefficient of overhead medium-voltage (OV MV) BPL networks, the well-established hybrid method, which is employed to examine the behavior of various multiconductor transmission line (MTL) structures, is also adopted in this paper [4], [6]-[10], [13]-[24]. Given as inputs the OV MV BPL network topology, OV MV MTL configuration and the applied coupling scheme, the hybrid method gives as outputs the corresponding transfer function and reflection coefficients. Actually, hybrid method consists of: (i) a bottom-up approach that is based on the MTL theory, eigenvalue decomposition (EVD) and singular value decomposition (SVD); and (ii) a top-down approach that is denoted as TM2 method and is based on the concatenation of multidimensional chain scattering matrices. In this paper, TM2 method of the hybrid method, which is analytically presented in [17], is extended in order to cope with the various load terminations of the main line (terminal loads) of the distribution BPL networks since the original TM2 method assumes that terminal loads of OV MV BPL networks are matched.

Apart from the aforementioned adversarial factors that deteriorate the quality of service of OV MV BPL networks, a number of serious problematic conditions that causes temporary or permanent damage to the integrity of power grid can jeopardize the uninterrupted operation and availability of the power distribution. According to [23]-[27], depending on the affected pieces of power grid equipment, the problematic conditions can be divided into two main categories, say: faults and instabilities. In accordance with [27], the fault category describes all the interruptions that may occur across the main and branch lines of a power grid. Between these two cases, it comprises the fault subcategory of main line fault that defines the main interest of this paper. In fact, the main line fault subcategory forms the only fault case which cannot be treated by Topology Identification Methodology (TIM) and Fault and Instability Identification Methodology (FIIM) in [25], [26]. Since main distribution line faults can be assumed to behave as either short- or open-circuit terminal loads depending on the location of the conductors of the main distribution lines after the fault, the behavior of the extended TM2 method during the determination of its reflection coefficients of the aforementioned terminal loads is first examined in this paper. Furthermore, the reflection coefficients of the extended TM2 method during main distribution line faults are compared against the respective ones of the original TM2 method during the normal operation of OV MV BPL networks. The comparison of the reflection coefficients between the normal and fault condition is going to determine the fault appearance across main distribution lines.

The rest of this paper is organized as follows: In Sec.II, the OV MV MTL configuration, the indicative OV MV BPL topologies, the bottom-up approach of the hybrid method and the main distribution line fault subcategory are presented. Sec.III deals with the top-down approach of the hybrid method and, especially, with the extension of TM2 method. Special attention is given to the determination of the reflection coefficients of OV MV BPL topologies when main distribution line faults occur.

In Sec.IV, numerical results are provided, aiming at marking out the behavior of the extended TM2 method as well as the reflection coefficient differences between the extended and original TM2 method during the normal and fault operation, respectively. Sec.V recapitulates the conclusions of this paper.

2. OV MV MTL Configurations, OV MV BPL Topologies, Bottom-Up Approach of the Hybrid Method and Faults

2.1 OV MV MTL Configuration

The OV MV MTL configuration, which is examined in this paper, is presented in Fig. 1(a) of [4]. The OV MV MTL configuration consists of the three phase lines ($n^{\mathrm{OVMV}}=3$) of radius $r_{\mathrm{MV,p}}$ that are spaced by Δ_{MV} and hung at typical heights h_{MV} above ground. The imperfect ground is considered as the reference conductor with conductivity σ_{g} and relative permittivity $\varepsilon_{\mathrm{rg}}$. The exact values concerning the aforementioned properties are reported in [6], [7], [16], [18], [20], [28]-[30] while the analysis concerning the impact of imperfect ground on broadband signal propagation and transmission via OV MV MTL configurations are analyzed in [6], [7], [16], [18], [20], [31]-[33].

2.2 Indicative OV MV BPL Topologies

To cope with the significant BPL signal aggravation due to the channel attenuation and noise, OV MV BPL networks are divided into cascaded OV MV BPL topologies of average path lengths of the order of 1000m which are bounded by BPL repeaters. With reference to Fig. 1(a), a typical OV MV BPL topology is presented that is bounded by two repeaters at the position A and B. Arbitrarily, the repeater at the position A acts as the transmitting end whereas the other repeater acts as the receiving end. Depending on the number and length of the branches encountered across the BPL signal propagation, different OV MV BPL topologies may be considered. In these three papers, four indicative OV MV BPL topologies of average path length are examined, namely:

1. A typical urban topology (denoted as urban case) with N=3 branches (L_1=500m, L_2=200m, L_3=100m, L_4=200m, L_{b1}=8m, L_{b2}=13m, L_{b3}=10m).
2. A typical suburban topology (denoted as suburban case) with N=2 branches (L_1=500m, L_2=400m, L_3=100m, L_{b1}=50m, L_{b2}=10m).
3. A typical rural topology (denoted as rural case) with only N=1 branch (L_1=600m, L_2=400m, L_{b1}=300m).
4. The "LOS" transmission along the same end-to-end distance $L=L_1+\ldots+L_{N+1}$=1000m (denoted as "LOS" case) when no branches are encountered. This topology corresponds to Line of Sight transmission in wireless channels.

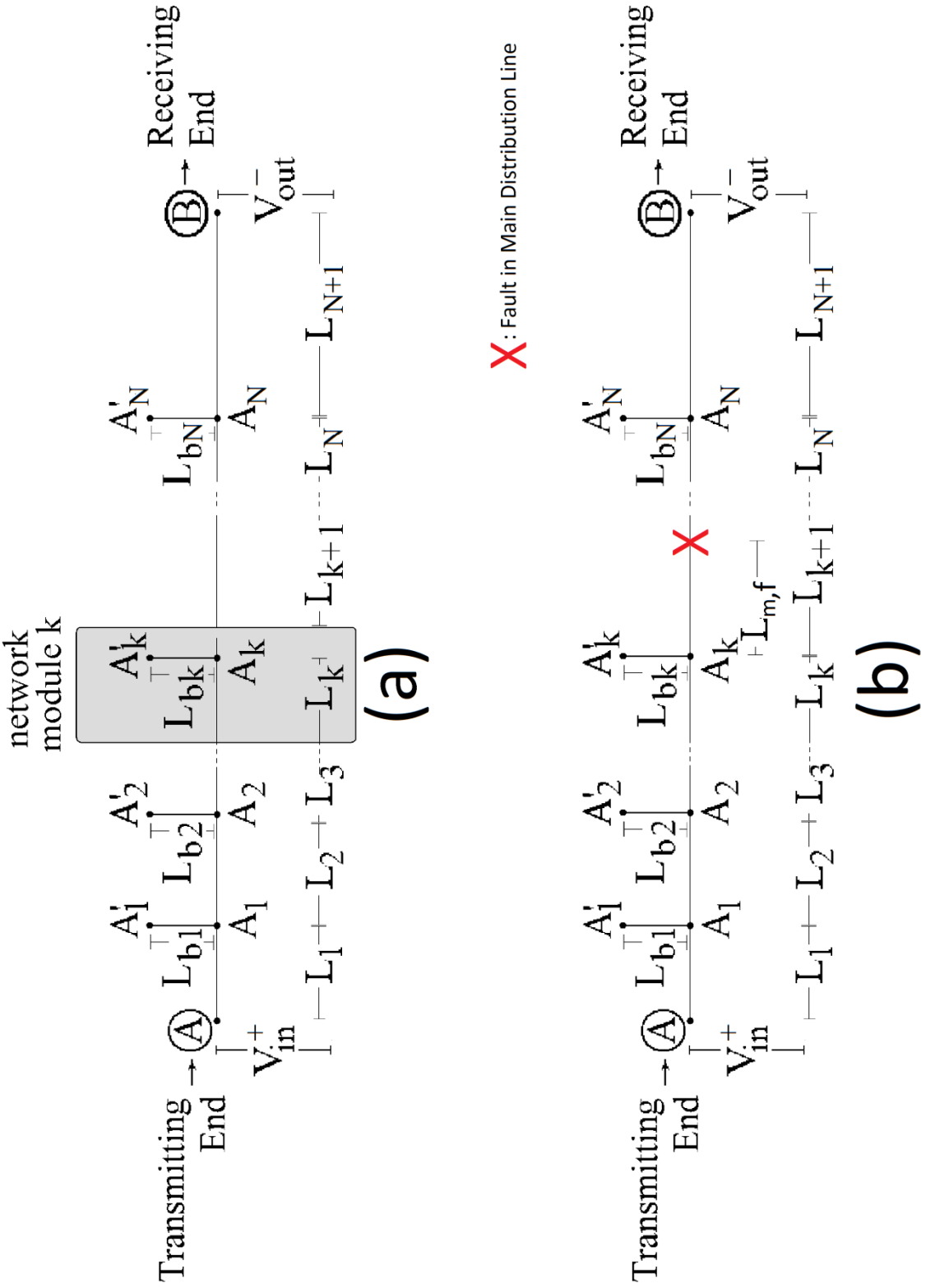

Figure 1. (a) General OV MV BPL topology [23]. (b) Main Distribution Line Fault in OV MV BPL topologies.

2.3 Bottom-Up Approach of the Hybrid Method, Coupling Schemes, Coupling Transfer Functions and Reflection Coefficients

Successfully tested in various transmission and distribution BPL networks [6]-[10], [13]-[22], [32]-[34], the well-established hybrid method consists of: (i) a bottom-up approach that is based on the MTL theory and eigenvalue decomposition (EVD) decomposition for the single-input single-output (SISO) systems of this paper; and (ii) a top-down approach that is denoted as TM2 method and is based on the concatenation of multidimensional chain scattering matrices. Through the original version of TM2 method, the hybrid method gives as outputs the corresponding modal transfer functions and modal reflection coefficients when the OV MV MTL configuration and OV MV BPL topology are given as inputs to the hybrid method.

On the basis of the applied coupling scheme, which is the practical way that the signals are injected into OV MV lines and the outputs of the hybrid method, coupling transfer functions and coupling reflection coefficients can be determined. In fact, two main categories of coupling schemes are mainly supported by the OV MV BPL networks, namely [4], [15], [17], [23], [24], [35]-[37]: (i) Wire-to-Ground (WtG) coupling schemes; and (ii) Wire-to-Wire (WtW) coupling schemes. In the case of WtG coupling schemes, which are examined in this paper, the WtG coupling transfer function $H^{\mathrm{WtG}^s}\{\cdot\}$ is given from

$$H^{\mathrm{WtG}^s}\{\cdot\} = \left[\mathbf{C}^{\mathrm{WtG}}\right]^{\mathrm{T}} \cdot \mathbf{T}_{\mathrm{V}} \cdot \mathbf{H}^{\mathrm{m}}\{\cdot\} \cdot \mathbf{T}_{\mathrm{V}}^{-1} \cdot \mathbf{C}^{\mathrm{WtG}} \tag{1}$$

while WtG coupling reflection coefficient $\Gamma^{\mathrm{WtG}^s}\{\cdot\}$ is determined by

$$\Gamma^{\mathrm{WtG}^s}\{\cdot\} = \left[\mathbf{C}^{\mathrm{WtG}}\right]^{\mathrm{T}} \cdot \mathbf{T}_{\mathrm{V}} \cdot \mathbf{\Gamma}_{\mathrm{in}}^{\mathrm{m}}\{\cdot\} \cdot \mathbf{T}_{\mathrm{V}}^{-1} \cdot \mathbf{C}^{\mathrm{WtG}} \tag{2}$$

where $\mathbf{C}^{\mathrm{WtG}}$ is an $n^{\mathrm{OVMV}} \times 1$ coupling column vector with zero elements except in row s where the value is equal to 1, $\mathbf{T}_{\mathrm{V}}$ is a $n^{\mathrm{OVMV}} \times n^{\mathrm{OVMV}}$ matrix that depends on the frequency, the OV MV MTL configuration and the physical properties of the cables, $\mathbf{H}^{\mathrm{m}}\{\cdot\}$ is the $n^{\mathrm{OVMV}} \times n^{\mathrm{OVMV}}$ EVD modal transfer function matrix and $\mathbf{\Gamma}_{\mathrm{in}}^{\mathrm{m}}\{\cdot\}$ is the $n^{\mathrm{OVMV}} \times n^{\mathrm{OVMV}}$ EVD modal reflection coefficient matrix. Both EVD modal transfer function matrix and EVD modal reflection coefficient matrix are given as outputs by the TM2 method [6]-[10], [13]-[17], [20], [28], [38].

To receive the WtG coupling transfer function and reflection coefficient of eqs. (1) and (2), respectively, certain assumptions for the circuital parameters of OV MV BPL topologies need to be taken into account during their determination of the original TM2 method. In accordance with [4], these assumptions are: (i) The branch lines are assumed identical to the main distribution ones; (ii) The interconnections between the main distribution and branch conductors of the lines are all connected; (iii) The transmitting and the receiving ends are assumed matched to the characteristic impedance of the modal channels; and (iv) The branch terminations are assumed open circuits.

2.4 Faults and Instabilities in OV MV BPL Topologies

During the continuous operation of the distribution power grid, critical problematic conditions can occur across it whose nature differs from the measurement differences. The presence of these problematic conditions endangers power quality and power distribution safety while these conditions are divided into two categories, namely: faults and instabilities [23]-[27]. Fault category, which describes all the interruptions that can occur in the lines of a distribution power grid, comprises two subcategories, say: main distribution line faults and branch line faults. Main distribution line faults that are of the interest of these three papers describe the condition where a main distribution line is interrupted due to physical or human reasons [27]. Main distribution line faults can be assumed to behave as either short- or open-circuit terminal loads. With reference to Fig. 1(b), let the main distribution line be broken at the position $\sum_{i=1}^{k} L_k + L_{\mathrm{m,f}}$ from the transmitting end. A critical incident that determines the presence of this fault is the immediate communications failure between the transmitting and receiving end. However, there is a number of reasons why an immediate communications failure may appear in an OV MV BPL network thus creating a cause ambiguity. In addition, even if a main distribution line fault occurs and is identified, the localization of the exact fault position can significantly facilitate the maintenance personnel. Various efforts concerning the main distribution line fault localization have already been presented in [31], [39]-[42]. In this paper, the identification of a main distribution line fault is secured via the study of the behavior of reflection coefficients that come from the hybrid method.

From the third assumption of Sec.IIC, which concerns the circuital parameters of the original TM2 method, it is assumed that the terminal load is matched to the characteristic impedance of the modal channels but this is a not valid assumption when a main distribution line fault arises. Since main distribution line faults can be assumed to behave as either short- or open-circuit terminal loads, the original TM2 method fails to handle this situation in terms of the occurred reflection coefficients. The extension of TM2 method to cope with the aforementioned load terminations in terms of the reflection coefficients is described in Sec.III.

3. Original and Extended TM2 Method

Based on the model description of [17], the original TM2 method is extended in this paper by exploiting the generic multidimensional network analysis of [21], [34]. This extension copes with the different terminal loads that may occur during a main distribution line fault. The extended TM2 method is suitable for both transmission and distribution BPL networks so that the respective main transmission and distribution line faults can be handled and, thus, simulated.

In accordance with the definition of the original TM2 method of [17] and with reference to Fig. 1(a), an end-to-end BPL topology is separated into network modules, each of them comprising the successive branches encountered. BPL signal transmission through the serial connection of the various network modules is taken into account through the concatenation of their respective chain scattering matrices. Each network module may be considered as a cascade of two submodules, say: (i) the "transmission" submodule representing a distribution line of length L_k ; and (ii) a "shunt" submodule representing the cascade of the branch termination A_k', the

branch line of length $L_{\mathrm{b}k}$ and the interconnection between the main and branch conductors. Based on the specialized algebra for handling multidimensional scattering matrices, which is analytically presented in [17], [21], [34], the $2n^{\mathrm{OVMV}} \times 2n^{\mathrm{OVMV}}$ chain scattering matrix of the network module $\mathbf{T}^{k}$ is determined by using the appropriate cascade rule order. The last module of the BPL topology is the distribution line of length L_{N+1} characterized by its $2n^{\mathrm{OVMV}} \times 2n^{\mathrm{OVMV}}$ chain scattering matrix $\mathbf{T}^{N+1}$. Having determined the chain scattering matrices of the various network modules encountered along the end-to-end connection, the $2n^{\mathrm{OVMV}} \times 2n^{\mathrm{OVMV}}$ overall end-to-end chain scattering matrix of the original TM2 method is evaluated through the multiplication rule from

$$\mathbf{T}^{\mathrm{overall,original}} = \left[\begin{array}{c|c} \mathbf{T}_{11}^{\mathrm{overall,original}} & \mathbf{T}_{12}^{\mathrm{overall,original}} \\ \hline \mathbf{T}_{21}^{\mathrm{overall,original}} & \mathbf{T}_{22}^{\mathrm{overall,original}} \end{array}\right] = \prod_{k=1}^{N+1} \mathbf{T}^{k} \tag{3}$$

where $\mathbf{T}_{11}^{\mathrm{overall,original}}$, $\mathbf{T}_{12}^{\mathrm{overall,original}}$, $\mathbf{T}_{21}^{\mathrm{overall,original}}$ and $\mathbf{T}_{22}^{\mathrm{overall,original}}$ are the $n^{\mathrm{OVMV}} \times n^{\mathrm{OVMV}}$ matrix elements of the $\mathbf{T}^{\mathrm{overall,original}}$ as evaluated from eq. (3). The respective $2n^{\mathrm{OVMV}} \times 2n^{\mathrm{OVMV}}$ overall end-to-end scattering matrix is obtained from [17], [21], [34]

$$\mathbf{S}^{\mathrm{overall,original}} = \left[\begin{array}{c|c} \mathbf{S}_{11}^{\mathrm{overall,original}} & \mathbf{S}_{12}^{\mathrm{overall,original}} \\ \hline \mathbf{S}_{21}^{\mathrm{overall,original}} & \mathbf{S}_{22}^{\mathrm{overall,original}} \end{array}\right] =$$

$$= \left[\begin{array}{c|c} \mathbf{T}_{21}^{\mathrm{overall,original}}\left[\mathbf{T}_{11}^{\mathrm{overall,original}}\right]^{-1} & \mathbf{T}_{22}^{\mathrm{overall,original}} - \mathbf{T}_{21}^{\mathrm{overall,original}}\left[\mathbf{T}_{12}^{\mathrm{overall,original}}\right]^{-1}\mathbf{T}_{11}^{\mathrm{overall,original}} \\ \hline \left[\mathbf{T}_{11}^{\mathrm{overall,original}}\right]^{-1} & -\left[\mathbf{T}_{12}^{\mathrm{overall,original}}\right]^{-1}\mathbf{T}_{11}^{\mathrm{overall,original}} \end{array}\right] \tag{4}$$

where $\mathbf{S}_{11}^{\mathrm{overall,original}}$, $\mathbf{S}_{12}^{\mathrm{overall,original}}$, $\mathbf{S}_{21}^{\mathrm{overall,original}}$ and $\mathbf{S}_{22}^{\mathrm{overall,original}}$ are the $n^{\mathrm{OVMV}} \times n^{\mathrm{OVMV}}$ elements of the $\mathbf{S}^{\mathrm{overall,original}}$ matrix as defined in eq. (4). Combining eqs. (1) and (4), the $n^{\mathrm{OVMV}} \times n^{\mathrm{OVMV}}$ EVD modal transfer function matrix is given by the $\mathbf{S}_{21}^{\mathrm{overall,original}}$ element of the $\mathbf{S}^{\mathrm{overall,original}}$ matrix, that is

$$\mathbf{H}^{\mathrm{m,original}}\{\cdot\} = \mathbf{S}_{21}^{\mathrm{overall,original}} = \left[\mathbf{T}_{11}^{\mathrm{overall,original}}\right]^{-1} \tag{5}$$

while the $n^{\mathrm{OVMV}} \times n^{\mathrm{OVMV}}$ EVD modal reflection coefficient matrix is given by

$$\mathbf{\Gamma}_{\mathrm{in}}^{\mathrm{m,original}}\{\cdot\} = \mathbf{S}_{11}^{\mathrm{overall,original}} \tag{6}$$

Here, it should be noted that the transmitting and receiving ends are assumed matched to the characteristic impedance of the modal channels during the determination of the aforementioned modal quantities. Indeed, this is the suitable assumption for the normal operation of OV MV BPL networks. However, the terminal loads differentiate from the matched termination when a main distribution line fault occurs.

On the basis of the specialized algebra for handling the various branch terminations and terminal loads [21], [34], extended TM2 method transforms the overall end-to-end chain scattering matrix of the original TM2 method, which is given in eq. (4), into the $n^{\mathrm{OVMV}} \times n^{\mathrm{OVMV}}$ EVD modal reflection coefficient matrix $\mathbf{\Gamma}_{\mathrm{in}}^{\mathrm{m,extended}}$ that is determined by

$$\mathbf{\Gamma}_{\mathrm{in}}^{\mathrm{m,extended}}\{\cdot\} = \mathbf{S}_{11}^{\mathrm{overall,original}} + \left[\mathbf{S}_{12}^{\mathrm{overall,original}} \cdot \left(\mathbf{I}_{n^{\mathrm{OVMV}}} - \mathbf{\Gamma}_{\mathrm{out}}^{\mathrm{m,extended}} \cdot \mathbf{S}_{22}^{\mathrm{overall,original}}\right)^{-1} \cdot \mathbf{\Gamma}_{\mathrm{out}}^{\mathrm{m,extended}} \cdot \mathbf{S}_{21}^{\mathrm{overall,original}}\right] \tag{7}$$

where $\mathbf{I}_{n^{\mathrm{OVMV}}}$ is a $n^{\mathrm{OVMV}} \times n^{\mathrm{OVMV}}$ identity matrix and $\mathbf{\Gamma}_{\mathrm{out}}^{\mathrm{m,extended}}$ is the $n^{\mathrm{OVMV}} \times n^{\mathrm{OVMV}}$ EVD modal reflection coefficient matrix of the terminal load. From the observation of eq. (7), $\mathbf{\Gamma}_{\mathrm{in}}^{\mathrm{m,extended}}$ degenerates into $\mathbf{S}_{11}^{\mathrm{overall,original}}$ during the normal operation of the OV MV BPL network since then the terminal load can be assumed matched to the characteristic impedance of the modal channels, which implies that $\mathbf{\Gamma}_{\mathrm{out}}^{\mathrm{m,extended}}$ is equal to a $n^{\mathrm{OVMV}} \times n^{\mathrm{OVMV}}$ zero matrix.

On the basis of eq. (7), the conversion of the original TM2 method to the extended TM2 method is also schematically given in Figs. 2(a) and (b). Comparing Fig. 2(a), which describes the output of the original TM2 method, and Fig. 2(b), which describes the output of the extended TM2 method, it is evident that the extended TM2 method assesses the reflection of the incident waves $\mathbf{a}_1$ and reflected waves $\mathbf{b}_1'$ at the transmitting end through the modal reflection coefficient matrix $\mathbf{\Gamma}_{\mathrm{in}}^{\mathrm{m,extended}}$ whereas it does not provide any transfer function details because no incident and reflected waves occur after the terminal load in contrast with the original TM2 method where incident waves $\mathbf{a}_2$ and reflected waves $\mathbf{b}_2$ appear at the receiving end and, afterwards, are measured.

As already been mentioned, the terminal load can be assumed matched to the characteristic impedance of the modal channels during the normal operation of the OV MV BPL networks whereas the terminal load may behave as either short- or open-circuit during a main distribution line fault depending on the location of the conductors of the main distribution lines after the fault. In order to assess and compare the previous behaviors in terms of their reflection coefficients when original and extended TM2 method is applied, $\mathbf{\Gamma}_{\mathrm{in}}^{\mathrm{m,original}}$ is given by eq. (6) during the normal operation whereas $\mathbf{\Gamma}_{\mathrm{in}}^{\mathrm{m,extended}}$ is given by eq. (7) during the main distribution line fault condition. In the latter case, $\mathbf{\Gamma}_{\mathrm{out}}^{\mathrm{m,extended}}$ is assumed to be equal to $-\mathbf{I}_{n^{\mathrm{OVMV}}}$ (short-circuit terminal load) or $\mathbf{I}_{n^{\mathrm{OVMV}}}$ (open-circuit terminal load) in order to evaluate $\mathbf{\Gamma}_{\mathrm{in}}^{\mathrm{m,extended}}$.

Summarizing the findings of this Section, the "real-life" operation of the OV MV BPL networks depends on the deployed coupling scheme systems across them. Since all the required modal quantities have been defined for the normal and fault operation by appropriately applying original and extended TM2 method, WtG coupling transfer function and WtG coupling reflection coefficient can easily be determined by eqs. (1) and (2), respectively, by appropriately replacing these modal quantities as previously outlined.

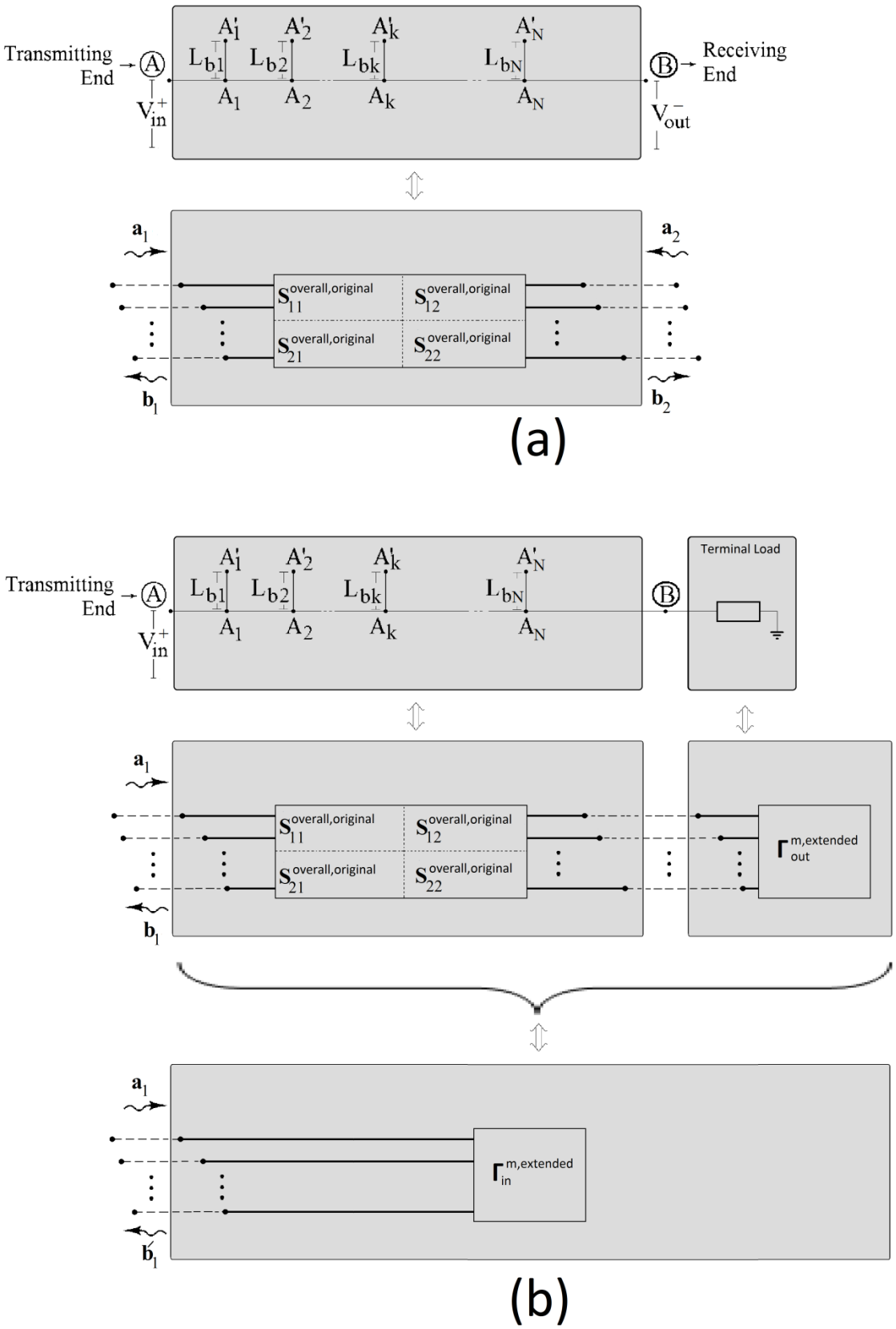

Figure 2. (a) Overall end-to-end scattering matrix of the original TM2 method. (b) Modal reflection coefficient matrix of the extended TM2 method when terminal load occurs at the receiving end.

4. Numerical Results and Discussion

4.1 Simulation Goals and Parameters

The indicative topologies of OV MV BPL networks are simulated with the purpose of identifying a main distribution line fault by comparing the results of reflection coefficient of the original TM2 method with the ones of the extended TM2 method. The behavior of reflection coefficients is further detailed for the different terminal loads (i.e., short- or open-circuit termination) when a main distribution line fault occurs.

As regards the simulation specifications, those are the same with [4], [23]-[27]. More specifically, the BPL frequency range and flat-fading subchannel frequency spacing are assumed equal to 1-30MHz and 1MHz, respectively. Therefore, the number of subchannels is equal to 30 in the examined frequency range. Arbitrarily, the WtG^3 coupling scheme is applied during the following simulations. As it is usually done [10], [13], [14], [16], [18], [23], [24], [43], the selection of representative coupling schemes is a typical procedure for the sake of reducing manuscript size.

4.2 Coupling Transfer Function and Coupling Reflection Coefficient for the Indicative OV MV BPL Topologies (Original TM2 Method)

Prior to study the behavior of OV MV BPL networks when a main distribution line fault occurs, the magnitude of coupling transfer function and coupling reflection coefficient of the indicative OV MV BPL topologies is outlined when their terminal loads are assumed matched to the modal characteristics impedances. The nature of the studied terminal loads implies that original TM2 method is applied during the following simulations. Note that the behavior of the coupling reflection coefficient during the normal operation, which is presented in this subsection, is going to act as the benchmark in order to identify the existence of a main distribution line fault (see Sec.IVD).

In Fig. 3, the coupling transfer function is plotted versus frequency for the four indicative OV MV BPL topologies of Sec.IIB when WtG^3 coupling scheme is applied. In Fig. 4, similar curves with Fig. 3 are shown but for the magnitude of coupling reflection coefficient.

From Fig. 3, it is clear that the existence of branches encountered across the BPL signal transmission in the examined OV MV BPL topologies imposes spectral notches in the coupling transfer functions, which are superimposed to the relatively steady “LOS” transfer function. The depth and the extent of these spectral notches mainly depend on the number and the electrical length of the branches as well as the nature of branch terminations. As concerns the characteristics of branches, OV MV BPL topologies with high number of branches and relatively low branch electrical length, such as the examined urban case one, create hostile and aggravated multipath environments for the BPL signal transmission. Conversely, when the presence of branches is scarce and the branch length is high, transfer function of these OV MV BPL topologies, such as the examined OV MV BPL rural one, tends to converge to the behavior of the “LOS” case where shallow and rare spectral notches are observed. In all the other OV MV BPL topology cases, the behavior of their transfer functions lies between the one of urban (worst case) and “LOS” (best case) [6], [7], [8], [9]. Anyway, the challenge of mitigating these horrible transmission characteristics push the recent

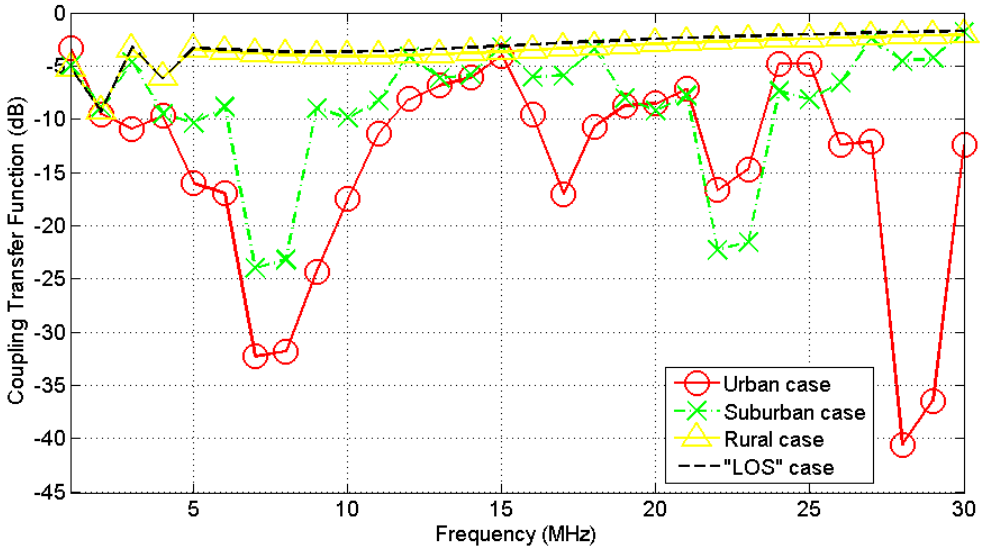

Figure 3. Coupling transfer function versus the frequency for the indicative OV MV BPL topologies when WtG^3 coupling scheme is applied and normal operation conditions are assumed (the frequency spacing is equal to 1MHz).

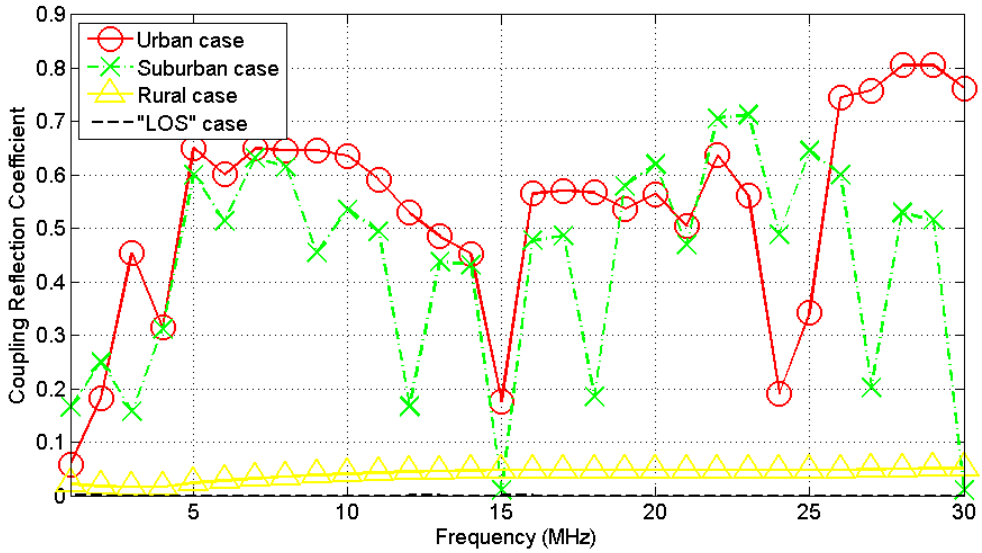

Figure 4. Coupling reflection coefficient versus the frequency for the indicative OV MV BPL topologies when WtG^3 coupling scheme is applied and normal operation conditions are assumed (the frequency spacing is equal to 1MHz).

research efforts towards communications solutions such as multi-hop repeater systems, multiple-input multiple-output consideration of the BPL channels and various resource allocation schemes [11], [18], [44], [45].

Similarly to coupling transfer functions, the magnitude of coupling reflection coefficients of the indicative OV MV BPL topologies present significant fluctuations in comparison with the almost zero reflection coefficient of the "LOS" case (matched termination load). In fact, the branch presence along the transmission path creates a

spectral environment that resembles to that of power dividers [10], [32], [33]. Since different number and length of branches are connected to the main distribution line, this has as a result that the input impedance at the transmitting end presents a frequency-dependent behavior, which further affects the reflection coefficient at the same point. In general terms, the spectral behavior of the reflection coefficient can be approached in a similar way with the behavior of the transfer function; say, topologies with high number of branches having relatively short lengths of branches superimpose significant reflection and spectral notches to the "LOS" case whereas topologies with low number of branches and long lengths tend to render their reflection coefficient similar to the "LOS" case ones.

Observing both Figs. 3 and 4, it is obvious that the trend smoothness of transfer function and reflection coefficient curves, the extrema of the curves and the extent and depth of curve notches may act as an identity pattern for the OV MV BPL topologies. This unique property of the aforementioned curves is going to be exploited by the main line fault localization methodology (MLFLM) in the accompanying papers in order to localize the main distribution line faults that may occur in OV MV BPL networks [23]-[26].

4.3 Coupling Reflection Coefficient for the Indicative OV MV BPL Topologies when Main Distribution Line Faults Occur (Extended TM2 Method)

Already been mentioned, critical problematic conditions, such as the main distribution line faults, can occur across the distribution power grid during its operation. With reference to Fig. 1(b), let the main distribution line be broken at 750m from the transmitting end. The four modified indicative OV MV BPL topologies are then differentiated as follows:

1. The modified urban topology (denoted as modified urban case) with N=2 branches (L_1=500m, L_2=200m, L_3=50m, L_{b1}=8m, L_{b2}=13m).
2. The modified suburban topology (denoted as modified suburban case) with N=1 branch (L_1=500m, L_2=250m, L_{b1}=50m).
3. The modified rural topology (denoted as modified rural case) with N=1 branch (L_1=600m, L_2=150m, L_{b1}=300m).
4. The "LOS" transmission along the same end-to-end distance $L=L_1+\ldots+L_{N+1}$=750m (denoted as modified "LOS" case) when no branches are encountered.

Here, it should be noted that the terminal load, which is located at the receiving end of the modified OV MV BPL topologies, is assumed equal to either short- or open-circuit. Hence, two sets of the four modified OV MV BPL topologies are examined in this subsection.

In accordance with Sec.III, the study of the behavior of OV MV BPL networks when a main distribution line fault occurs is focused on the examination of the reflection coefficients as dictated by eq. (7) through the application of the extended TM2 method. In Fig. 5, the magnitude of coupling reflection coefficient is plotted versus frequency for the four modified OV MV BPL topologies when WtG[3] coupling scheme is applied and the terminal load is assumed to be short-circuit. In Fig. 6, similar curves with Fig. 5 are shown with the assumption that the terminal load is an open-circuit.

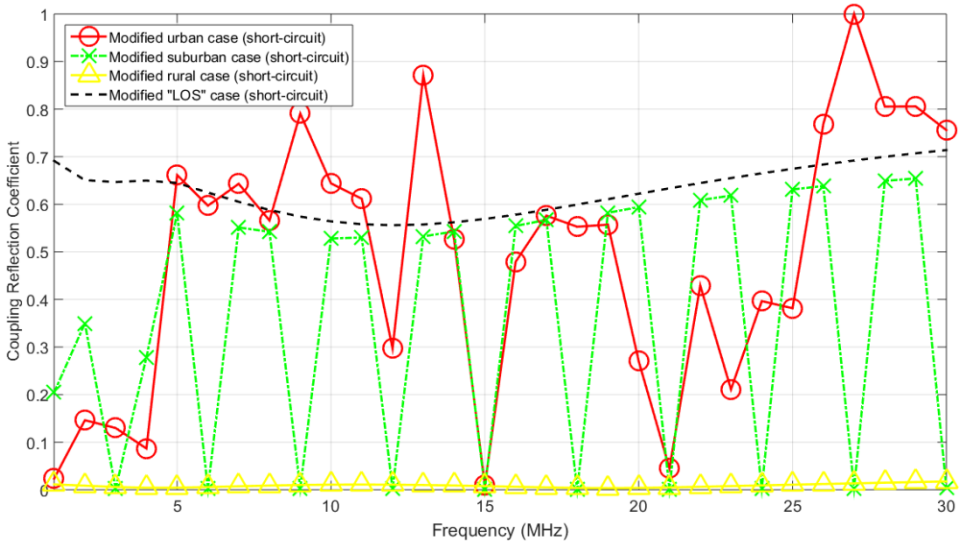

Figure 5. Coupling reflection coefficient versus the frequency for the modified OV MV BPL topologies when WtG[3] coupling scheme is applied and short-circuit is assumed as the terminal load (the frequency spacing is equal to 1MHz).

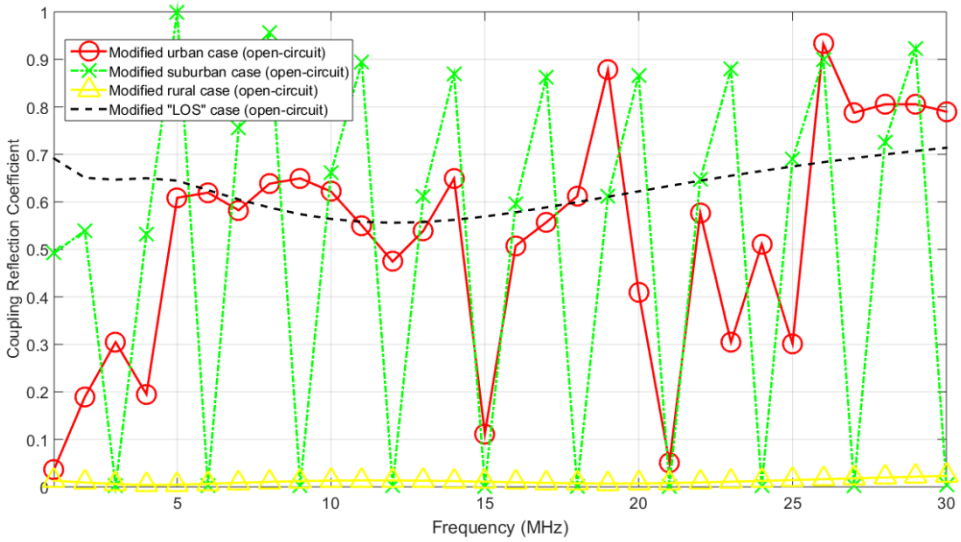

Figure 6. Same plots with Fig.5 but for an open-circuit terminal load.

The first fact that implies the presence of a main distribution line fault is the immediate communications failure between the transmitting and receiving end while the validation of the fault presence comes from the examination of the reflection coefficient at the transmitting end as highlighted in Figs. 4-6. In fact, the nature of the terminal load critically determines the form of the coupling reflection coefficient; say, any termination load, which differs from the matched terminal load of the normal operation of the OV MV BPL networks, significantly differentiates the coupling reflection coefficient from the one presented during the normal operation regardless of the examined topology.

Comparing Figs. 4-6, it deserves special attention the behavior of the magnitude of the coupling reflection coefficient of the "LOS" case. First, the values of the reflection coefficient of "LOS" case drastically change from the zero when the terminal load connected at the receiving end takes a value that differs from the matched termination. Actually, the magnitudes of the reflection coefficient coincide when the terminal load is assumed to be either short- or open-circuit. Anyway, this is explained by eq. (7) and the values assigned to $\mathbf{\Gamma}_{out}^{m,extended}$ in Sec.III for each of the aforementioned terminal load cases.

From the aforementioned observations, it is evident that the identification and further localization of a main distribution line fault comes from the difference of reflection coefficients that occurs between the normal and fault operation, which is highlighted in the following subsection.

4.4 Coupling Reflection Coefficient Differences between the Normal and Fault Operation of the Indicative OV MV BPL Topologies

Already been reported in Sec.IVC, the main distribution line faults differentiate the reflection coefficient behavior between the normal and fault operation. In this subsection, a study is undergone focusing on the comparative behavior of OV MV BPL topologies during the main distribution line faults.

In Fig. 7, the reflection coefficient differences of the indicative OV MV BPL topologies between their normal and fault operation is plotted versus frequency when WtG^3 coupling scheme is applied and the terminal load is assumed to be short-circuit termination. The main distribution line fault is located at 750m from the transmitting end and the reflection coefficient difference, which is presented in Fig.7, essentially defines the difference between Figs. 5 and 6 for given OV MV BPL topology. In Figs. 8-10, same plots with Fig. 7 but for the main distribution line fault to be located at 1m, 520m and 910m, respectively. Similar curves with Figs. 7-10 are given in Figs. 11-14, but for the open-circuit terminal load case.

Examining Figs. 7-14, several interesting conclusions can be deduced:

- When the main distribution line fault is located immediately after the transmitting end, the impact of the presence of the transmission line is limited. Indeed, when the main distribution line fault is located at 1m from the transmitting end, the reflection coefficient is equal to -1 or 1 if the terminal load is a short- or open-circuit termination, respectively. Therefore, the magnitude of the reflection coefficients is equal to 1 in both the cases. As presented in Figs. 8 and 12, it is expected that the coupling reflection coefficient difference of the "LOS" case is equal to -1 since the absolute value of the reflection coefficient of the "LOS" topology during its normal operation is equal to 0.
- Apart from the "LOS" case where the main distribution line fault is located at the transmitting end, the coupling reflection coefficient differences of OV MV BPL topologies with branches present fluctuations that are distributed around the zero regardless of the terminal load.
- When a communications failure between the transmitting and receiving end persists and the coupling reflection coefficient differences insist on differing from zero in the frequency domain a main distribution line fault is present.

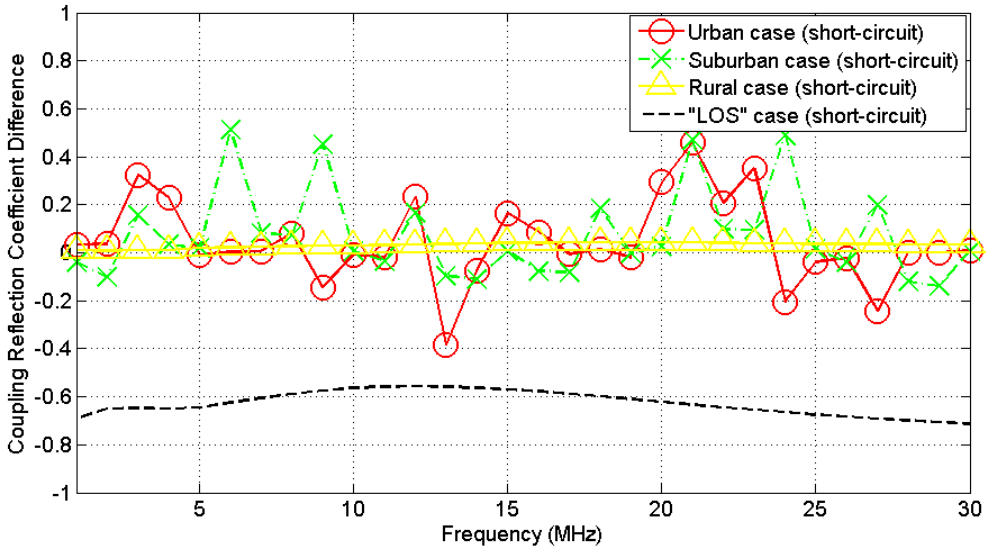

Figure 7. Coupling reflection coefficient difference versus the frequency between the original and modified indicative OV MV BPL topologies when WtG^3 coupling scheme is applied and short-circuit is assumed as the terminal load at 750m from the transmitting end (the frequency spacing is equal to 1MHz).

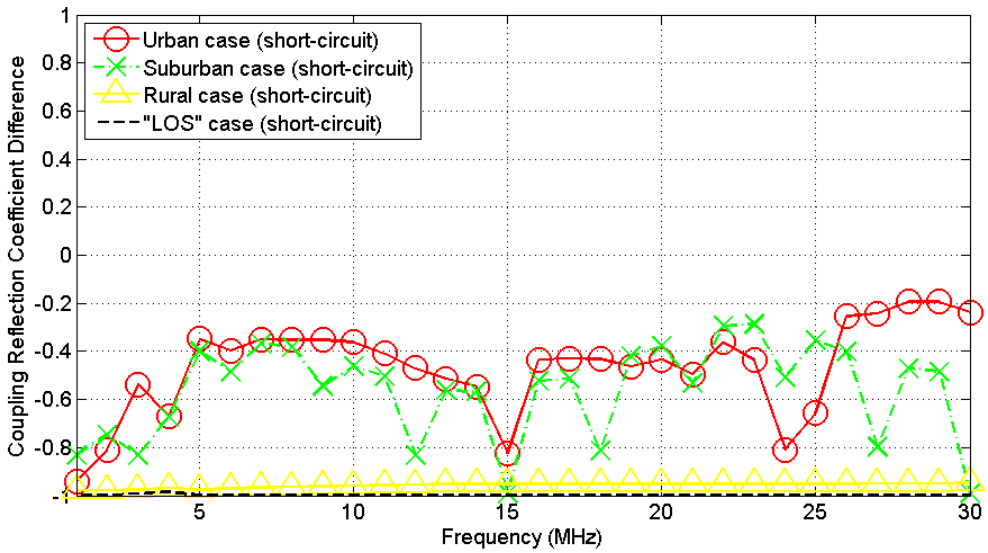

Figure 8. Coupling reflection coefficient difference versus the frequency between the original and modified indicative OV MV BPL topologies when WtG^3 coupling scheme is applied and short-circuit is assumed as the terminal load at 1m from the transmitting end (the frequency spacing is equal to 1MHz).

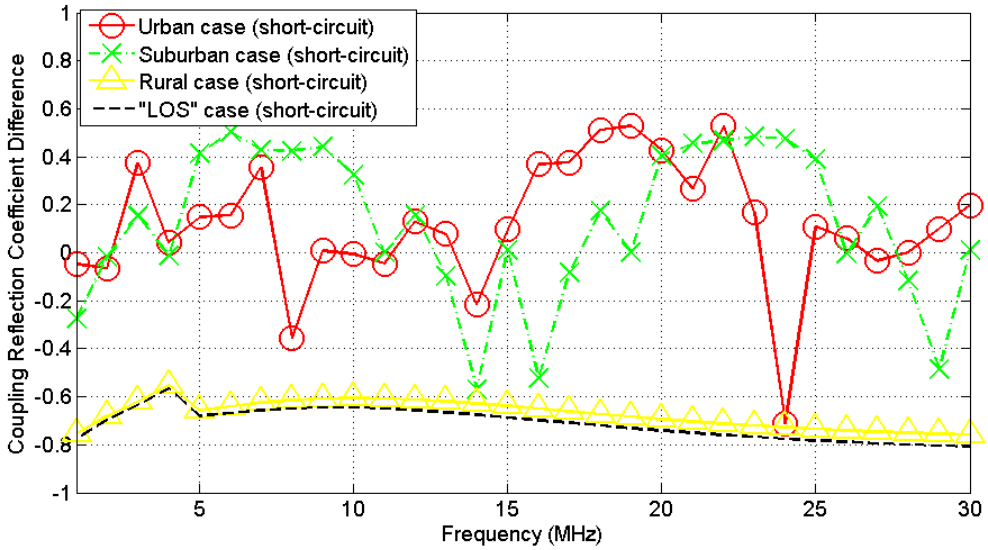

Figure 9. Coupling reflection coefficient difference versus the frequency between the original and modified indicative OV MV BPL topologies when WtG^3 coupling scheme is applied and short-circuit is assumed as the terminal load at 520m from the transmitting end (the frequency spacing is equal to 1MHz).

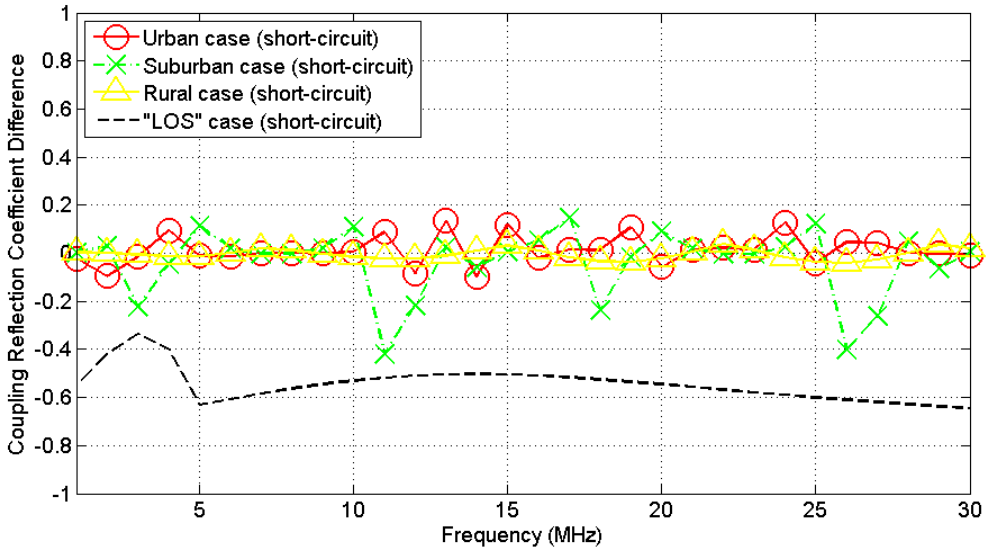

Figure 10. Coupling reflection coefficient difference versus the frequency between the original and modified indicative OV MV BPL topologies when WtG^3 coupling scheme is applied and short-circuit is assumed as the terminal load at 910m from the transmitting end (the frequency spacing is equal to 1MHz).

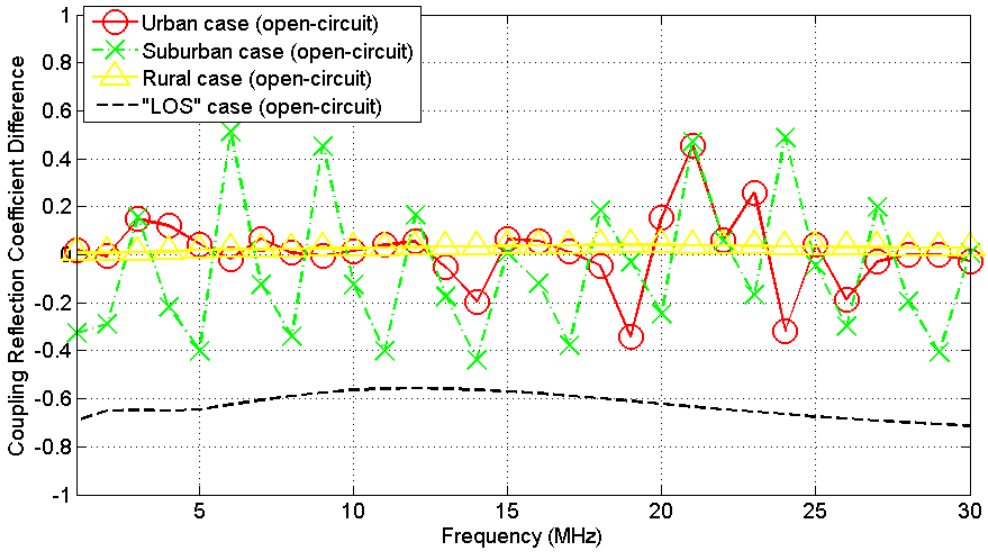

Figure 11. Same plots with Fig.7 but for an open-circuit terminal load.

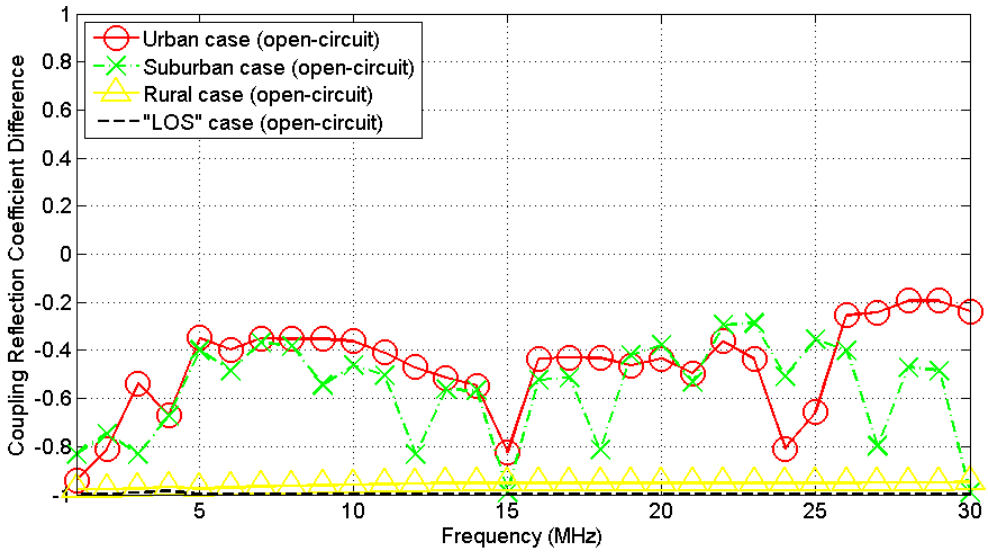

Figure 12. Same plots with Fig.8 but for an open-circuit terminal load.

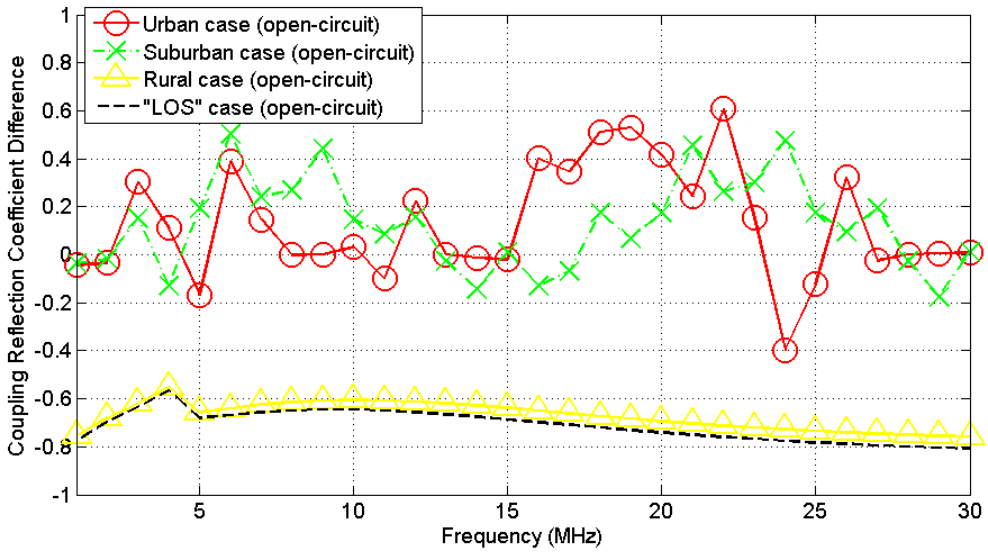

Figure 13. Same plots with Fig.9 but for an open-circuit terminal load.

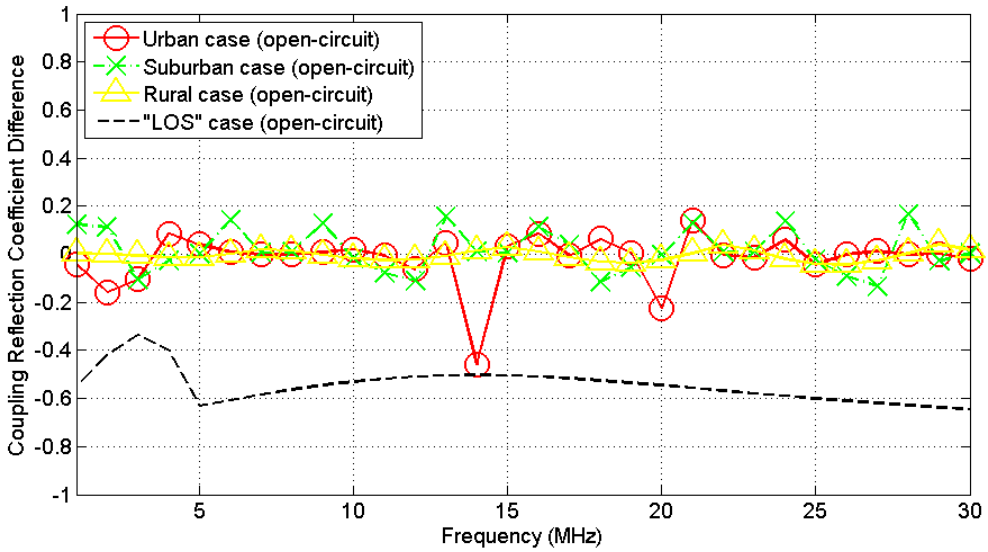

Figure 14. Same plots with Fig.10 but for an open-circuit terminal load.

Here, the identification of a main distribution line fault is secured and the localization of main distribution line faults through MLFLM procedure can be initiated (for more details concerning the localization of main distribution line faults and MLFLM, see [46]).

- The detection of a main distribution line fault is easier in the OV MV BPL topologies with more branches than in the "LOS" case since the fluctuations of the coupling reflection coefficient differences around zero get severe in the aggravated topology cases. In contrast, rural and "LOS" OV MV BPL topologies demand more attention when the identification of main distribution line faults is undergone since their fluctuations are milder.

- Similarly to the findings regarding the unique appearance of transfer functions and reflection coefficients of OV MV BPL topologies, the unique characteristics of the coupling reflection coefficient differences (i.e., the trend of the curve, the extrema of the curves and the extent and depth of curve notches) are exploited as the identity pattern in order to exact localize main distribution line faults in [46], [47].
- Although the identification of a main distribution line fault has been theoretically secured in all the OV MV BPL topologies through the coupling reflection coefficient differences, the identification of these faults can be problematic in the "real-life" conditions since measurement differences can be added during the determination of reflection coefficients (fault alarm case). The countermeasures against the measurement differences by using piecewise monotonic data approximations (PMAs) as well as the identification efficiency of a main distribution line fault through the reflection coefficient differences is examined in [47].
- Apart from the identification of a main distribution line fault, the goal of these papers is the exact localization of the fault. On the basis of the PMA benchmark results of [47] and the extended TM2 method, TIM of [23] and FIIM of [24] can further be upgraded in order to deal with the main distribution line faults that constitute the only fault case which cannot be identified by TIM and FIIM in [25], [26]. MLFLM is going to exploit the unique characteristics of reflection coefficients of OV MV BPL topologies as well as the findings of this paper and [47] in order to exactly localize the main distribution line faults that may occur in OV MV BPL networks in [46].

Conclusions

In this first paper, the identification methodology of main distribution line faults in OV MV BPL networks has been presented and assessed. Initially, the extension of TM2 method has been analyzed on the basis of the original TM2 method through its generic multidimensional network analysis. In fact, the identification of main distribution line faults is based on the coupling reflection coefficients derived from the original and the extended TM2 method as well as their differences. The assessment of the identification of main distribution line faults has been applied to four indicative OV MV BPL topologies when their terminal loads are assumed to be either matched or short-circuit or open-circuit. Actually, the pattern of the coupling reflection coefficients significantly depends on the examined OV MV BPL topology as well as the nature of the terminal loads, thus implying that there are significant differences in coupling reflection coefficients between the normal and fault condition for given OV MV BPL topology. Synoptically, the coupling reflection coefficient may act as an identity pattern for given OV MV BPL topology and terminal load while the communications failure between the transmitting and receiving end and the fluctuations of coupling reflection differences at the transmitting end marks the existence of a main distribution line fault across the OV MV BPL topology.

The influence of the measurements differences during the identification of main distribution line faults, the countermeasures against measurement differences by applying PMAs and the proposal of MLFLM with the intention to localize the main distribution line faults are going to be investigated in the following two papers.

CONFLICTS OF INTEREST

The author declares that there is no conflict of interests regarding the publication of this paper.

References

[1] G. Kaddoum and N. Tadayon, "Differential Chaos Shift Keying: A Robust Modulation Scheme for Power-Line Communications," *IEEE Trans. on Circuits and Systems II: Express Briefs*, vol. 64, no. 1, pp. 31-35, 2017.

[2] A. Milioudis, G. Andreou, and D. Labridis, "Optimum transmitted power spectral distribution for broadband power line communication systems considering electromagnetic emissions," *Elsevier Electric Power Systems Research*, vol. 140, pp. 958-964, Nov. 2016.

[3] K. Sharma and L. M. Saini, "Power-line Communications for Smart Grid: Progress, Challenges, Opportunities and Status," *Elsevier Renewable and Sustainable Energy Reviews*, vol. 67, pp. 704-751, 2017.

[4] A. G. Lazaropoulos, "Best L1 Piecewise Monotonic Data Approximation in Overhead and Underground Medium-Voltage and Low-Voltage Broadband over Power Lines Networks: Theoretical and Practical Transfer Function Determination," *Hindawi Journal of Computational Engineering*, vol. 2016, Article ID 6762390, 24 pages, 2016. doi:10.1155/2016/6762390. [Online]. Available: https://www.hindawi.com/journals/jcengi/2016/6762390/cta/

[5] C. Cano, A.Pittolo, D. Malone, L. Lampe, A. M.Tonello, and A. Dabak, "State-of-the-art in Power Line Communications: From the Applications to the Medium," *IEEE J. Sel. Areas Commun.*,vol. 34, pp. 1935-1952, 2016.

[6] A. G. Lazaropoulos and P. G. Cottis, "Transmission characteristics of overhead medium voltage power line communication channels," *IEEE Trans. Power Del.*, vol. 24, no. 3, pp. 1164-1173, Jul. 2009.

[7] A. G. Lazaropoulos and P. G. Cottis, "Capacity of overhead medium voltage power line communication channels," *IEEE Trans. Power Del.*, vol. 25, no. 2, pp. 723-733, Apr. 2010.

[8] A. G. Lazaropoulos and P. G. Cottis, "Broadband transmission via underground medium-voltage power lines-Part I: transmission characteristics," *IEEE Trans. Power Del.*, vol. 25, no. 4, pp. 2414-2424, Oct. 2010.

[9] A. G. Lazaropoulos and P. G. Cottis, "Broadband transmission via underground medium-voltage power lines-Part II: capacity," *IEEE Trans. Power Del.*, vol. 25, no. 4, pp. 2425-2434, Oct. 2010.

[10] A. G. Lazaropoulos, "Broadband transmission characteristics of overhead high-voltage power line communication channels," *Progress in Electromagnetics Research B*, vol. 36, pp. 373-398, 2012. [Online]. Available: http://www.jpier.org/PIERB/pierb36/19.11091408.pdf

[11] A. G. Lazaropoulos, "Capacity Performance of Overhead Transmission Multiple-Input Multiple-Output Broadband over Power Lines Networks: The Insidious Effect of Noise and the Role of Noise Models," *Trends in Renewable Energy*, vol. 2, no. 2, pp. 61-82,

Jan. 2016. [Online]. Available: http://futureenergysp.com/index.php/tre/article/view/23

[12] Homeplug, AV2Whitepaper, 2011, [Online]. Available: http://www.homeplug.org/techresources/resources/

[13] A. G. Lazaropoulos, "Factors Influencing Broadband Transmission Characteristics of Underground Low-Voltage Distribution Networks," *IET Commun.*, vol. 6, no. 17, pp. 2886-2893, Nov. 2012.

[14] A. G. Lazaropoulos, "Towards broadband over power lines systems integration: Transmission characteristics of underground low-voltage distribution power lines," *Progress in Electromagnetics Research B*, 39, pp. 89-114, 2012. [Online]. Available: http://www.jpier.org/PIERB/pierb39/05.12012409.pdf

[15] A. G. Lazaropoulos, "Broadband transmission and statistical performance properties of overhead high-voltage transmission networks,"*Hindawi Journal of Computer Networks and Commun.*, 2012, article ID 875632, 2012. [Online]. Available: http://www.hindawi.com/journals/jcnc/aip/875632/

[16] A. G. Lazaropoulos, "Towards modal integration of overhead and underground low-voltage and medium-voltage power line communication channels in the smart grid landscape: model expansion, broadband signal transmission characteristics, and statistical performance metrics (Invited Paper)," *ISRN Signal Processing*, vol. 2012, Article ID 121628, 17 pages, 2012. [Online]. Available: http://www.isrn.com/journals/sp/aip/121628/

[17] A. G. Lazaropoulos, "Review and Progress towards the Common Broadband Management of High-Voltage Transmission Grids: Model Expansion and Comparative Modal Analysis," *ISRN Electronics*, vol. 2012, Article ID 935286, pp. 1-18, 2012. [Online]. Available: http://www.hindawi.com/isrn/electronics/2012/935286/

[18] A. G. Lazaropoulos, "Review and Progress towards the Capacity Boost of Overhead and Underground Medium-Voltage and Low-Voltage Broadband over Power Lines Networks: Cooperative Communications through Two- and Three-Hop Repeater Systems," *ISRN Electronics*, vol. 2013, Article ID 472190, pp. 1-19, 2013. [Online]. Available: http://www.hindawi.com/isrn/electronics/aip/472190/

[19] A. G. Lazaropoulos, "Green Overhead and Underground Multiple-Input Multiple-Output Medium Voltage Broadband over Power Lines Networks: Energy-Efficient Power Control," *Springer Journal of Global Optimization*, vol. 2012 / Print ISSN 0925-5001, pp. 1-28, Oct. 2012.

[20] P. Amirshahi and M. Kavehrad, "High-frequency characteristics of overhead multiconductor power lines for broadband communications," *IEEE J. Sel. Areas Commun.*, vol. 24, no. 7, pp. 1292-1303, Jul. 2006.

[21] T. Sartenaer, "Multiuser communications over frequency selective wired channels and applications to the powerline access network" Ph.D. dissertation, Univ. Catholique Louvain, Louvain-la-Neuve, Belgium, Sep. 2004. [Online} Available: https://dial.uclouvain.be/pr/boreal/en/object/boreal%3A5010/datastream/PDF_12/view

[22] T. Calliacoudas and F. Issa, ""Multiconductor transmission lines and cables solver," An efficient simulation tool for plc channel networks development," presented at the *IEEE Int. Conf. Power Line Communications and Its Applications*, Athens, Greece, Mar. 2002.

[23] A. G. Lazaropoulos, "Measurement Differences, Faults and Instabilities in Intelligent Energy Systems – Part 1: Identification of Overhead High-Voltage Broadband over Power Lines Network Topologies by Applying Topology Identification Methodology (TIM)," *Trends in Renewable Energy*, vol. 2, no. 3, pp. 85 – 112, Oct. 2016.

[24] A. G. Lazaropoulos, "Measurement Differences, Faults and Instabilities in Intelligent Energy Systems – Part 2: Fault and Instability Prediction in Overhead High-Voltage Broadband over Power Lines Networks by Applying Fault and Instability Identification Methodology (FIIM)," *Trends in Renewable Energy*, vol. 2, no. 3, pp. 113 – 142, Oct. 2016. [Online]. Available: http://futureenergysp.com/index.php/tre/article/view/27/33

[25] A. G. Lazaropoulos, "Power Systems Stability through Piecewise Monotonic Data Approximations – Part 1: Comparative Benchmarking of L1PMA, L2WPMA and L2CXCV in Overhead Medium-Voltage Broadband over Power Lines Networks," *Trends in Renewable Energy*, vol. 3, no. 1, pp. 2 – 32, Jan. 2017. [Online]. Available: http://futureenergysp.com/index.php/tre/article/view/29/34

[26] A. G. Lazaropoulos, "Power Systems Stability through Piecewise Monotonic Data Approximations – Part 2: Adaptive Number of Monotonic Sections and Performance of L1PMA, L2WPMA and L2CXCV in Overhead Medium-Voltage Broadband over Power Lines Networks," *Trends in Renewable Energy*, vol. 3, no. 1, pp. 33 – 60, Jan. 2017. [Online]. Available: http://futureenergysp.com/index.php/tre/article/view/30/35

[27] A. G. Lazaropoulos, "Improvement of Power Systems Stability by Applying Topology Identification Methodology (TIM) and Fault and Instability Identification Methodology (FIIM) – Study of the Overhead Medium-Voltage Broadband over Power Lines (OV MV BPL) Networks Case," *Trends in Renewable Energy*, vol. 3, no. 2, pp. 102 – 128, Apr. 2017. [Online]. Available: http://futureenergysp.com/index.php/tre/article/view/34/pdf

[28] P. Amirshahi, "Broadband access and home networking through powerline networks" Ph.D. dissertation, Pennsylvania State Univ., University Park, PA, May 2006. [Online]. Available: http://etda.libraries.psu.edu/theses/approved/WorldWideIndex/ETD-1205/index.html

[29] M. D'Amore and M. S. Sarto, "Simulation models of a dissipative transmission line above a lossy ground for a wide-frequency range-Part I: Single conductor configuration," *IEEE Trans. Electromagn. Compat.*, vol. 38, no. 2, pp. 127-138, May 1996.

[30] M. D'Amore and M. S. Sarto, "Simulation models of a dissipative transmission line above a lossy ground for a wide-frequency range-Part II: Multi-conductor configuration," *IEEE Trans. Electromagn. Compat.*, vol. 38, no. 2, pp. 139-149, May 1996.

[31] A. Milioudis, G. T. Andreou, and D. P. Labridis, "Detection and location of high impedance faults in multiconductor overhead distribution lines using power line communication devices," *IEEE Trans. on Smart Grid*, vol. 6, no. 2, pp. 894-902, 2015.

[32] A. G. Lazaropoulos, "Designing Broadband over Power Lines Networks Using the Techno-Economic Pedagogical (TEP) Method – Part I: Overhead High Voltage Networks and Their Capacity Characteristics," *Trends in Renewable*

Energy, vol. 1, no. 1, pp. 16-42, Mar. 2015. [Online]. Available: http://futureenergysp.com/index.php/tre/article/view/2

[33] A. G. Lazaropoulos, "Designing Broadband over Power Lines Networks Using the Techno-Economic Pedagogical (TEP) Method – Part II: Overhead Low-Voltage and Medium-Voltage Channels and Their Modal Transmission Characteristics," *Trends in Renewable Energy*, vol. 1, no. 2, pp. 59-86, Jun. 2015. [Online]. Available: http://futureenergysp.com/index.php/tre/article/view/6/16

[34] T. Sartenaer and P. Delogne, "Deterministic modelling of the (Shielded) outdoor powerline channel based on the multiconductor transmission line equations," *IEEE J. Sel. Areas Commun.*, vol. 24, no. 7, pp. 1277-1291, Jul. 2006.

[35] A. G. Lazaropoulos, "Policies for Carbon Energy Footprint Reduction of Overhead Multiple-Input Multiple-Output High Voltage Broadband over Power Lines Networks," *Trends in Renewable Energy*, vol. 1, no. 2, pp. 87-118, Jun. 2015. [Online]. Available: http://futureenergysp.com/index.php/tre/article/view/11/17

[36] A. G. Lazaropoulos, "Wireless Sensor Network Design for Transmission Line Monitoring, Metering and Controlling: Introducing Broadband over PowerLines-enhanced Network Model (BPLeNM)," *ISRN Power Engineering*, vol. 2014, Article ID 894628, 22 pages, 2014. doi:10.1155/2014/894628. [Online]. Available: http://www.hindawi.com/journals/isrn.power.engineering/2014/894628/

[37] A. G. Lazaropoulos, "Wireless Sensors and Broadband over PowerLines Networks: The Performance of Broadband over PowerLines-enhanced Network Model (BPLeNM) (Invited Paper)," *ICAS Publishing Group Transaction on IoT and Cloud Computing*, vol. 2, no. 3, pp. 1-35, 2014. [Online]. Available: http://citeseerx.ist.psu.edu/viewdoc/download;jsessionid=741EE7C15693046FFFF5E9749149F579?doi=10.1.1.679.8217&rep=rep1&type=pdf

[38] A. G. Lazaropoulos, "The Impact of Noise Models on Capacity Performance of Distribution Broadband over Power Lines (BPL) Networks," *Hindawi Computer Networks and Communications*, vol. 2016, Article ID 5680850, 14 pages, 2016. doi:10.1155/2016/5680850. [Online]. Available: http://www.hindawi.com/journals/jcnc/2016/5680850/

[39] A. N. Milioudis, G. T. Andreou, and D. P. Labridis, "Enhanced Protection Scheme for Smart Grids Using Power Line Communications Techniques—Part II: Location of High Impedance Fault Position," *IEEE Trans. on Smart Grid*, no. 3, vol. 4, pp. 1631-1640, 2012.

[40] A. Milioudis, G. Andreou, and D. Labridis, "High impedance fault detection using power line communication techniques," in *Proc. 2010 45th Int. Univ. Power Eng. Conf. (UPEC)*, pp. 1–6, Cardiff, U.K., 2010.

[41] A. Milioudis, G. Andreou, and D. Labridis, "High impedance fault evaluation using narrowband power line communication techniques," in *Proc. 2011 IEEE Trondheim PowerTech*, Trondheim, Norway, pp. 1–6.

[42] A. Milioudis, G. Andreou, and D. Labridis, "Enhanced protection scheme for smart grids using power line communications techniques—Part I: Detection of high impedance fault occurrence," *IEEE Trans. Smart Grid*, vol. 3, no. 4, pp. 1621–1630, Dec. 2012.

[43] A. G. Lazaropoulos, "Deployment Concepts for Overhead High Voltage Broadband over Power Lines Connections with Two-Hop Repeater System: Capacity Countermeasures against Aggravated Topologies and High Noise

Environments," *Progress in Electromagnetics Research B*, vol. 44, pp. 283-307, 2012. [Online]. Available: http://www.jpier.org/PIERB/pierb44/13.12081104.pdf

[44] S. Liu, F. Yang, and J. Song, "An Optimal Interleaving Scheme with Maximum Time-Frequency Diversity for PLC Systems," *IEEE Trans. on Power Del.*, vol. 31, no. 3, pp. 1007-1014, 2016.

[45] G. Prasad, L. Lampe, and S. Shekhar, "In-Band Full Duplex Broadband Power Line Communications," *IEEE Trans. on Commun.*, vol. 64, no. 9, pp. 3915-3931, 2016.

[46] A. G. Lazaropoulos, "Main Line Fault Localization Methodology in Smart Grid – Part 3: Main Line Fault Localization Methodology (MLFLM)," *Trends in Renewable Energy*, vol. 3, no. 3, pp. 62-81, 2017.

[47] A. G. Lazaropoulos, "Main Line Fault Localization Methodology in Smart Grid – Part 2: Extended TM2 Method, Measurement Differences and L1 Piecewise Monotonic Data Approximation for the Overhead Medium-Voltage Broadband over Power Lines Networks Case," *Trends in Renewable Energy*, vol. 3, no. 3, pp. 26-61, 2017.

Trends in Renewable Energy
OPEN ACCESS ISSN: 2376-2144
Peer-Reviewed Article futureenergysp.com/index.php/tre

Main Line Fault Localization Methodology in Smart Grid – Part 2: Extended TM2 Method, Measurement Differences and L1 Piecewise Monotonic Data Approximation for the Overhead Medium-Voltage Broadband over Power Lines Networks Case

Athanasios G. Lazaropoulos[1]

1: School of Electrical and Computer Engineering / National Technical University of Athens / 9 Iroon Polytechniou Street / Zografou, GR 15780

Received June 13, 2017; Accepted September 2, 2017; Published October 2, 2017

Enriching the fault identification methodology of the first paper, this second paper investigates the performance of the identification of main distribution line faults when broadband over power lines (BPL) networks are deployed. The main issue that is concerned in this paper is the impact of measurement differences on the fault identification process performance.
The main contribution of this paper, which is focused on the identification of the main distribution line faults when measurement differences occur, is the application of the L1 piecewise monotonic data approximation (l1PMA) in order to cope with the measurement differences that influence the reflection coefficients derived from the extended TM2 method. Through the L1PMA application, measurement differences are confronted in order to prevent the trigger of a false alarm about the existence of a main distribution line fault. The combined operation of the extended TM2 method and L1PMA concludes the introductory phase (fault identification) of the main line fault localization methodology (MLFLM).

Keywords: Smart Grid; Intelligent Energy Systems; Broadband over Power Lines (BPL) Networks; Power Line Communications (PLC); Faults; Fault Analysis; Fault Localization; Distribution Power Grids

1. Introduction

The need for more intelligent, stable and autonomous transmission and distribution power grids is met by the deployment of the smart grid package, which comprises both hardware and software proposals, across the entire vintage power grid infrastructure [1]-[4]. As concerns the smart grid hardware, broadband over power lines (BPL) networks have rightfully attracted the attention among the available wired and wireless communications media, which anyway may interoperate in the smart grid environment [5]-[7]. A major advantage of the BPL networks is the fact that their deployment is based on the already existent power grid equipment devoted to transfer and deliver power. As concerns the smart grid software, a myriad of smart grid applications

Corresponding author: AGLazaropoulos@gmail.com

Tr Ren Energy, 2017, Vol.3, No.3, 26-61. doi: 10.17737/tre.2017.3.3.0037

can be supported by all the available wired and wireless communication solutions of smart grid, including BPL technology, since the traditional power grid can be further treated as an integrated intelligent IP-based network environment [2], [8]-[10].

As concerns the determination of the channel attenuation and reflection coefficient of overhead medium-voltage (OV MV) BPL networks, the well-established hybrid method, which consists of [6], [10]-[26]: (i) a bottom-up approach that is based on the multiconductor transmission line (MTL) theory, eigenvalue decomposition (EVD) and singular value decomposition (SVD); and (ii) a top-down approach that is denoted as TM2 method and is based on the concatenation of multidimensional chain scattering matrices. In accordance with [1], original TM2 method gives as outputs the corresponding transfer function and reflection coefficients for the normal operation of OV MV BPL networks whereas extended TM2 method gives as output the reflection coefficients for the operation where a main distribution line fault occurs (fault operation). In fact, the main distribution line fault subcategory forms the only fault case which cannot be treated by the available tools for identifying and localizing faults and instabilities, say Topology Identification Methodology (TIM) and Fault and Instability Identification Methodology (FIIM) of [3], [4]. The identification of main distribution line faults is going to be treated by the approach of reflection coefficients of the extended TM2 method, which has initially been presented in [1]. As presented in [1], the comparison of the reflection coefficients between the normal operation, as given by the original TM2 method, and the fault operation, as determined by the extended TM2 method, defines the existence of main distribution line faults.

As already been mentioned in [3], [4], [6], [10], [26], measurement differences between the experimental and theoretical results occur during the transfer function determination of OV MV BPL topologies because of a number of practical reasons and "real-life" conditions. Similar measurement differences also occur during the determination of reflection coefficients. Following the same methodology to counteract the measurement differences of reflection coefficients with those of transfer functions, piecewise monotonic data approximations (PMAs), such as L1PMA, L2WPMA and L2CXCV, are also applied to the reflection coefficient measurements in order to restore the theoretical reflection coefficient [3], [4], [6], [10], [26]. Among the available PMAs that have been applied to BPL networks, L1PMA, which has been thoroughly analyzed and assessed in [3], [26], is selected to be applied to the restoration of theoretical values of reflection coefficients. In this paper, the performance of L1PMA is assessed when various intensities of measurement differences are considered regardless of the examined OV MV BPL topology and the nature of the terminal load. Synoptically, the primary objective of this paper is to identify the main distribution line faults even if measurement differences occur while the fault alarm can be prevented due to the measurement differences.

The rest of this paper is organized as follows: In Sec.II, the findings of [1] that are used in this paper are briefly outlined. In Sec.III, a brief presentation of the measurement differences in BPL networks and L1PMA is given. Also, the suitable performance metrics for assessing the mitigation against measurement differences and for identifying a main distribution line fault are demonstrated. Sec.IV discusses the simulations of various OV MV BPL networks intending to mark out the mitigation performance of L1PMA against measurement differences during the main distribution line fault identification. Sec.V concludes this paper.

2. Brief Presentation of the OV MV MTL Configurations, OV MV BPL Topologies, Hybrid Method and the Main Distribution Line Faults

In accordance with [1], the OV MV MTL configuration, which is used in these three papers, is presented in Fig. 1(a) of [26] while its structure properties concerning the number of phase lines, the phase line spacings and the configuration heights are reported in [12], [13], [19], [21], [23], [27]-[29]. As the ground properties are considered, the impact of imperfect ground on broadband signal propagation and transmission via OV MV MTL configurations is analyzed in [12], [13], [19], [21], [23], [30]-[32].

According to [1], OV MV BPL networks are divided into cascaded OV MV BPL topologies. These OV MV BPL topologies are characterized by average path lengths of the order of 1000m which are bounded by BPL repeaters. With reference to Fig. 1(a) of [1], a typical OV MV BPL topology is presented while four indicative OV MV BPL topologies of average path length are defined and examined in these three papers. The topological specifications of the four indicative OV MV BPL topologies are detailed in [1] in order to describe respective typical urban, suburban, rural and "LOS" cases. Certain assumptions for the circuital parameters of OV MV BPL topologies, which are required by the hybrid method, are also given in [1].

Similarly to [1], [11]-[25], [31]-[33], the well-established hybrid method is applied in these three papers. More analytically, the hybrid method consists of: (i) a bottom-up approach that is based on the MTL theory, EVD and SVD decomposition; and (ii) a top-down approach that further comprises either the original TM2 method for the normal operation or the extended TM2 method for the main distribution line fault operation. The output of the hybrid method, which is the EVD modal reflection coefficient matrix $\mathbf{\Gamma}_{\text{in}}^{\text{m}}\{\cdot\}$, is further processed by the coupling scheme module that determines the practical way of the BPL signal injection into OV MV lines. In the case of Wire-to-Ground (WtG) coupling schemes, which are examined in these papers, the WtG coupling reflection coefficient $\Gamma^{\text{WtG}^{\text{s}}}\{\cdot\}$ is determined by [1]

$$\Gamma^{\text{WtG}^{\text{s}}}\{\cdot\} = \left[\mathbf{C}^{\text{WtG}}\right]^{\text{T}} \cdot \mathbf{T}_{\text{V}} \cdot \mathbf{\Gamma}_{\text{in}}^{\text{m}}\{\cdot\} \cdot \mathbf{T}_{\text{V}}^{-1} \cdot \mathbf{C}^{\text{WtG}} \tag{2}$$

where $\mathbf{C}^{\text{WtG}}$ is the coupling column vector and $\mathbf{T}_{\text{V}}$ is a matrix that depends on the frequency, the OV MV MTL configuration and the physical properties of the cables.

Already been mentioned in [1], critical problematic conditions can occur across the distribution power grid during its continuous normal operation. These problematic conditions differ from the measurement differences and can be divided into two categories, namely: faults and instabilities [3]-[6], [10]. Main distribution line faults, which are examined in these three papers, define a subcategory of the fault operation and describe the condition where a main distribution line is interrupted due to physical or human reasons [5]. Depending on the location of the conductors of the main distribution lines after the fault, main distribution line faults can be assumed to behave as either short- or open-circuit terminal loads whether the lines lie in the air or on the ground, respectively.

3. Measurement Differences, Presentation of L1PMA and Performance Metric

Apart from the faults and instabilities that cause critical damages to the transmission and distribution power grid infrastructure, a set of practical reasons and "real-life" conditions create significant differences between experimental measurements and theoretical results during the various determinations relating with the BPL networks. In accordance with [6], the set of measurement difference causes can be grouped into six categories, namely: (i) Isolation difficulties of specific MTL parameters in time- and frequency-domain; (ii) Low accuracy and sensitivity of the used equipment during measurements; (iii) Cross-talk and resonant phenomena due to the parasitic capacitances and inductances of lines; (iv) The weakness of including specific wiring and grounding practices; (v) Practical impedance deviations of lines, branches, terminations and transmitting/receiving ends; and (vi) The isolation lack of the noise effect during the transfer function computations.

The acquired PMA experience in the case of BPL coupling transfer functions across transmission and distribution power grids is here extended in order to cope with the measurement differences that may be present during the measurement of reflection coefficients. In accordance with [3]-[6], [10], [26], PMAs are going to exploit their piecewise monotonicity property by decomposing the reflection coefficient data into separate monotonous data sections between adjacent turning points (primary extrema). Then, PMAs separately handle the monotonous sections by proposing suitable regression approximations. Similarly to the coupling transfer function case, L1PMA software is modified in order to receive as inputs the measured OV MV BPL reflection coefficient data (i.e., either from the original TM2 method or the extended TM2 method), the measurement frequencies and the number of monotonic sections (i.e., either user- or computer-defined) and give as outputs the optimal primary extrema and the best fit of the measured OV MV BPL reflection coefficient data. In mathematical terms and with reference to eq. (2), the measured OV MV BPL reflection coefficient $\overline{\Gamma^{\mathrm{WtG^s}}}$ for given WtG^s coupling scheme is determined by

$$\overline{\Gamma^{\mathrm{WtG^s}}}(f_i)=\Gamma^{\mathrm{WtG^s}}(f_i)+e(f_i),\ i=1,\ldots,u \tag{3}$$

where f_i, $i=1,\ldots,u$ denotes the measurement frequency, $e(f_i)$ synopsizes the total measurement difference due to the aforementioned six categories and u is the number of subchannels in the examined frequency range.

Generalizing eq. (3), the measured OV MV BPL reflection coefficient column vector $\overline{\mathbf{\Gamma}^{\mathrm{WtG}}}$ is then determined by

$$\overline{\mathbf{\Gamma}^{\mathrm{WtG}}}\equiv\overline{\mathbf{\Gamma}^{\mathrm{WtG}}}(\mathbf{f})=\left[\overline{\Gamma^{\mathrm{WtG}}}(f_1)\ \cdots\ \overline{\Gamma^{\mathrm{WtG}}}(f_i)\ \cdots\ \overline{\Gamma^{\mathrm{WtG}}}(f_u)\right]^{\mathrm{T}} \tag{3}$$

where $\mathbf{f}=\left[f_1\ \cdots\ f_i\ \cdots\ f_u\right]^{\mathrm{T}}$ is the measurement frequency column vector. Similarly to the measured OV MV BPL reflection coefficient column vector $\overline{\mathbf{\Gamma}^{\mathrm{WtG}}}$, the theoretical OV MV BPL reflection coefficient column vector $\mathbf{\Gamma}^{\mathrm{WtG}}$ can also be defined. With reference to [26], the theoretical OV MV BPL reflection coefficient column vector, the measured OV MV BPL reflection coefficient column vector, the measurement frequency column vector and the number of monotonic sections are

received by the L1PMA software presented in [34]. L1PMA software processes its inputs and gives as outputs the approximated theoretical OV MV BPL reflection coefficient column vector $\overline{\overline{\mathbf{\Gamma}}}_{\text{theor}}^{\text{WtG}}$ and the approximated measured OV MV BPL reflection coefficient column vector $\overline{\overline{\mathbf{\Gamma}}}_{\text{meas}}^{\text{WtG}}$.

Similarly to the performance metric CSPpM of FIIM [5], the proposed main distribution line fault identification percentage metric (MDLFI), which acts as the accompanying performance metric of the identification of main distribution line faults when measurement differences occur, is given by

$$MDLFI = \frac{\sum_{k_{\text{sect}}=k_{\text{sect,min}}}^{k_{\text{sect,max}}} MDLFI_{\text{par}}\left(k_{\text{sect}}\right)}{\left(k_{\text{sect,max}} - k_{\text{sect,min}} + 1\right)\times u} \tag{4}$$

where

$$MDLFI_{\text{par}}\left(k_{\text{sect}}\right) = \sum_{i=1}^{u} \frac{\left|\overline{\overline{\mathbf{\Gamma}}}_{\text{meas}}^{\text{WtG}}\left(f_i, k_{\text{sect}}\right) - \overline{\overline{\mathbf{\Gamma}}}_{\text{theor}}^{\text{WtG}}\left(f_i, k_{\text{sect}}\right)\right|}{\left|\overline{\overline{\mathbf{\Gamma}}}_{\text{theor}}^{\text{WtG}}\left(f_i, k_{\text{sect}}\right)\right|} \tag{5}$$

, $k_{\text{sect,min}}$ is the lower monotonic section bound, which is assumed to be equal to 1 in this paper, and $k_{\text{sect,max}}$ is the upper monotonic section bound, which is assumed to be equal to 20 in this paper. Overall, note that MDLFI describes the relative error between L1PMA approximations of the measured and theoretical data by receiving the arithmetic mean of its $\text{MDLFI}_{\text{par}}$ components. The behavior of the aforementioned percentage metric is going to be examined in Sec.IV in comparison with the magnitude of the measurement differences while a critical threshold of the MDLFI ($\text{MDLFI}_{\text{thr}}$) that is going to act as the warning limit of a main distribution line fault is also analyzed. Relative decisions regarding the dependencies of $\text{MDLFI}_{\text{thr}}$ on various parameters are also presented in Sec.IV.

4. Numerical Results and Discussion

4.1 Simulation Goals and Parameters

Various types of OV MV BPL topologies and measurement difference distributions are simulated with the purpose of evaluating the L1PMA mitigation performance against measurement differences and the accuracy of identifying a main distribution line fault when it occurs by eliminating the false alarm likelihood. Similarly to the measurement differences of OV MV BPL coupling transfer functions, the measurement differences that occur in OV MV BPL networks during the determination of reflection coefficients are typically described by continuous uniform distributions (CUDs) with range from 0 to a maximum CUD value that is equal to α_{MD}.

As regards the operation parameters of hybrid method and L1PMA, the BPL frequency range and the flat-fading subchannel frequency spacing are assumed equal to 1-30MHz and 1MHz, respectively. Therefore, the number of subchannels u in the examined frequency range is equal to 30. In accordance with [1], the WtG^3 coupling scheme is applied during the following simulations. Finally, the maximum number of monotonic sections that is going to be used is assumed to be equal to 20 [26].

As the indicative OV MV BPL topologies are concerned, their topological characteristics concerning the number of branches, the length of main distribution lines and branches as well as the fault location have already been determined in [1].

4.2 Measurement Differences and Faults in Indicative OV MV BPL Topologies

Already been presented in [1], the main distribution line faults differentiate the reflection coefficient behavior between the normal and fault operation. Hence, significant differences occur between the theoretical and measured reflection coefficients. At the same time, there are also six categories, which have been reported in Sec.III, that may create additional measurement differences between the existing coupling reflection coefficients of the normal and fault operation for given OV MV BPL topology.

For comparison reasons only, the aforementioned four measurement difference distributions are first applied to the theoretical coupling reflection coefficients. In Figs. 1(a)-(d), the magnitude of the theoretical coupling reflection coefficients are plotted versus frequency for the four indicative OV MV BPL topologies –i.e., urban, suburban, rural and "LOS" case of Sec.2.2 of [1]–, respectively, when the four indicative measurement difference CUDs are applied for a given indicative OV MV BPL topology. Note that during the normal operation the terminal load is assumed to be matched to the characteristic impedance of the modal channels.

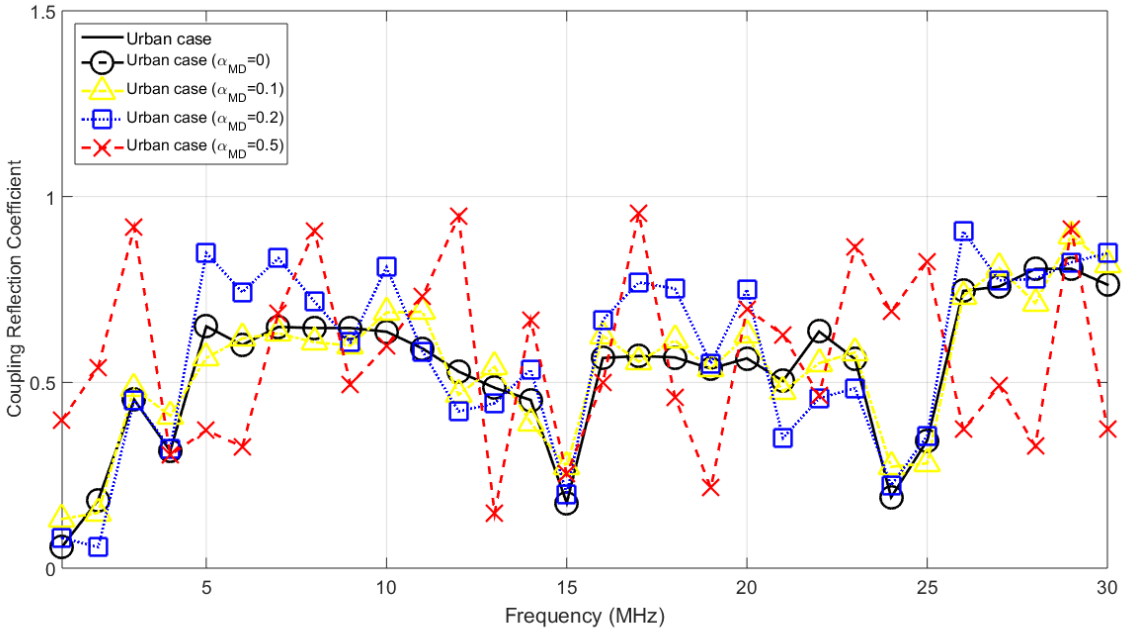
Urban case
Urban case (α_{MD}=0)
Urban case (α_{MD}=0.1)
Urban case (α_{MD}=0.2)
Urban case (α_{MD}=0.5)
Coupling Reflection Coefficient
Frequency (MHz)
0
0.5
1
1.5
5
10
15
20
25
30

(a)

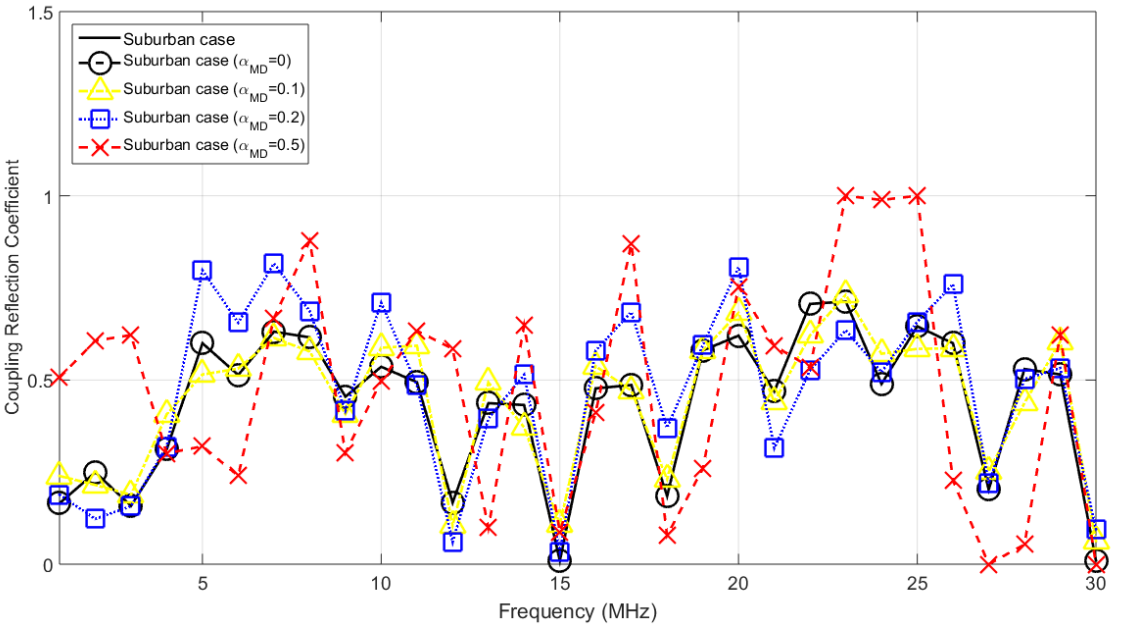
Suburban case
Suburban case (α_{MD}=0)
Suburban case (α_{MD}=0.1)
Suburban case (α_{MD}=0.2)
Suburban case (α_{MD}=0.5)
Coupling Reflection Coefficient
Frequency (MHz)
0
0.5
1
1.5
5
10
15
20
25
30

(b)

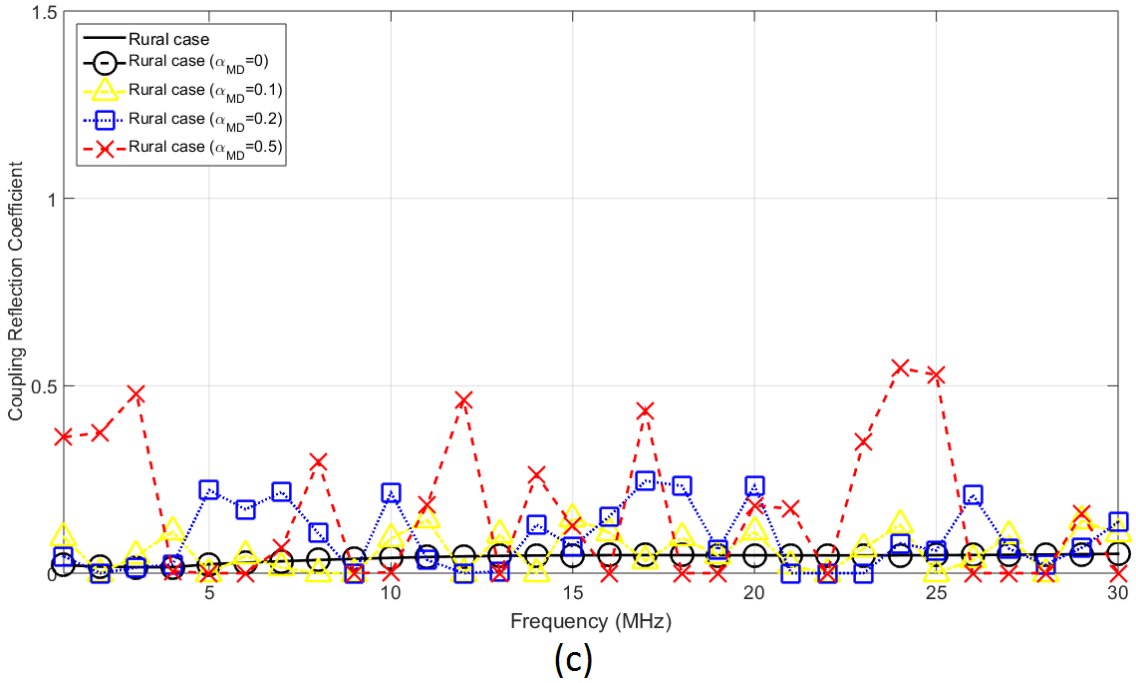

Figure 1. Magnitude of theoretical coupling reflection coefficients of OV MV BPL topologies contaminated by the four indicative measurement difference distributions (CUD/a_{MD}=0, CUD/a_{MD}=0.1, CUD/a_{MD}=0.2 and CUD/a_{MD}=0.5). (a) Urban case. (b) Suburban case. (c) Rural case. (d) "LOS" case.

The combined impact of the measurement differences and the main distribution line faults on the OV MV BPL coupling reflection coefficient is here investigated. More specifically, in Figs. 2(a)-(d), the theoretical coupling reflection coefficient is plotted versus frequency for the indicative OV MV BPL topologies, respectively –i.e., urban, suburban, rural and "LOS" case of Sec.2.2 of [1]–. In each figure,

the measured coupling reflection coefficient after the main distribution line fault at 750 m from the transmitting end is also given for the respective modified OV MV BPL topology –i.e., modified urban, suburban, rural and "LOS" case of Sec.4.3 of [1]– when measurement differences follow four indicative measurement difference distributions, namely: (i) CUD with a_{MD}=0 (no measurement differences); (ii) CUD with a_{MD}=0.1; (iii) CUD with a_{MD}=0.2; and (iv) CUD with a_{MD}=0.5. Similarly to [1], it should be noted that the magnitude of the OV MV BPL coupling reflection coefficients is demonstrated in the following figures of this paper while the terminal loads during the fault operation are assumed to be short-circuits in Figs. 2(a)-(d). In Figs. 3(a)-(d), same figures with Figs. 2(a)-(d) are shown but for the case of open-circuit terminal loads.

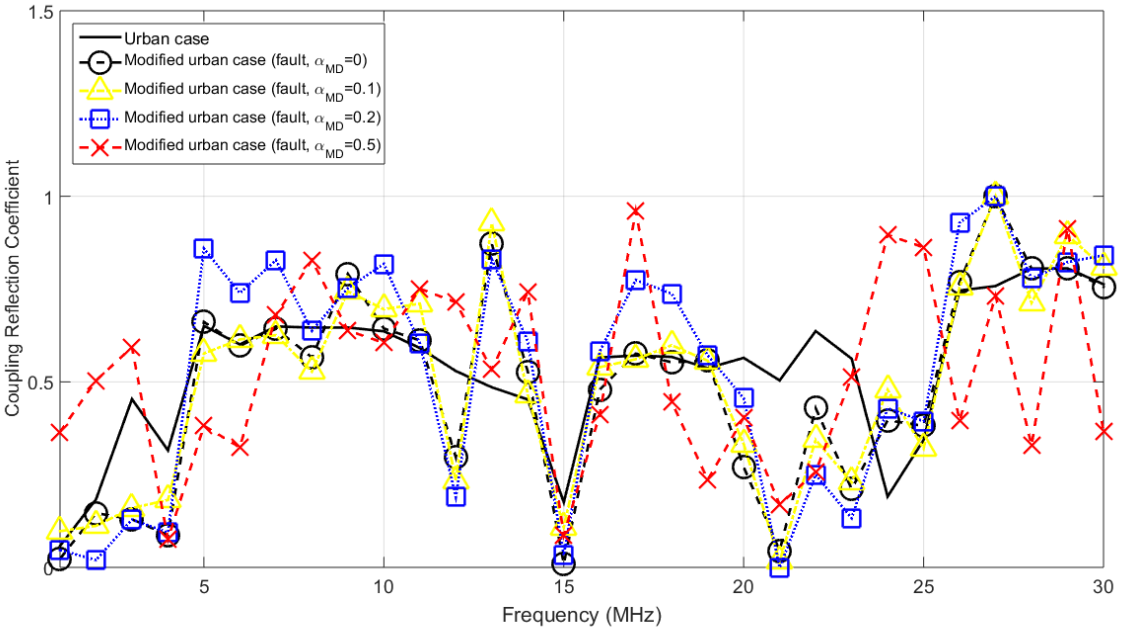
Urban case
Modified urban case (fault, α_{MD}=0)
Modified urban case (fault, α_{MD}=0.1)
Modified urban case (fault, α_{MD}=0.2)
Modified urban case (fault, α_{MD}=0.5)
Coupling Reflection Coefficient
Frequency (MHz)
0
0.5
1
1.5
5
10
15
20
25
30

(a)

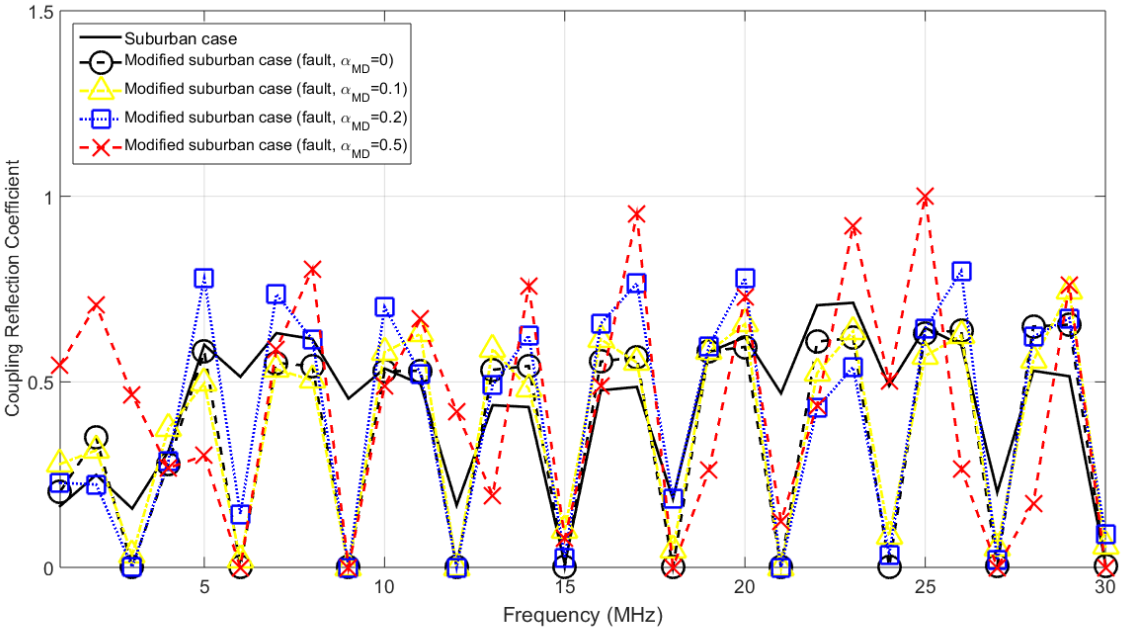
Suburban case
Modified suburban case (fault, α_{MD}=0)
Modified suburban case (fault, α_{MD}=0.1)
Modified suburban case (fault, α_{MD}=0.2)
Modified suburban case (fault, α_{MD}=0.5)
Coupling Reflection Coefficient
Frequency (MHz)
0
0.5
1
1.5
5
10
15
20
25
30

(b)

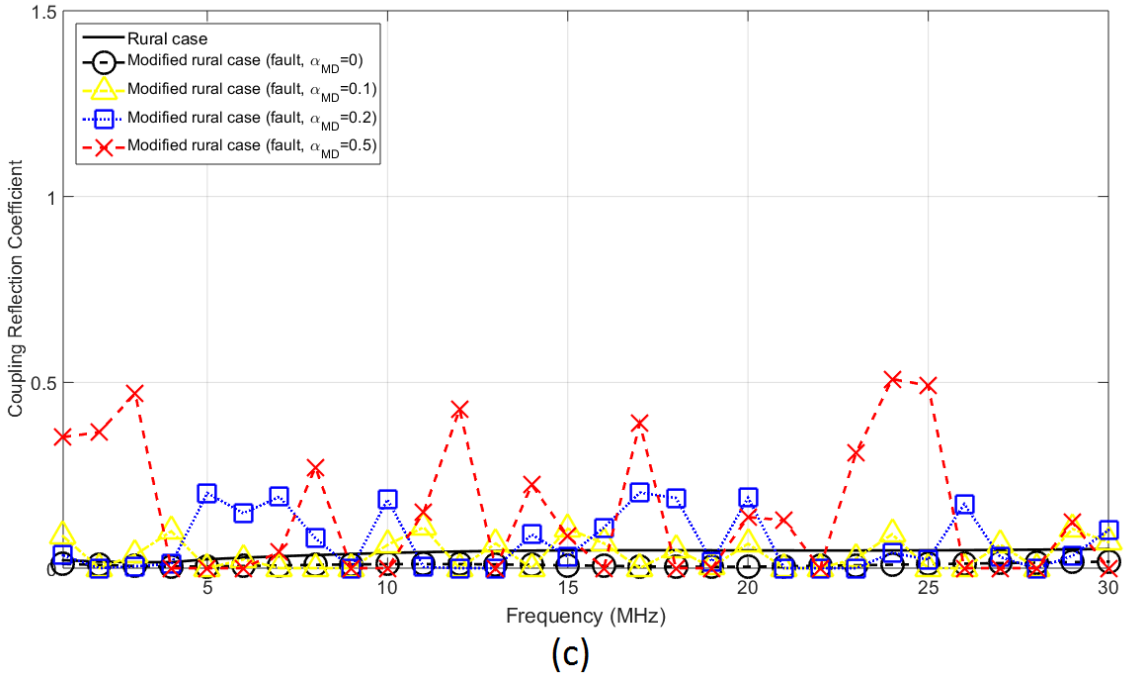

Figure 2. Theoretical and measured coupling reflection coefficients (measurement differences and main distribution line fault) of OV MV BPL topologies when four indicative measurement difference distributions (CUD/a_{MD}=0, CUD/a_{MD}=0.1, CUD/a_{MD}=0.2 and CUD/a_{MD}=0.5) are applied while the terminal load is assumed to be short-circuit. (a) Urban and modified urban case. (b) Suburban and modified suburban case. (c) Rural and modified rural case. (d) "LOS" and modified "LOS" case.

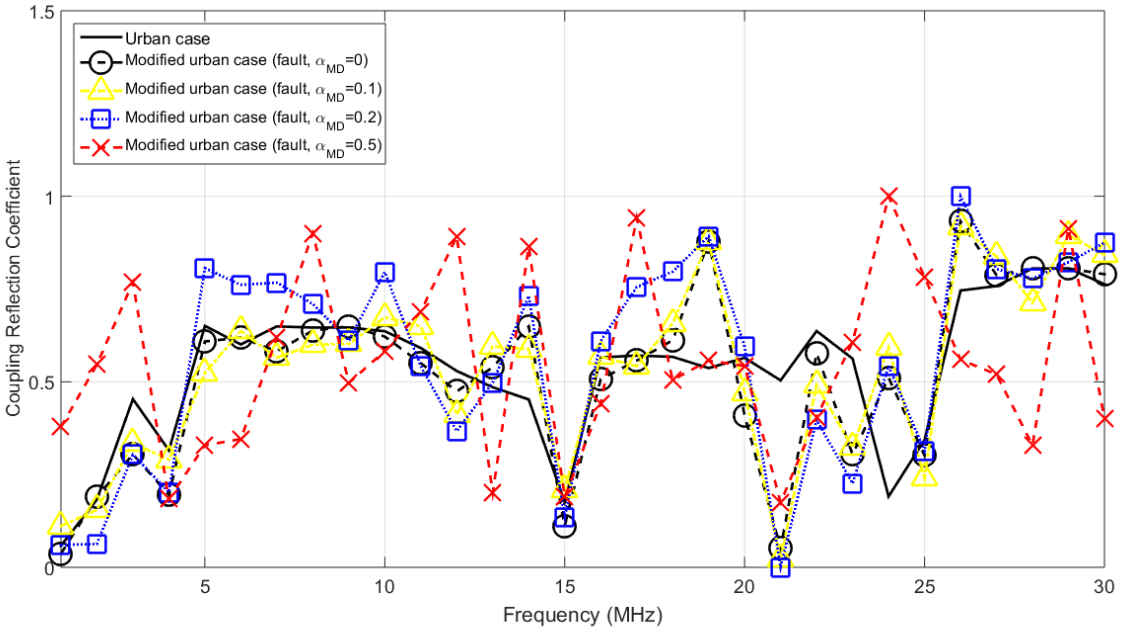
Urban case
Modified urban case (fault, α_{MD}=0)
Modified urban case (fault, α_{MD}=0.1)
Modified urban case (fault, α_{MD}=0.2)
Modified urban case (fault, α_{MD}=0.5)
Coupling Reflection Coefficient
Frequency (MHz)
0
0.5
1
1.5
5
10
15
20
25
30

(a)

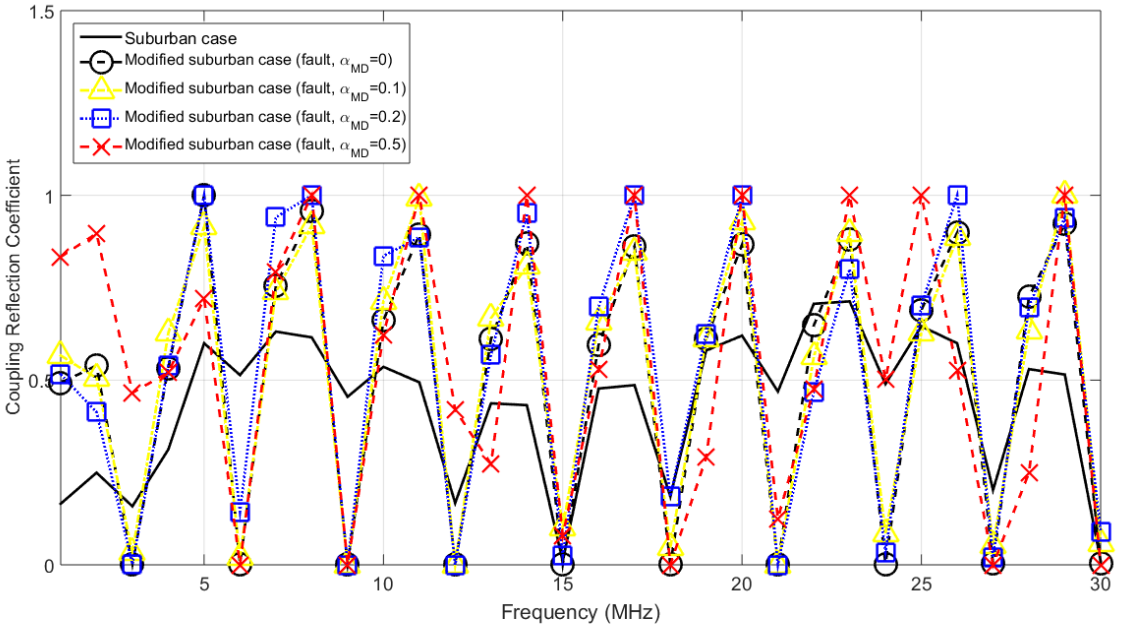
Suburban case
Modified suburban case (fault, α_{MD}=0)
Modified suburban case (fault, α_{MD}=0.1)
Modified suburban case (fault, α_{MD}=0.2)
Modified suburban case (fault, α_{MD}=0.5)
Coupling Reflection Coefficient
Frequency (MHz)
0
0.5
1
1.5
5
10
15
20
25
30

(b)

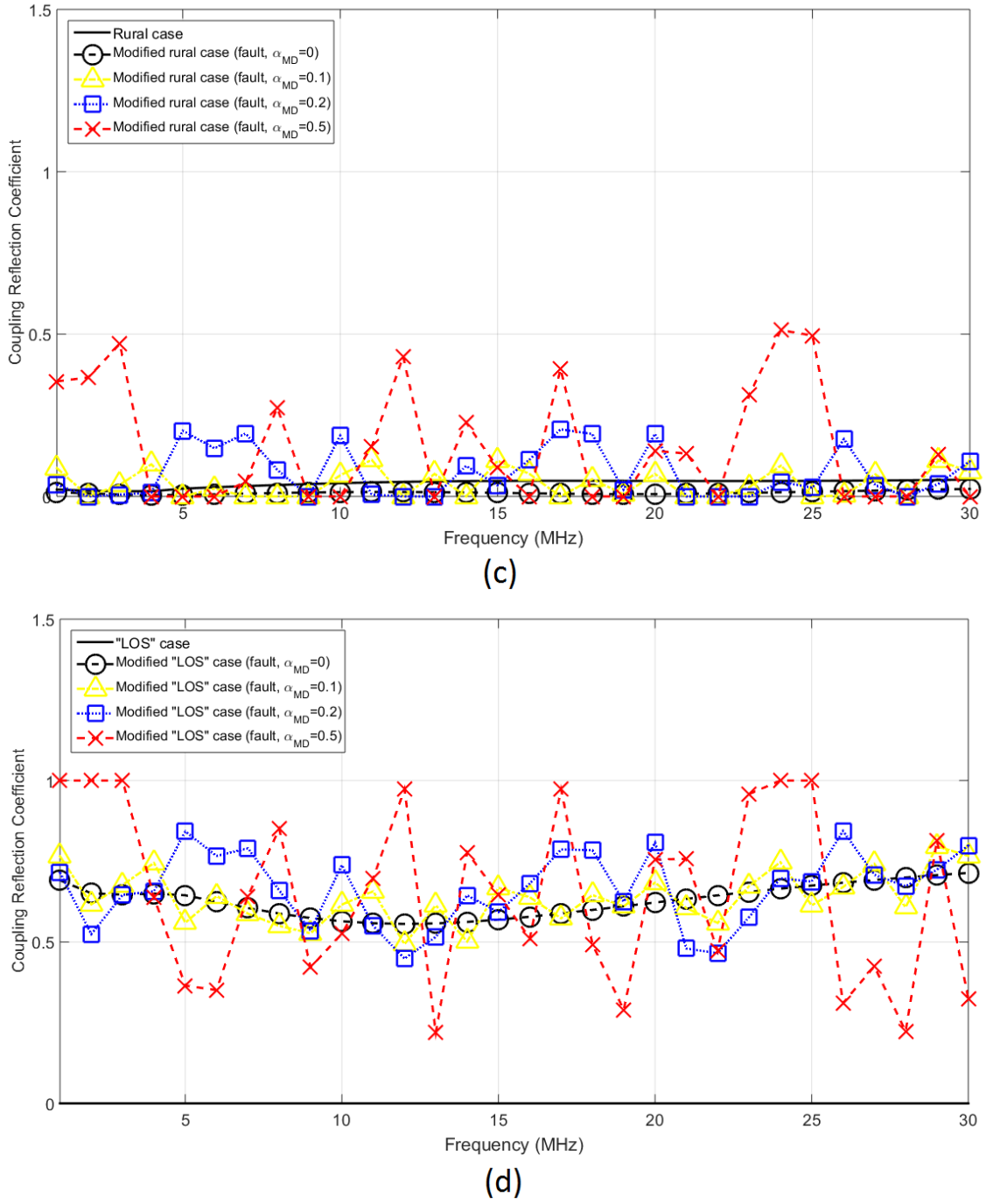

Figure 3. Same plots with Figure 2 but for open-circuit terminal loads during the fault operation.

Depending on the examined OV MV BPL topology, the notches of measurement differences incommode the identification of a main distribution line fault by creating different levels of difficulty. Observing Figs. 1(c) and 1(d), the OV MV BPL topologies of low number of branches, such as rural and "LOS" cases, are characterized by rare and shallow notches. When a main distribution line fault occurs, the coupling reflection coefficient curves of the fault operation significantly differ from the respective curves of the normal operation. The superimposed notches, which come from the measurement

differences, imply the presence of a main distribution line fault because the curves of the theoretical and measured reflection coefficients still significantly differ. Conversely, OV MV BPL topologies of high number of short branches maintain significant notches due to the multipath environment.

Already been mentioned in [1], the first sign of the presence of a main distribution line fault is the immediate communications failure between the transmitting and receiving end but it is not the only sign. From Figs. 2(a)-(d) and Figs. 3(a)-(d), it is evident that significant coupling reflection coefficient differences occur between the normal and fault operation even if measurement differences are neglected (i.e., CUD/a_{MD}=0). Regardless of the terminal load (i.e., short- or open-circuit terminations), when a main distribution line fault occurs, the superposition of the measurement differences to the reflection coefficients of the fault operation deteriorates the identification process of a main distribution line fault. In fact, as the maximum value a_{MD} of CUD increases so do the notches across the reflection coefficient curves.

Comparing Figs. 1(a) and 1(b) with Figs. 2(a), 2(b), 3(a) and 3(b), the coupling reflection coefficients of the fault operation satisfactorily differ from the ones of the normal operation when a main distribution line fault occurs. However, in the more aggravated OV MV BPL topologies, such as urban and suburban cases, the imposed notches of measurement differences are tangled with the notches of the coupling reflection coefficients. The plethora of notches creates confusion when a decision needs to be taken whether a noisy environment or main distribution line fault occurs.

4.3 L1PMA Mitigation of Measurement Differences and $MDLFI_{par}$

Already been presented in Sec. 4.2, measurement differences can create significant deviations between experimental measurements and theoretical results during the determination of OV MV BPL coupling reflection coefficients, thus, creating ambiguity, whether a main distribution line fault or noisy environment occurs. On the basis of [3], [4], piecewise monotonic data approximations, such as L1PMA, L2WPMA and L2CXCV, achieve to mitigate the additive measurement differences by simply maintaining the monotonicity pattern of each OV MV BPL coupling transfer function. Extending the previous concept, L1PMA is here applied to coupling reflection coefficients so that the mitigation of measurement differences may occur and a robust decision regarding the existence of a main distribution line fault can be supported. Actually, the mitigation performance of L1PMA mainly depends on the magnitude of measurement differences and the applied number of monotonic sections.

In accordance with [3], L1PMA identifies the primary extrema of the examined curves and, then, interpolate the data at these extrema. In the case of L1PMA, which is examined in this paper, the low number of monotonic sections blocks the high fluctuations imposed by the high magnitudes of measurement differences, thus giving a general data approximation that follows the monotonicity pattern. Conversely, when a high number of monotonic sections is adopted, L1PMA very efficiently approximate the curves by following them in the depth and the extent of spectral notches but the data approximation cannot mitigate the measurement differences in that sense. In the last case, L1PMA considers measurement differences as part of the OV MV BPL coupling reflection coefficients.

The proposed MDLFI of eq. (4) tries to overall exploit the result versatility of the application of different number of monotonic sections through $MDLFI_{par}$ of eq. (5) by

considering $k_{sect,min}$ and $k_{sect,max}$ to be equal to 1 and 20, respectively. In Fig. 4(a), $MDLFI_{par}$ is plotted versus the number of monotonic sections for the indicative theoretical OV MV BPL urban case when the four indicative measurement difference distributions of Sec.4.2 are applied. In Figs. 4(b)-(d), same curves with Fig. 4(a) are presented but for the case of the indicative OV MV BPL suburban, rural and "LOS" case, respectively.

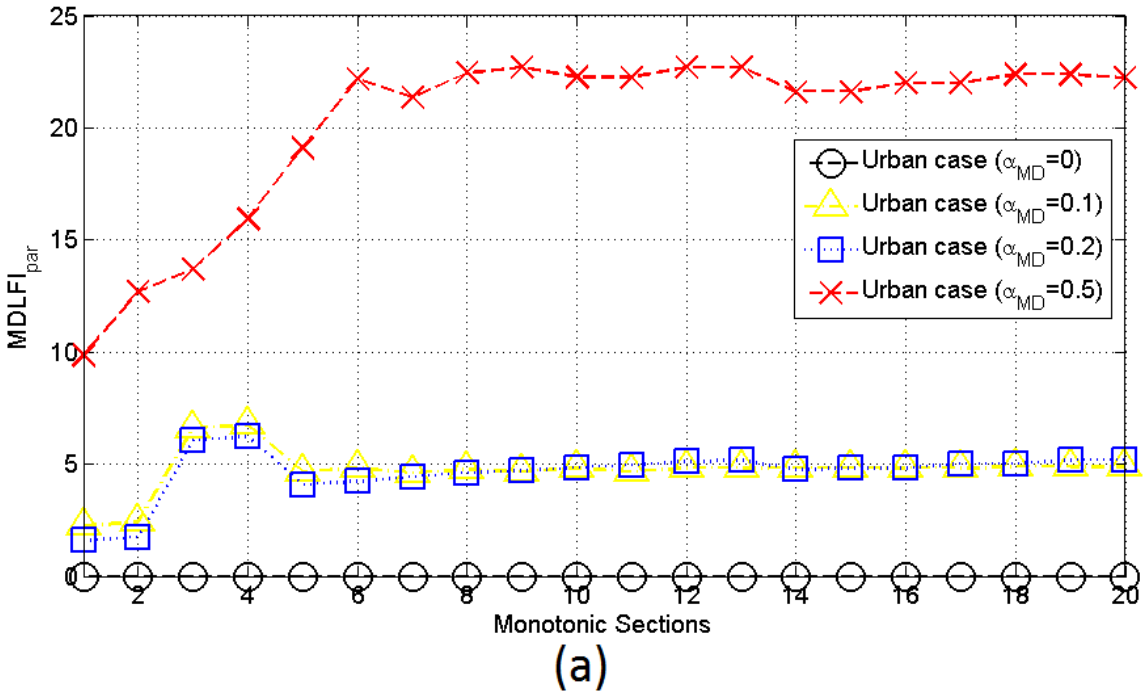

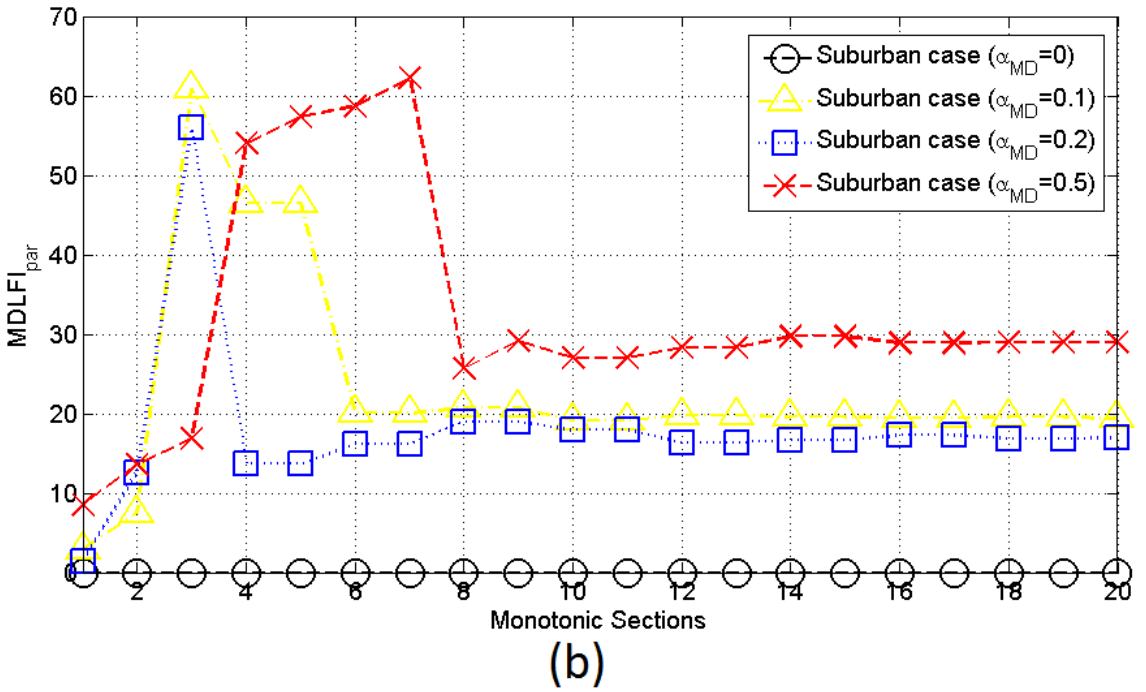

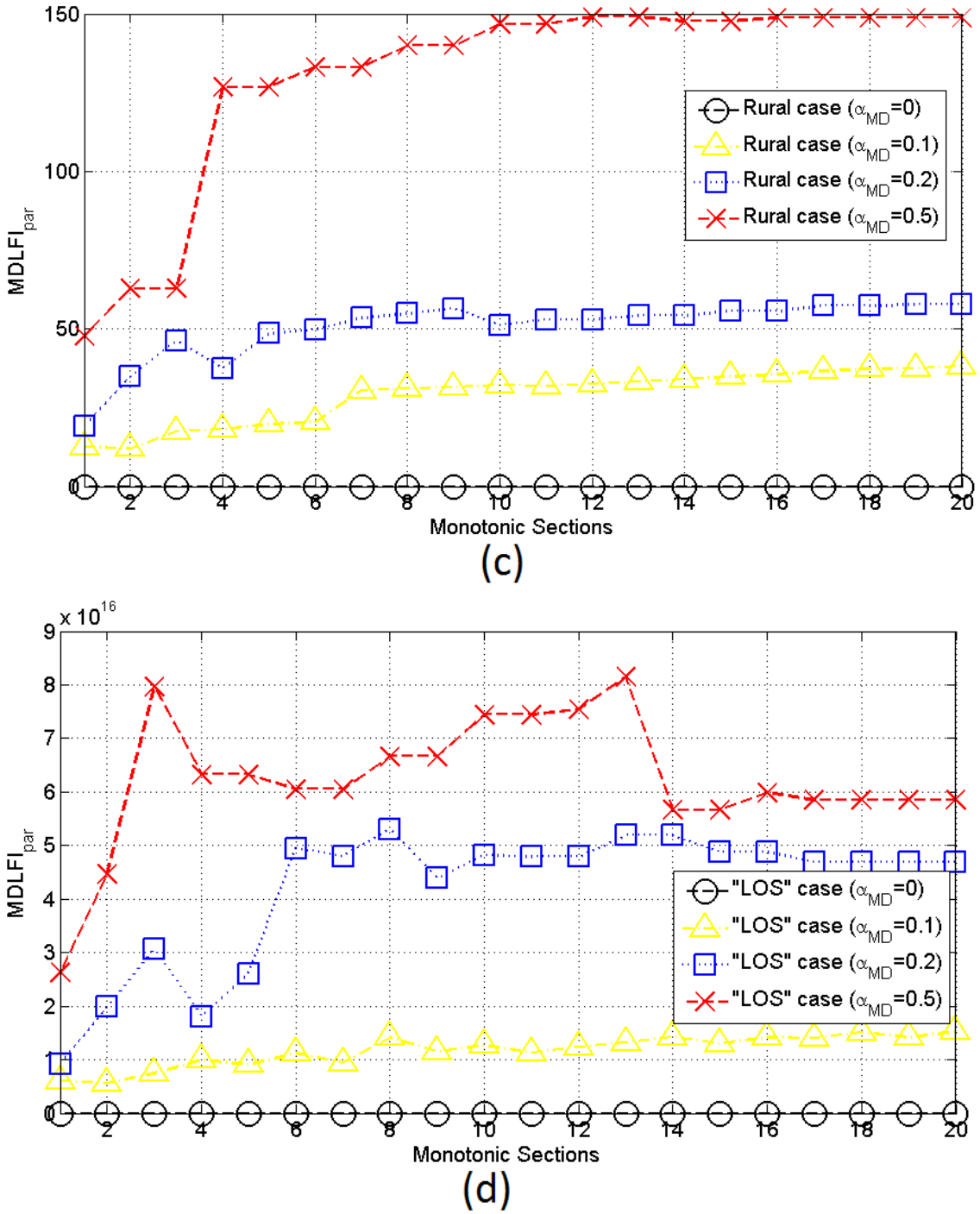

Figure 4. $MDLFI_{par}$ of OV MV BPL topologies contaminated by the four indicative measurement difference distributions ($CUD/a_{MD}=0$, $CUD/a_{MD}=0.1$, $CUD/a_{MD}=0.2$ and $CUD/a_{MD}=0.5$). (a) Urban case. (b) Suburban case. (c) Rural case. (d) "LOS" case.

From Figs. 4(a)-(d), it is obvious that $MDLFI_{par}$ uniquely characterizes an OV MV BPL topology however its curve depends on the severity of the imposed measurement differences and the examined OV MV BPL topology. For given OV MV BPL topology, the theoretical coupling reflection coefficient is already known and, thus, $MDLFI_{par}$ is equal to zero when measurement differences are neglected. As the

magnitude a_{MD} of measurement difference CUD increases, $MDLFI_{par}$ differentiates from zero presenting increased values.

The combined impact of measurement differences and main distribution line faults on the OV MV BPL coupling reflection coefficient is also investigated through $MDLFI_{par}$. More specifically, in Figs. 5(a)-(d), $MDLFI_{par}$ is plotted versus the number of monotonic sections for the indicative OV MV BPL topologies, respectively –i.e., urban, suburban, rural and "LOS" case of Sec.4.2–. In each figure, $MDLFI_{par}$ after the main distribution line fault at 750m from the transmitting end is given for the respective modified OV MV BPL topology when measurement differences follow four indicative measurement difference distributions, namely: (i) CUD with a_{MD}=0 (no measurement differences); (ii) CUD with a_{MD}=0.1; (iii) CUD with a_{MD}=0.2; and (iv) CUD with a_{MD}=0.5. In Figs. 5(a)-(d), the terminal loads during the fault operation are assumed to be short-circuits. In Figs. 6(a)-(d), same figures with Figs. 5(a)-(d) are shown but for the case of open-circuit terminal loads.

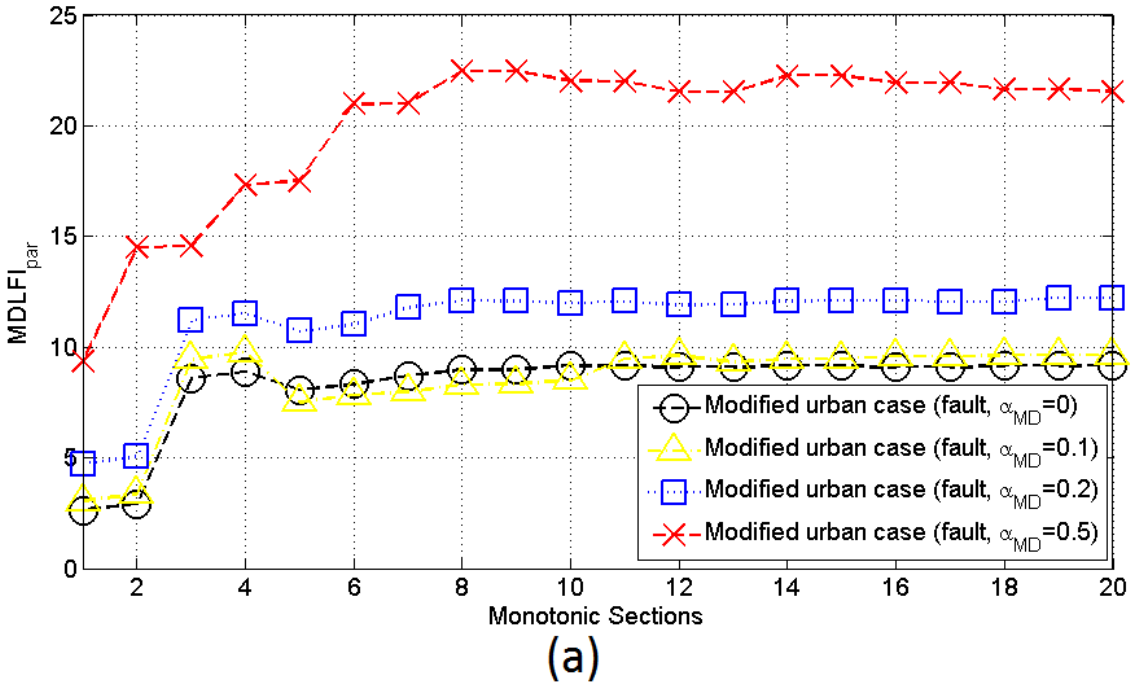
MDLFI_par
Monotonic Sections
Modified urban case (fault, α_MD=0)
Modified urban case (fault, α_MD=0.1)
Modified urban case (fault, α_MD=0.2)
Modified urban case (fault, α_MD=0.5)

(a)

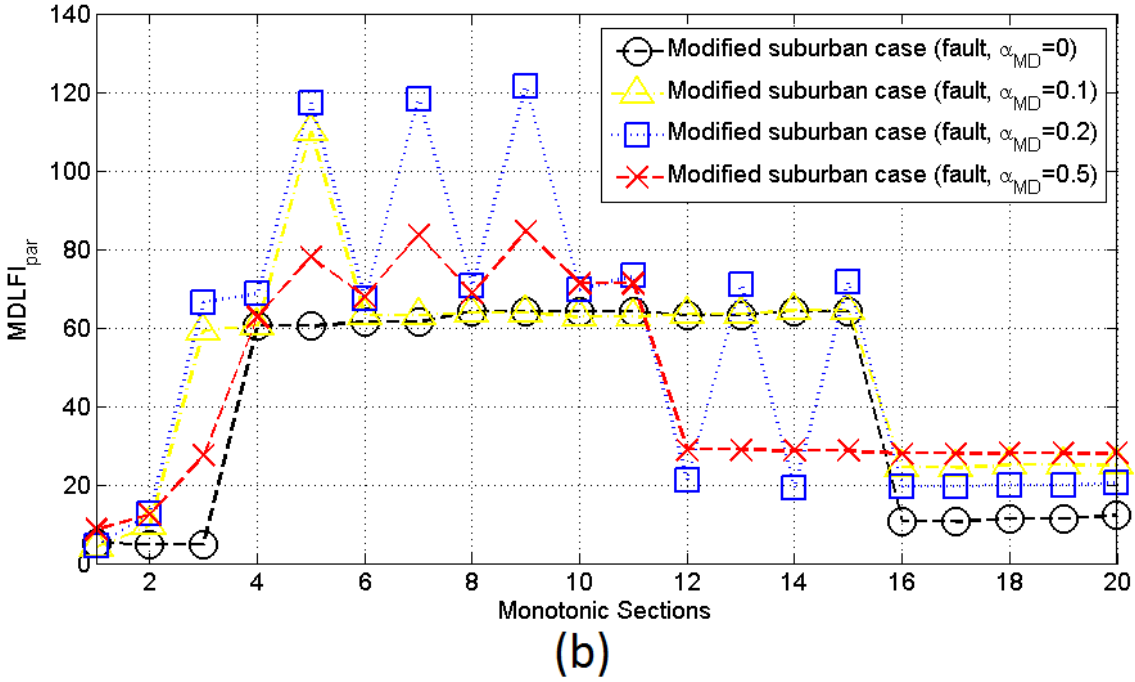
MDLFI_par
Monotonic Sections
Modified suburban case (fault, α_MD=0)
Modified suburban case (fault, α_MD=0.1)
Modified suburban case (fault, α_MD=0.2)
Modified suburban case (fault, α_MD=0.5)

(b)

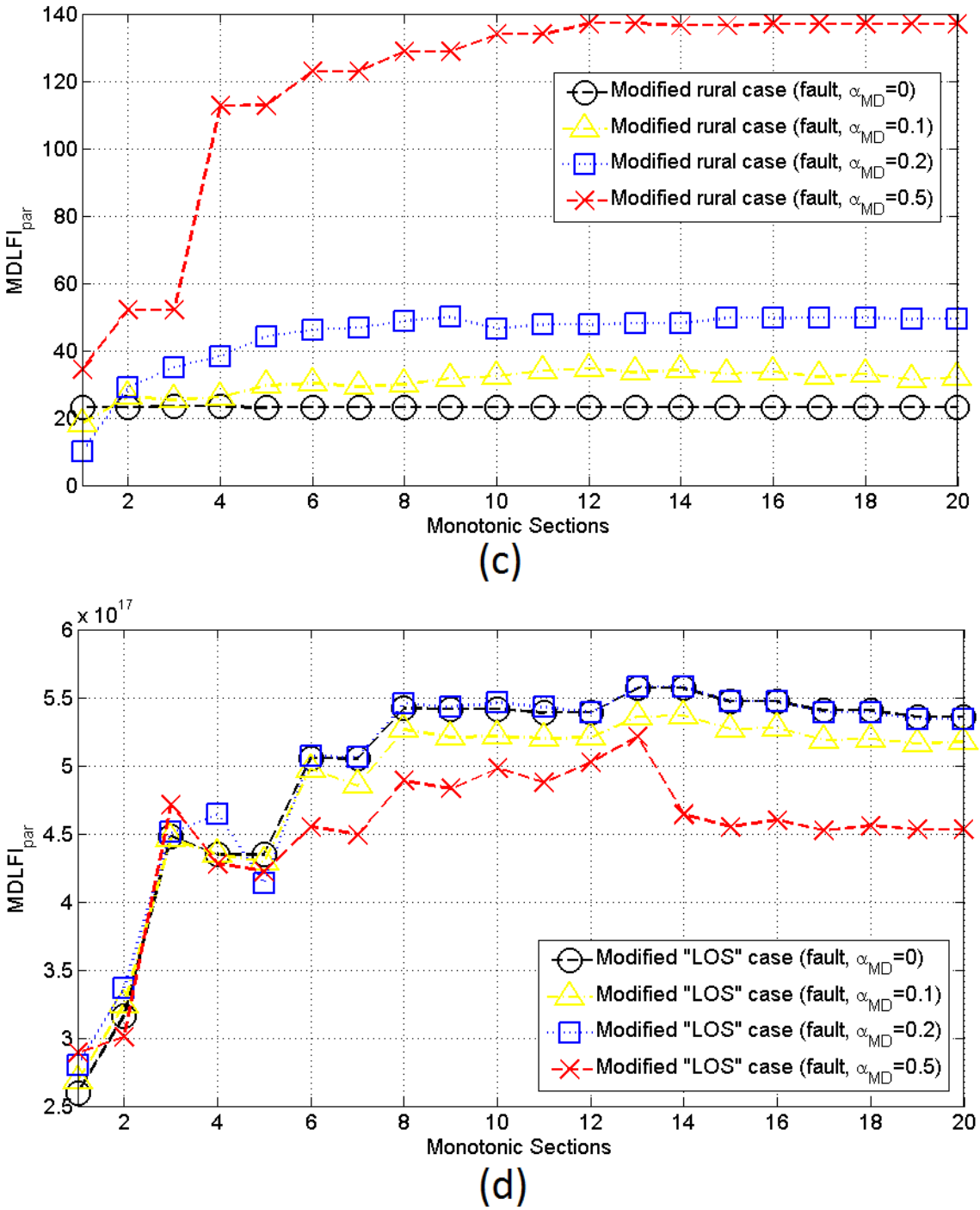

Figure 5. $MDLFI_{par}$ of modified OV MV BPL topologies with short-circuit terminal loads contaminated by the four indicative measurement difference distributions (CUD/a_{MD}=0, CUD/a_{MD}=0.1, CUD/a_{MD}=0.2 and CUD/a_{MD}=0.5). (a) Modified urban case. (b) Modified suburban case. (c) Modified rural case. (d) Modified "LOS" case.

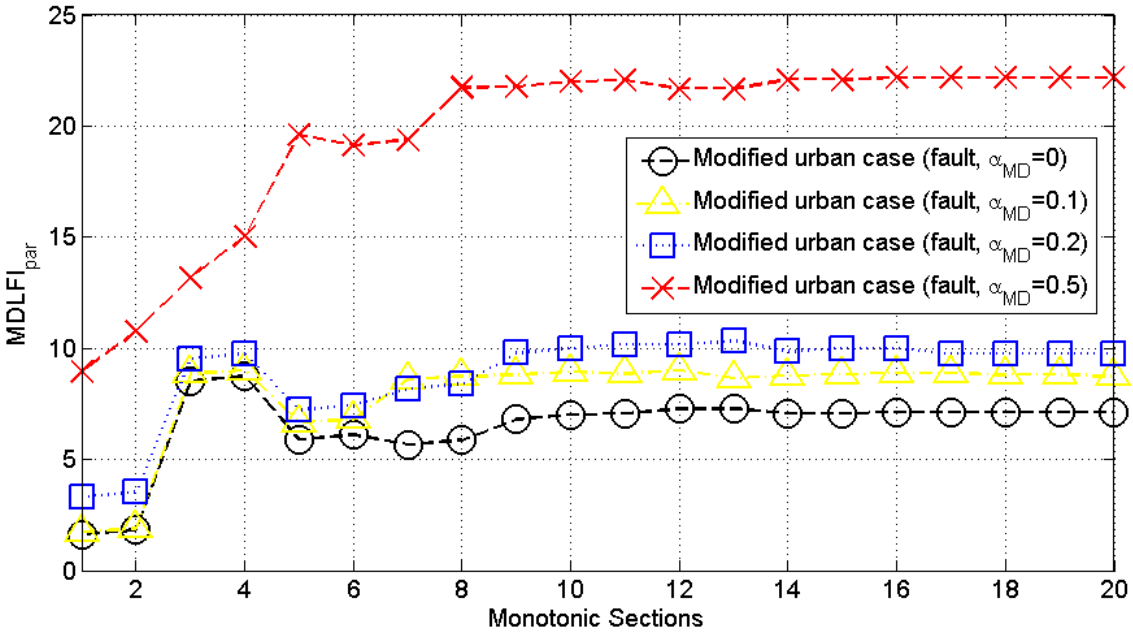
MDLFI_par
Monotonic Sections
Modified urban case (fault, α_MD=0)
Modified urban case (fault, α_MD=0.1)
Modified urban case (fault, α_MD=0.2)
Modified urban case (fault, α_MD=0.5)

(a)

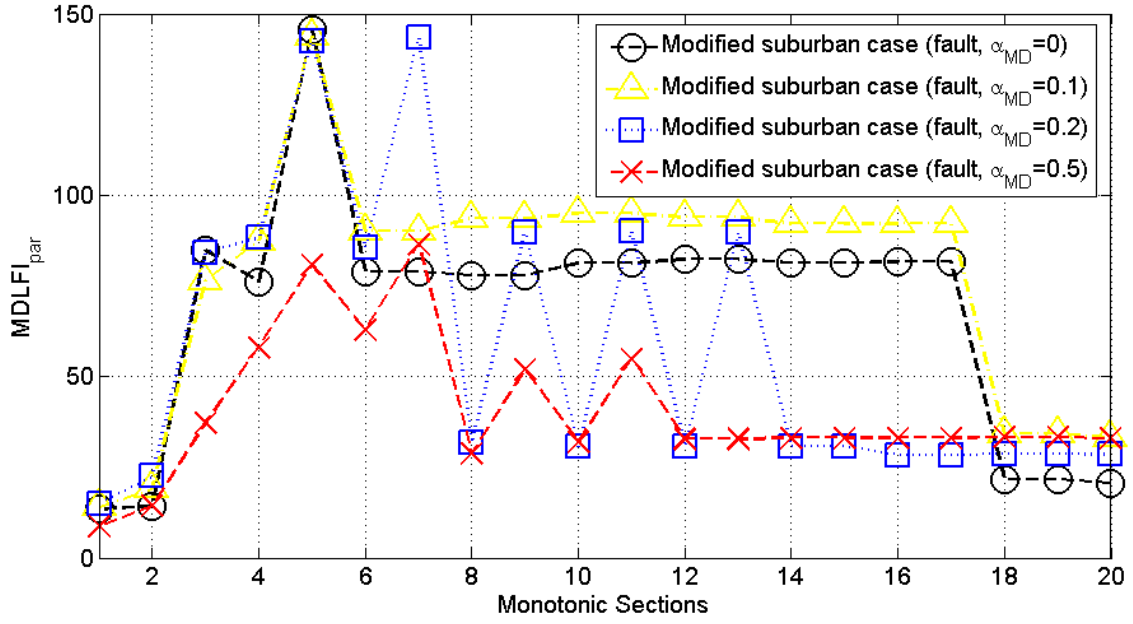
MDLFI_par
Monotonic Sections
Modified suburban case (fault, α_MD=0)
Modified suburban case (fault, α_MD=0.1)
Modified suburban case (fault, α_MD=0.2)
Modified suburban case (fault, α_MD=0.5)

(b)

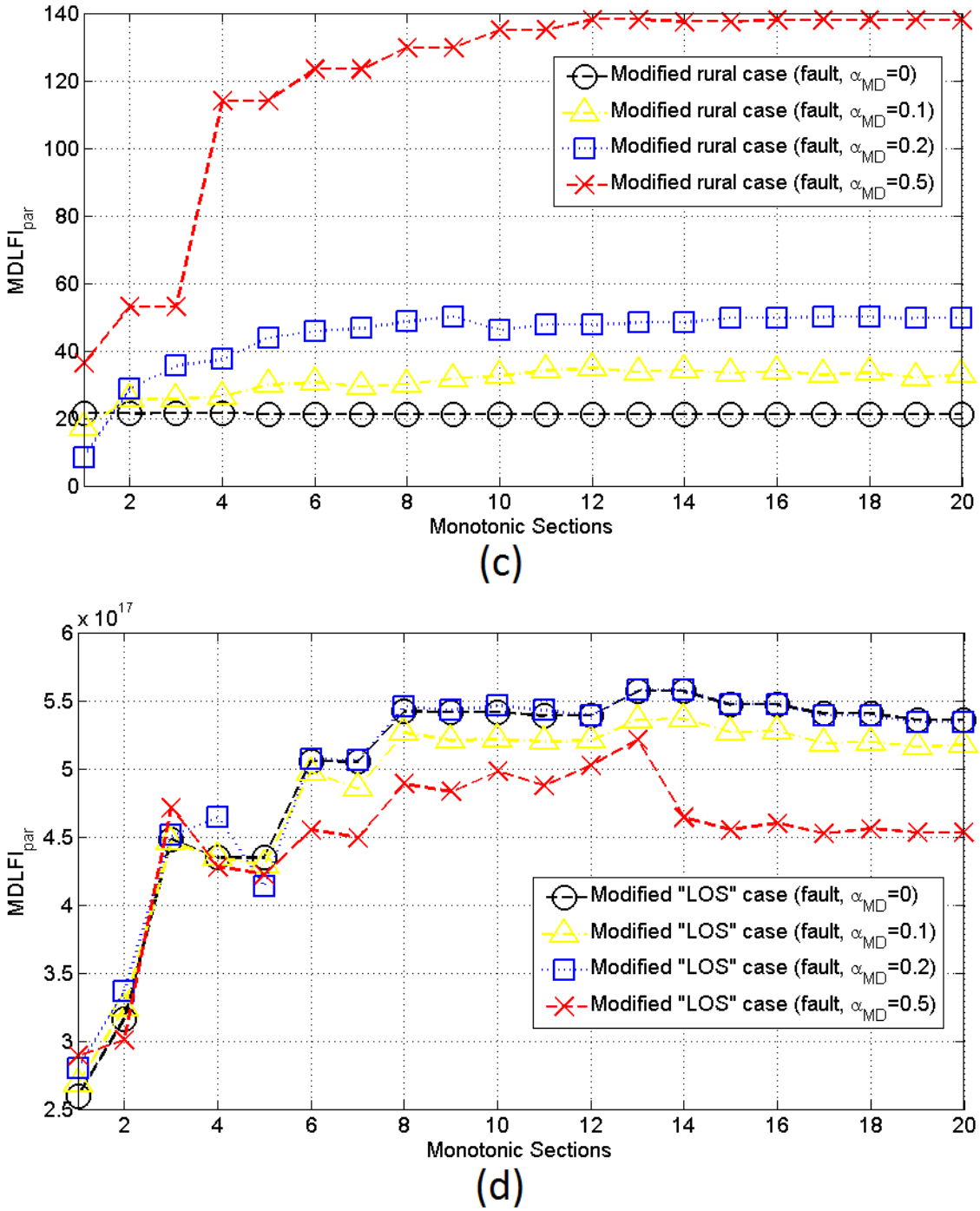

Figure 6. Same plots with Figure 5 but for open-circuit terminal loads during the fault operation.

To facilitate the comparison between Figs 4(a)-(d) with the respective Figs. 5(a)-(d), $\Delta MDLFI_{par}$ that describes the difference between the $MDLFI_{par}$ of modified OV MV BPL topologies and of respective original OV MV BPL topologies is plotted versus the number of monotonic sections in Figs. 7(a)-(d) when short-circuit terminal loads are assumed. In Figs. 8(a)-(d), same curves with Figs. 7(a)-(d) are

presented but for the case of open-circuit terminal loads; say, the graphical comparison of Figs. 4(a)-(d) with the respective Figs. 6(a)-(d).

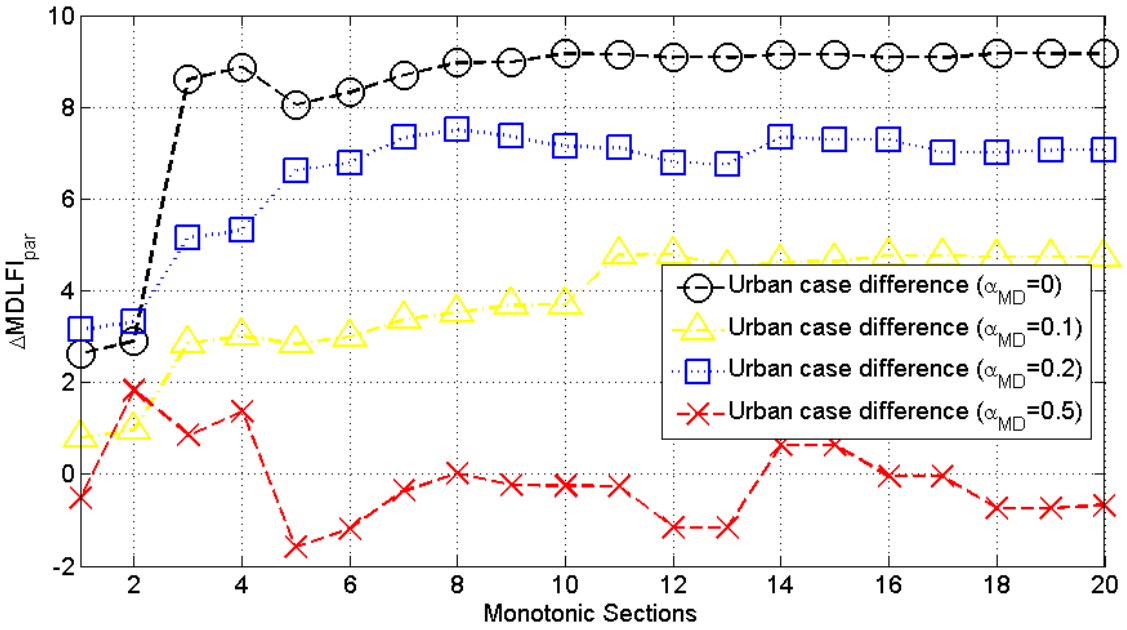

(a)

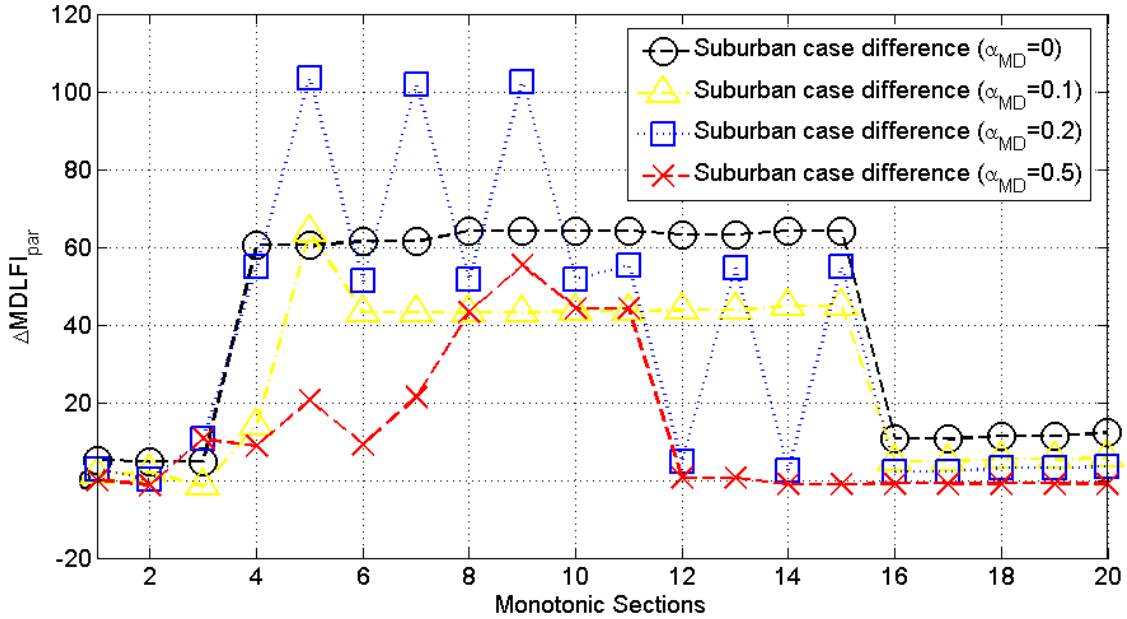

(b)

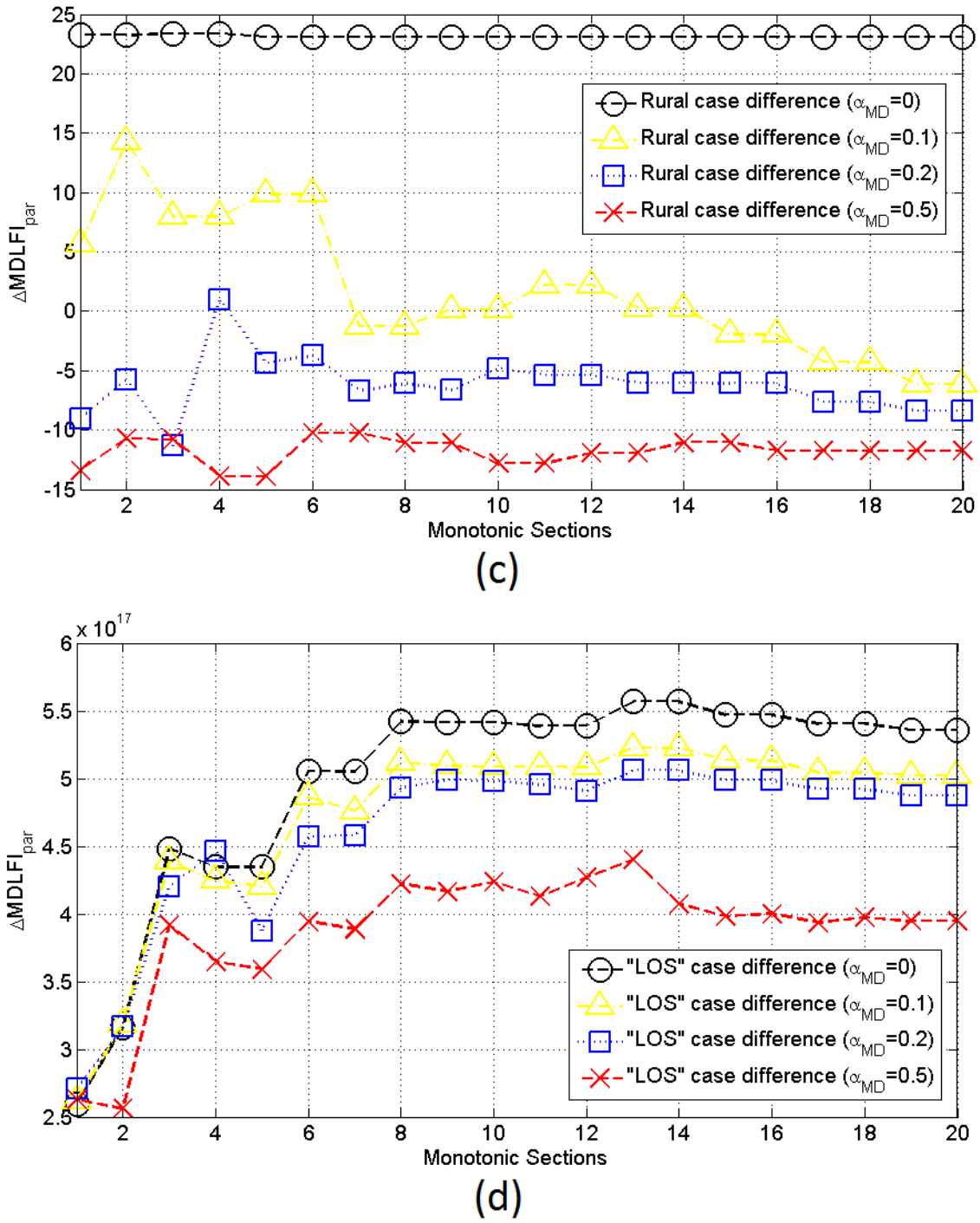

Figure 7. $\Delta MDLFI_{par}$ between modified OV MV BPL topologies with short-circuit terminal loads and original OV MV BPL topologies when the four indicative measurement difference distributions are applied (CUD/a_{MD}=0, CUD/a_{MD}=0.1, CUD/a_{MD}=0.2 and CUD/a_{MD}=0.5). (a) Urban case difference. (b) Suburban case difference. (c) Rural case difference. (d) "LOS" case difference.

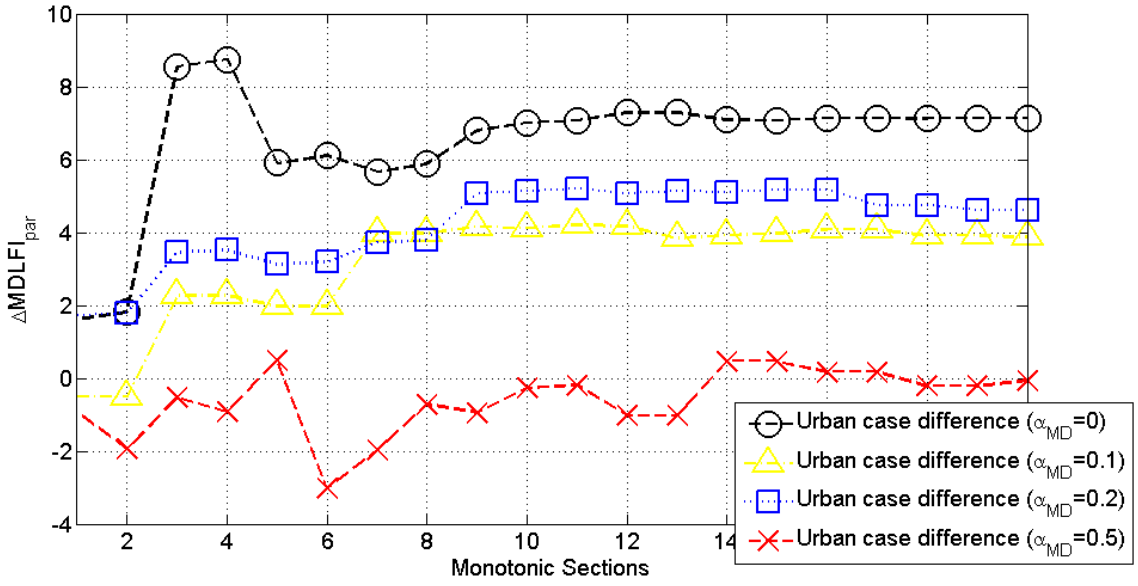
ΔMDLFI_par
Monotonic Sections
Urban case difference (α_MD=0)
Urban case difference (α_MD=0.1)
Urban case difference (α_MD=0.2)
Urban case difference (α_MD=0.5)

(a)

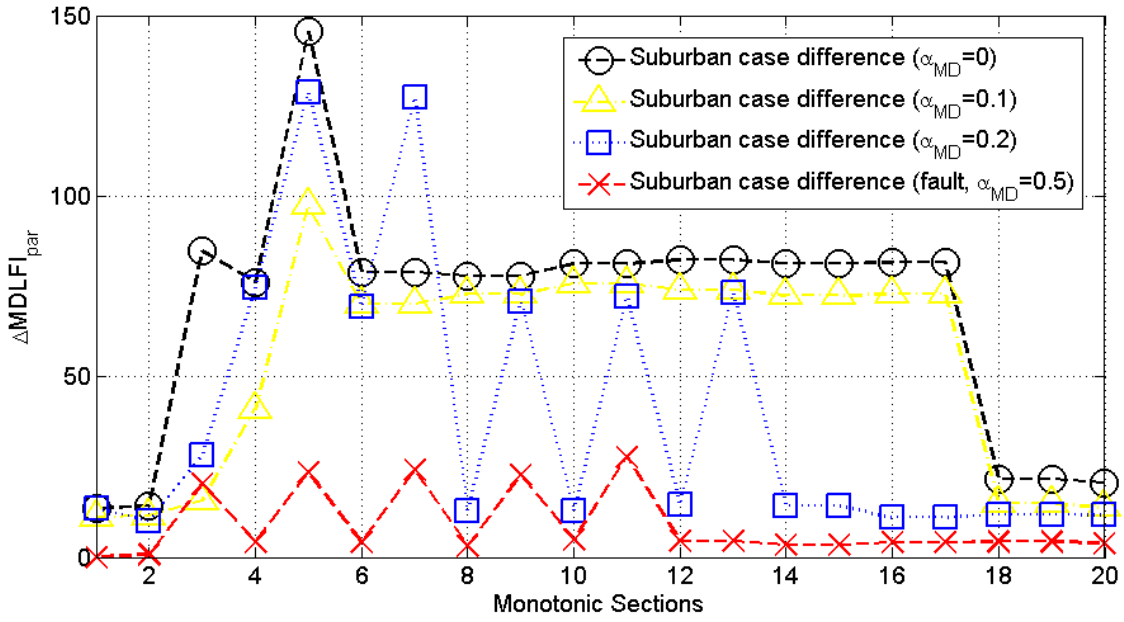
ΔMDLFI_par
Monotonic Sections
Suburban case difference (α_MD=0)
Suburban case difference (α_MD=0.1)
Suburban case difference (α_MD=0.2)
Suburban case difference (fault, α_MD=0.5)

(b)

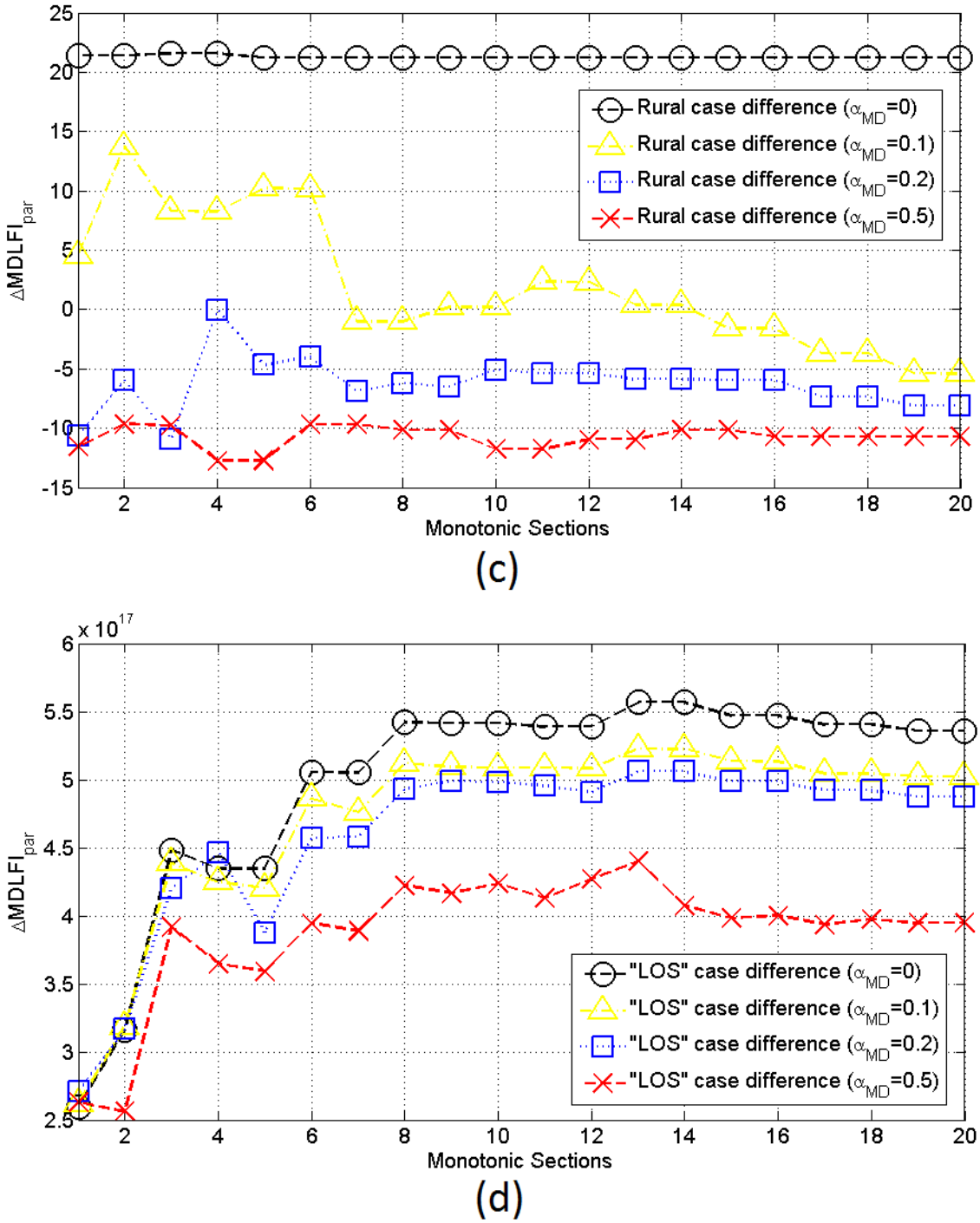

Figure 8. Same plots with Figure 7 but for open-circuit terminal loads during the fault operation.

Comparing Figs. 4(a)-(d), 5(a)-(d), 6(a)-(d), 7(a)-(d) and 8(a)-(d), it is obvious that $MDLFI_{par}$ differences occur between the original and modified OV MV BPL topologies. Although the direct comparison among curves is a difficult task, it is clear that $\Delta MDLFI_{par}$ implies the existence of a main distribution line fault when the magnitude a_{MD} of measurement differences is assumed to be equal to zero or remain low (e.g., below 0.1). When the magnitude a_{MD} increases above 0.2 the identification of main

distribution line faults become a precarious venture because it is not clear if the coupling reflection coefficient differences derive from either the modified OV MV BPL topology or the measurement differences. In order to bypass the examination of $MDLFI_{par}$ curves among different OV MV BPL topology cases and quantify the identification problem of main distribution line faults, MDLFI is further calculated in the following subsection. Actually, MDLFI is a derivative performance metric since it is based on $MDLFI_{par}$ of this subsection. Since MDLFI is, in essence, a performance metric similar to the relative error –see eq. (4)–, MDLFI can be straightforward compared to the magnitude a_{MD} of measurement difference distribution.

4.4 MDLFI, MDLFI Thresholds and Decisions Concerning Main Distribution Line Faults in OV MV BPL Topologies

The decision of the existence of a main distribution line fault remains precarious if intense measurement differences should be counteracted during the determination of OV MV BPL coupling reflection coefficients. However, MDLFI that expresses a deviation percentage between the measured and theoretical OV MV BPL coupling reflection coefficients can provide a benchmark result, which further can be compared to the magnitude a_{MD} of the measurement differences taking into account the examined OV MV BPL topology. In this way, MDLFI can support a decision concerning the existence of main distribution line faults. It should be reminded that the original OV MV BPL topologies consist of the four indicative 1000m average path length OV MV BPL topologies whereas modified OV MV BPL topologies, which have been examined until now, comprise the respective original OV MV BPL topologies but for a main distribution line fault that occurs at 750m from the transmitting end by simultaneously implying terminal loads that behave either as short- or open-circuit terminations.

In order to examine the impact of the measurement differences on MDLFI and on relative decisions concerning the existence of faults across the main distribution lines of the examined topologies, MDLFI of the original and modified OV MV BPL topologies of Sec.4.2 is reported in Table 1. MDLFI of Table 1 is investigated when different magnitudes a_{MD} of CUD measurement differences and terminal loads are assumed. Note that the terminal loads of the original OV MV BPL topologies are assumed to be matched to the supported modal characteristic impedances whereas modified OV MV BPL topologies are examined when short- and open-circuit terminations are applied.

By observing the values of Table 1, some interesting remarks can be pointed out, namely:

- From all the columns of MDLFI concerning both original and modified OV MV BPL topologies, it is clear that as the magnitude a_{MD} of CUD measurement differences increases so does MDLFI for given topology, in general.
- Since MDLFI of the original OV MV BPL topologies describes the dissimilarity between the respective theoretical and measured coupling reflection coefficients of original topologies, it is expected that even if small measurement differences get appeared, the coupling reflection coefficient differences of the OV MV BPL topologies with shallow and rare notches (i.e., rural and “LOS” cases) are going to be significantly differentiated. The latter is reflected to high values of MDLFI.

TABLE 1
MDLFI of the Original and Modified OV MV BPL Topologies for Different Magnitudes of Measurement Differences

Magnitude a_{MD} of CUD Measurement Differences	MDLFI											
	Original OV MV BPL Topologies (matched terminal loads)				Modified OV MV BPL Topologies (short-circuit terminal loads)				Modified OV MV BPL Topologies (open-circuit terminal loads)			
	Urban	Suburban	Rural	"LOS"	Urban	Suburban	Rural	"LOS"	Urban	Suburban	Rural	"LOS"
0	0	0	0	0	0.28	1.38	0.77	1.7×10^{16}	0.22	2.28	0.71	1.7×10^{16}
0.1	0.16	0.77	0.96	3.9×10^{14}	0.28	1.67	1.02	1.6×10^{16}	0.26	2.59	1.03	1.6×10^{16}
0.2	0.15	0.59	1.68	1.4×10^{15}	0.37	1.79	1.47	1.7×10^{16}	0.29	1.91	1.47	1.7×10^{16}
0.5	0.67	1.07	4.34	2.1×10^{15}	0.67	1.49	3.95	1.5×10^{16}	0.65	1.35	3.98	1.5×10^{16}

- When a high number of deep spectral notches already occurs in coupling reflection coefficient curves (i.e., curves of original urban and suburban OV MV BPL topologies), the impact of measurement differences on MDLFI is less important in comparison with that of original rural and "LOS" OV MV BPL topologies. Since the spectral notch origin remains unclear, MDLFI values stay low. Therefore, ΔMDLFI between the respective values of original and modified OV MV BPL topologies also remains low implying that harder decision regarding the existence of main distribution line faults could be supported.
- Since the BPL networks are deployed across transmission and distribution networks, theoretical OV MV BPL coupling reflection coefficients and real-time measurements concerning the coupling reflection coefficients can be continuously available. Since theoretical OV MV BPL coupling reflection coefficients are already known for given OV MV BPL topology, an estimation of the magnitude a_{MD} of CUD measurement differences can be achieved by comparing MDLFI of the measured coupling reflection coefficients with the respective theoretical MDLFI values exposed to measurement differences of different magnitudes.

- Real-time measurements of coupling reflection coefficients and an estimation of the magnitude a_{MD} of CUD measurement differences can be easily saved in a database (see MLFLM database of [35]). Since frequent measurements are available and can be retreated right before the main distribution line fault, an estimation of the magnitude a_{MD} of CUD measurement differences can be available at the moment of the appearance of a main distribution line fault. Since measurement differences are not directly affected by the existence of a main distribution line fault, the magnitude a_{MD} of CUD measurement differences that is used during the MDLFI determination can be considered as already known.
- In general terms, the values of the column of MDLFI concerning original OV MV BPL topologies (see grey column of Table 1) can act as the MDLFI threshold for given magnitude a_{MD} of CUD measurement differences and OV MV BPL topology. By observing Table 1, if the grey column values are assumed to be the benchmark metric $MDLFI_{thr}$, the identification of a main distribution line fault is achieved in 26 of 32 cases, say in 81.25%.

To validate the previous findings about the identification of a main distribution line fault through MDLFI, all the possible main distribution line faults that can occur across a given original OV MV BPL topology should be examined for different magnitude a_{MD} of CUD measurement differences. If the previous assertion is valid, MDLFI of the examined OV MV BPL topologies with main distribution line faults should always remain higher than $MDLFI_{thr}$ for given original OV MV BPL topology and magnitude a_{MD} of CUD measurement differences.

Let assume that the identification of a main distribution line fault across the original OV MV BPL urban case is examined. First, the set of all the possible locations of a main distribution line fault should be taken into account when the terminal load is assumed to be either short- or open-circuit termination. In order to create an extended set of possible fault OV MV BPL topologies, the distance of the main distribution line fault from the transmitting end is assumed to be multiples of 50m in this subsection. On the basis of the original OV MV BPL topology, in Fig. 9(a), MDLFI of each possible fault OV MV BPL topology is plotted versus the main distribution line fault distance from the transmitting end when the terminal load is assumed to be short-circuit. MDLFI is computed for the four indicative magnitude a_{MD} of CUD measurement differences that have already been applied in Secs. 4.2 and 4.3. Also, in accordance with the grey column of Table 1, for each magnitude a_{MD} of CUD measurement differences, the respective $MDLFI_{thr}$ is also plotted in Fig. 9(a). Same curves with Fig. 9(a) are given in Fig. 9(b) but for the case of the fault OV MV BPL urban topology with open-circuit termination. In Figs. 10(a) and 10(b), same plots are presented with Figs. 9(a) and 9(b) but for the case of the fault OV MV BPL rural topology.

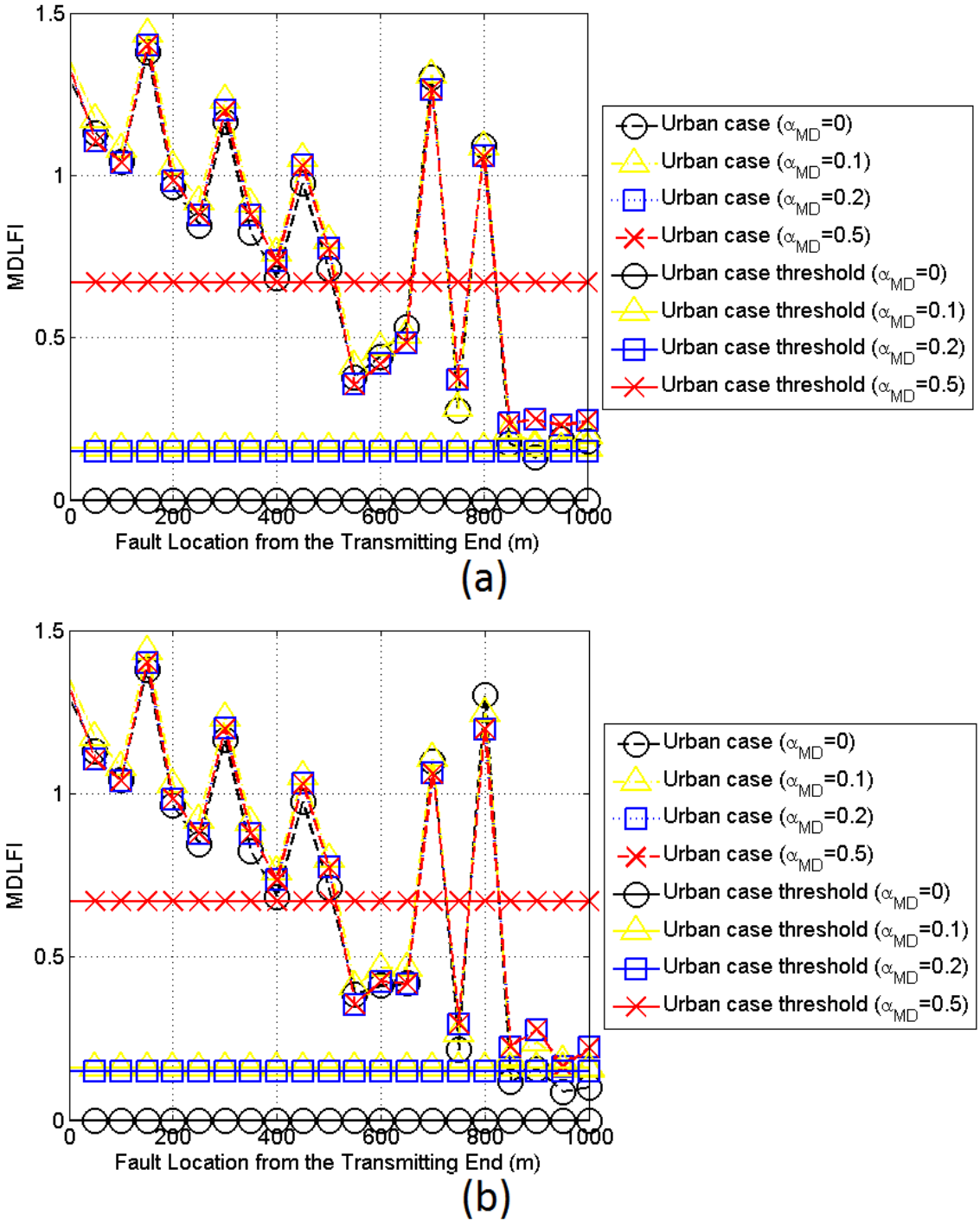

Figure 9. MDLFI of modified OV MV BPL topologies with short-circuit terminal loads and original OV MV BPL topologies when the four indicative measurement difference distributions are applied (CUD/a_{MD}=0, CUD/a_{MD}=0.1, CUD/a_{MD}=0.2 and CUD/a_{MD}=0.5). (a) Urban case difference. (b) Suburban case difference. (c) Rural case difference. (d) "LOS" case difference.

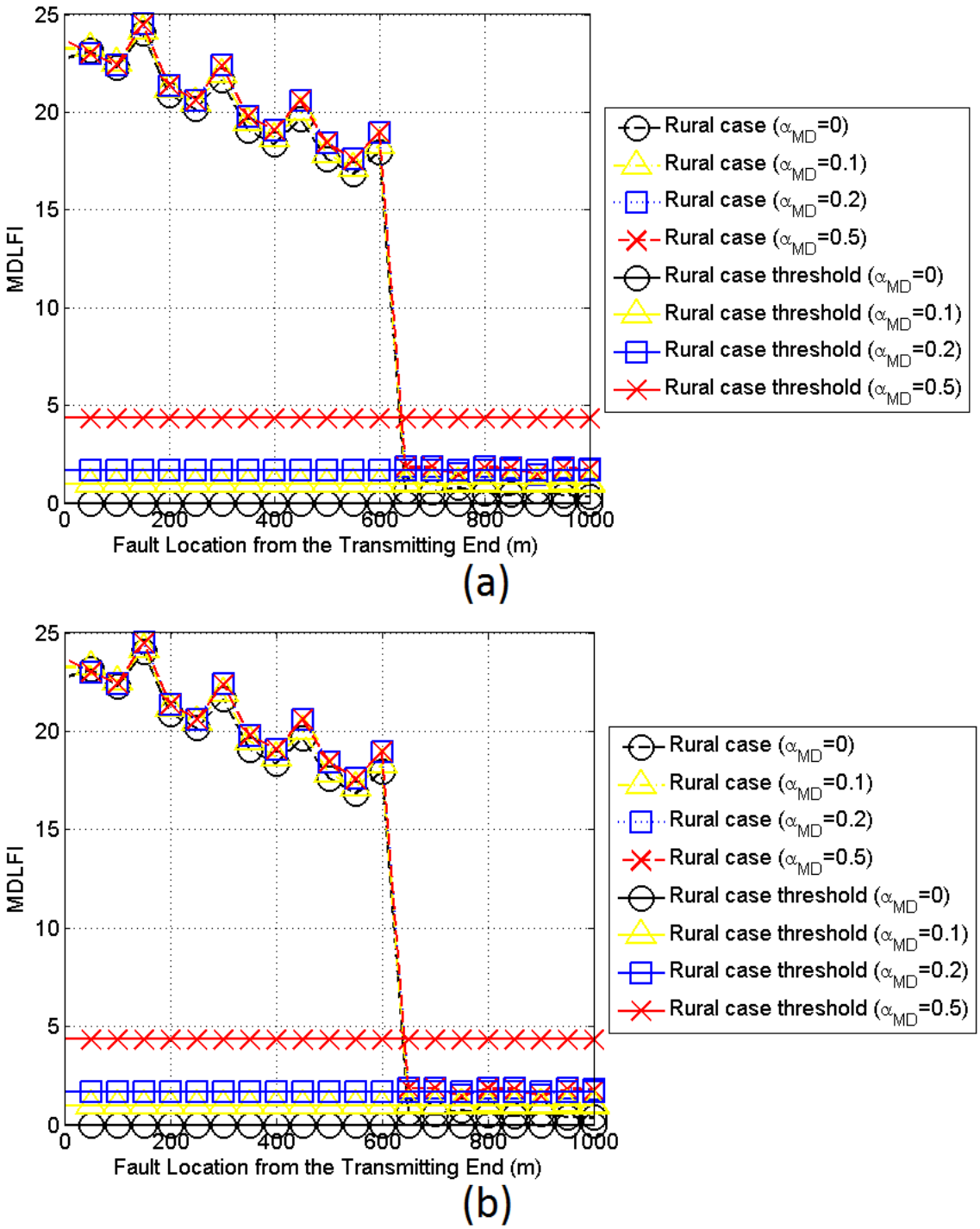

Figure 10. Same plots with Figure 9 but for the identification of main distribution line faults across the original OV MV BPL rural topology.

With reference to Figs. 9(a), 9(b), 10(a) and 10(b), several interesting conclusions concerning the application of MDLFI as well as the corresponding decisions about the identification of a main distribution line fault across the OV MV BPL topologies can be pointed out, namely:

- Already been mentioned in this subsection, MDLFI strongly depends on the examined OV MV BPL topology since it is considered as a dissimilarity metric between the original and fault case. This explains the fact that MDLFI values of fault rural OV MV BPL topologies always remain higher than the ones of fault urban OV MV BPL topologies.
- MDLFI slightly depends on the terminal load of the examined fault OV MV BPL topology. In fact, coupling reflection coefficient differences can be observed when the terminal load is assumed to be equal to short- or open-circuit termination. However, the coupling reflection coefficients for given OV MV BPL topology when terminal loads vary from short- to open-circuit remain low implying low differences between the respective MDLFIs. Hence, apart from the identification of a main distribution line fault, a first idea regarding the nature of the fault and thus the type of the main distribution line fault (day, fault line in the air or on the ground) can be given.
- MDLFI strongly depends on the location of the main distribution line fault across the OV MV BPL topology. In fact, when the fault is located near to the transmitting end, MDLFI receives higher values in comparison with the respective ones of a main distribution line fault located near to the receiving end. Since the identification of the fault is achieved through the comparison of MDLFI of the fault OV MV BPL topology against the $MDLFI_{thr}$ of the original one, this implies that the identification of a main distribution line fault becomes easier when it is located near to the transmitting end than far away from it. This is a logical result since the fault OV MV BPL topology is critically modified in comparison with the original one when the fault is near to the transmitting end. Not only the overall transmission length of the fault OV MV BPL topology becomes lower than the average length of 1000m but a number of branches can be omitted in the fault OV MV BPL topology. In order to cope with this fault location sensitivity, MLFLM exploits MDLFI measurements of both the available sides of an OV MV BPL topology –say, transmitting and receiving end– (for more details concerning the combined MLFLM application of MDLFI, see [35]).
- Already been recognized from Table 1, as the magnitude a_{MD} of measurement differences increases so does the difficulty of identifying a main distribution line fault. This can be explained by the fact that the magnitude increase of measurement differences creates an increase to $MDLFI_{thr}$ that anyway defines the critical line between the normal and fault operation. As $MDLFI_{thr}$ increases, the distinction between the normal and fault condition becomes problematic. From the Figures, it is clear that MDLFI of the examined OV MV BPL topologies always remains above $MDLFI_{thr}$ when magnitudes a_{MD} of measurement differences remain low (e.g., $a_{MD}=0$ and $a_{MD}=0.1$). In these cases of low measurement differences, the difference between MDLFI and $MDLF_{thr}$ remains large enough so that a robust decision regarding the existence of a main distribution line fault can be supported. Conversely, when magnitudes a_{MD} of

measurement differences start to get high, the difference between MDLFI and $MDLFI_{thr}$ diminishes, thus confusing and creating a decision ambiguity whether a main distribution line fault exists. Marginally, when the magnitude a_{MD} of measurement differences is equal to 0.5, the decision of the existence of a main distribution line fault becomes critically uncertain. Numerically, in all the four OV MV BPL topologies examined in Figs. 9(a), 9(b), 10(a) and 10(b), although a main distribution line fault occurs, a safe decision concerning this existence cannot be safely supported in 8 of the 20 cases when the magnitude a_{MD} of the measurement differences is assumed to be equal to 0.5. Here, it should be noted that all the 8 problematic main distribution line fault cases are situated near to the receiving end, which is a problematic condition for a single MDLFI measurement from the transmitting end, as already been mentioned.

The identification of main distribution line faults in OV MV BPL topologies regardless of the presence of measurement differences and the nature of the terminal load concludes the main prerequisite of applying MLFLM. Since the existence of main distribution line faults can be secured with a high degree of accuracy, the next phase of MLFLM that is the exact localization of the fault across the examined OV MV BPL topology is analyzed in [35].

5. Conclusions

The main distribution line fault identification methodology of the first paper has further been extended in this paper so that measurement differences of the coupling reflection coefficients can be mitigated. Through the application of L1PMA and its accompanying metrics, such as $MDLFI_{par}$, MDLFI and $MDLFI_{thr}$, a secure identification of a main distribution line fault across the OV MV BPL networks can be achieved when magnitude a_{MD} of measurement differences that follow CUD remains low or normal (i.e., a_{MD} lower than 0.2). In the vast majority of the cases examined, the decision regarding the fault identification remains robust when magnitude a_{MD} remains, indeed, low or normal. In contrast, when the magnitude a_{MD} of measurement differences becomes significant and comparable to the depth of the spectral notches of the coupling reflection coefficients (i.e., a_{MD} higher than 0.2), decisions regarding the existence of main distribution line fault become insecure especially when the faults are situated near to the receiving end, far away from the measurement site. Anyway, the decision regarding the identification of main distribution line faults are considered to be more reliable when the faults are located near to the transmitting end of the examined OV MV BPL topologies.

The combined operation of extended TM2 method, L1PMA and set of MDLFI-related metrics concludes the introductory phase of MLFLM. However, the main phase of MLFLM that has to do with the exact localization of main distribution line faults across the OV MV BPL topologies is analyzed in the third paper.

CONFLICTS OF INTEREST

The author declares that there is no conflict of interests regarding the publication of this paper.

References

[1] A. G. Lazaropoulos, "Main Line Fault Localization Methodology in Smart Grid – Part 1: Extended TM2 Method for the Overhead Medium-Voltage Broadband over Power Lines Networks Case," *Trends in Renewable Energy*, vol. 3, no. 3, pp. 2-25, 2017.

[2] A. G. Lazaropoulos, A. Sarafi, and P. G. Cottis, "The emerging smart grid — A pilot MV/BPL network installed at Lavrion, Greece," in *Proc. Workshop on Applications for Powerline Communications WSPLC 2008*, Thessaloniki, Greece, Oct. 2008. [Online]. Available: http://newton.ee.auth.gr/WSPLC08/Abstracts%5CSG_3.pdf

[3] A. G. Lazaropoulos, "Power Systems Stability through Piecewise Monotonic Data Approximations – Part 1: Comparative Benchmarking of L1PMA, L2WPMA and L2CXCV in Overhead Medium-Voltage Broadband over Power Lines Networks," *Trends in Renewable Energy*, vol. 3, no. 1, pp. 2 – 32, Jan. 2017. [Online]. Available: http://futureenergysp.com/index.php/tre/article/view/29/34

[4] A. G. Lazaropoulos, "Power Systems Stability through Piecewise Monotonic Data Approximations – Part 2: Adaptive Number of Monotonic Sections and Performance of L1PMA, L2WPMA and L2CXCV in Overhead Medium-Voltage Broadband over Power Lines Networks," *Trends in Renewable Energy*, vol. 3, no. 1, pp. 33 – 60, Jan. 2017. [Online]. Available: http://futureenergysp.com/index.php/tre/article/view/30/35

[5] A. G. Lazaropoulos, "Improvement of Power Systems Stability by Applying Topology Identification Methodology (TIM) and Fault and Instability Identification Methodology (FIIM) – Study of the Overhead Medium-Voltage Broadband over Power Lines (OV MV BPL) Networks Case," *Trends in Renewable Energy*, vol. 3, no. 2, pp. 102 – 128, Apr. 2017. [Online]. Available: http://futureenergysp.com/index.php/tre/article/view/34/pdf

[6] A. G. Lazaropoulos, "Measurement Differences, Faults and Instabilities in Intelligent Energy Systems – Part 1: Identification of Overhead High-Voltage Broadband over Power Lines Network Topologies by Applying Topology Identification Methodology (TIM)," *Trends in Renewable Energy*, vol. 2, no. 3, pp. 85 – 112, Oct. 2016.

[7] A. G. Lazaropoulos and P. Lazaropoulos, "Financially Stimulating Local Economies by Exploiting Communities' Microgrids: Power Trading and Hybrid Techno-Economic (HTE) Model," *Trends in Renewable Energy*, vol. 1, no. 3, pp. 131-184, Sep. 2015. [Online]. Available: http://futureenergysp.com/index.php/tre/article/view/14

[8] L. Lutz, A. M. Tonello, and T. G. Swart, *Power Line Communications: Principles, Standards and Applications from multimedia to smart grid*, John Wiley & Sons, 2016.

[9] G. Artale, A. Cataliotti, V. Cosentino, D. Di Cara, R. Fiorelli, S. Guaiana, and G. Tine, "A New Low Cost Coupling System for Power Line Communication on Medium Voltage Smart grids," *IEEE Trans. on Smart Grid*, to be published, 2017.

[10] A. G. Lazaropoulos, "Measurement Differences, Faults and Instabilities in Intelligent Energy Systems – Part 2: Fault and Instability Prediction in Overhead High-Voltage Broadband over Power Lines Networks by Applying Fault and

Instability Identification Methodology (FIIM)," *Trends in Renewable Energy*, vol. 2, no. 3, pp. 113 – 142, Oct. 2016. [Online]. Available: http://futureenergysp.com/index.php/tre/article/view/27/33

[11] A. G. Lazaropoulos, "Factors Influencing Broadband Transmission Characteristics of Underground Low-Voltage Distribution Networks," *IET Commun.*, vol. 6, no. 17, pp. 2886-2893, Nov. 2012.

[12] A. G. Lazaropoulos and P. G. Cottis, "Transmission characteristics of overhead medium voltage power line communication channels," *IEEE Trans. Power Del.*, vol. 24, no. 3, pp. 1164-1173, Jul. 2009.

[13] A. G. Lazaropoulos and P. G. Cottis, "Capacity of overhead medium voltage power line communication channels," *IEEE Trans. Power Del.*, vol. 25, no. 2, pp. 723-733, Apr. 2010.

[14] A. G. Lazaropoulos and P. G. Cottis, "Broadband transmission via underground medium-voltage power lines-Part I: transmission characteristics," *IEEE Trans. Power Del.*, vol. 25, no. 4, pp. 2414-2424, Oct. 2010.

[15] A. G. Lazaropoulos and P. G. Cottis, "Broadband transmission via underground medium-voltage power lines-Part II: capacity," *IEEE Trans. Power Del.*, vol. 25, no. 4, pp. 2425-2434, Oct. 2010.

[16] A. G. Lazaropoulos, "Broadband transmission characteristics of overhead high-voltage power line communication channels," *Progress in Electromagnetics Research B*, vol. 36, pp. 373-398, 2012. [Online]. Available: http://www.jpier.org/PIERB/pierb36/19.11091408.pdf

[17] A. G. Lazaropoulos, "Towards broadband over power lines systems integration: Transmission characteristics of underground low-voltage distribution power lines," *Progress in Electromagnetics Research B*, 39, pp. 89-114, 2012. [Online]. Available: http://www.jpier.org/PIERB/pierb39/05.12012409.pdf

[18] A. G. Lazaropoulos, "Broadband transmission and statistical performance properties of overhead high-voltage transmission networks,"*Hindawi Journal of Computer Networks and Commun.*, 2012, article ID 875632, 2012. [Online]. Available: http://www.hindawi.com/journals/jcnc/aip/875632/

[19] A. G. Lazaropoulos, "Towards modal integration of overhead and underground low-voltage and medium-voltage power line communication channels in the smart grid landscape: model expansion, broadband signal transmission characteristics, and statistical performance metrics (Invited Paper)," *ISRN Signal Processing*, vol. 2012, Article ID 121628, 17 pages, 2012. [Online]. Available: http://www.isrn.com/journals/sp/aip/121628/

[20] A. G. Lazaropoulos, "Review and Progress towards the Common Broadband Management of High-Voltage Transmission Grids: Model Expansion and Comparative Modal Analysis," *ISRN Electronics*, vol. 2012, Article ID 935286, pp. 1-18, 2012. [Online]. Available: http://www.hindawi.com/isrn/electronics/2012/935286/

[21] A. G. Lazaropoulos, "Review and Progress towards the Capacity Boost of Overhead and Underground Medium-Voltage and Low-Voltage Broadband over Power Lines Networks: Cooperative Communications through Two- and Three-Hop Repeater Systems," *ISRN Electronics*, vol. 2013, Article ID 472190, pp. 1-19, 2013. [Online]. Available: http://www.hindawi.com/isrn/electronics/aip/472190/

[22] A. G. Lazaropoulos, "Green Overhead and Underground Multiple-Input Multiple-Output Medium Voltage Broadband over Power Lines Networks: Energy-

Efficient Power Control," *Springer Journal of Global Optimization*, vol. 2012 / Print ISSN 0925-5001, pp. 1-28, Oct. 2012.

[23] P. Amirshahi and M. Kavehrad, "High-frequency characteristics of overhead multiconductor power lines for broadband communications," *IEEE J. Sel. Areas Commun.*, vol. 24, no. 7, pp. 1292-1303, Jul. 2006.

[24] T. Sartenaer, "Multiuser communications over frequency selective wired channels and applications to the powerline access network" Ph.D. dissertation, Univ. Catholique Louvain, Louvain-la-Neuve, Belgium, Sep. 2004. [Online} Available: https://dial.uclouvain.be/pr/boreal/en/object/boreal%3A5010/datastream/PDF_12/view

[25] T. Calliacoudas and F. Issa, ""Multiconductor transmission lines and cables solver," An efficient simulation tool for plc channel networks development," presented at the *IEEE Int. Conf. Power Line Communications and Its Applications*, Athens, Greece, Mar. 2002.

[26] A. G. Lazaropoulos, "Best L1 Piecewise Monotonic Data Approximation in Overhead and Underground Medium-Voltage and Low-Voltage Broadband over Power Lines Networks: Theoretical and Practical Transfer Function Determination," *Hindawi Journal of Computational Engineering*, vol. 2016, Article ID 6762390, 24 pages, 2016. doi:10.1155/2016/6762390. [Online]. Available: https://www.hindawi.com/journals/jcengi/2016/6762390/cta/

[27] P. Amirshahi, "Broadband access and home networking through powerline networks" Ph.D. dissertation, Pennsylvania State Univ., University Park, PA, May 2006. [Online]. Available: http://etda.libraries.psu.edu/theses/approved/WorldWideIndex/ETD-1205/index.html

[28] M. D'Amore and M. S. Sarto, "Simulation models of a dissipative transmission line above a lossy ground for a wide-frequency range-Part I: Single conductor configuration," *IEEE Trans. Electromagn. Compat.*, vol. 38, no. 2, pp. 127-138, May 1996.

[29] M. D'Amore and M. S. Sarto, "Simulation models of a dissipative transmission line above a lossy ground for a wide-frequency range-Part II: Multi-conductor configuration," *IEEE Trans. Electromagn. Compat.*, vol. 38, no. 2, pp. 139-149, May 1996.

[30] A. Milioudis, G. T. Andreou, and D. P. Labridis, "Detection and location of high impedance faults in multiconductor overhead distribution lines using power line communication devices," *IEEE Trans. on Smart Grid*, vol. 6, no. 2, pp. 894-902, 2015.

[31] A. G. Lazaropoulos, "Designing Broadband over Power Lines Networks Using the Techno-Economic Pedagogical (TEP) Method – Part I: Overhead High Voltage Networks and Their Capacity Characteristics," *Trends in Renewable Energy*, vol. 1, no. 1, pp. 16-42, Mar. 2015. [Online]. Available: http://futureenergysp.com/index.php/tre/article/view/2

[32] A. G. Lazaropoulos, "Designing Broadband over Power Lines Networks Using the Techno-Economic Pedagogical (TEP) Method – Part II: Overhead Low-Voltage and Medium-Voltage Channels and Their Modal Transmission Characteristics," *Trends in Renewable Energy*, vol. 1, no. 2, pp. 59-86, Jun. 2015. [Online]. Available: http://futureenergysp.com/index.php/tre/article/view/6/16

[33] T. Sartenaer and P. Delogne, "Deterministic modelling of the (Shielded) outdoor powerline channel based on the multiconductor transmission line equations," *IEEE J. Sel. Areas Commun.*, vol. 24, no. 7, pp. 1277-1291, Jul. 2006.
[34] http://cpc.cs.qub.ac.uk/summaries/ADRF
[35] A. G. Lazaropoulos, "Main Line Fault Localization Methodology in Smart Grid – Part 3: Main Line Fault Localization Methodology (MLFLM)," *Trends in Renewable Energy*, vol. 3, no. 3, pp. 62-81, 2017.

Main Line Fault Localization Methodology in Smart Grid – Part 3: Main Line Fault Localization Methodology (MLFLM)

Athanasios G. Lazaropoulos[1]

1: School of Electrical and Computer Engineering / National Technical University of Athens / 9 Iroon Polytechniou Street / Zografou, GR 15780

Received June 13, 2017; Accepted September 2, 2017; Published October 6, 2017

Since the main distribution line faults can be securely identified as outlined in the first and second paper, this third paper presents the methodology of localizing the main distribution line fault when broadband over power lines (BPL) networks have already been deployed across the distribution power grids. The main issue of this paper is the detailed presentation of the main line localization methodology (MLFLM) as well as well as its performance assessment when measurement differences occur.

The contribution of this paper, which is focused on the application of MLFLM, is double. First, the procedure, which is followed in order to create the database of faults and is used by MLFLM, is here analytically presented. This database is based on the application of the main distribution line fault identification percentage metric (MDLFI) to coupling reflection coefficients of all possible fault OV MV BPL topologies (modified OV MV BPL topologies). Second, the performance assessment of MLFLM is investigated with respect to the nature of the measurement differences and the location of main distribution line faults across the distribution power grid.

Keywords: Smart Grid; Intelligent Energy Systems; Broadband over Power Lines (BPL) Networks; Power Line Communications (PLC); Faults; Fault Analysis; Fault Localization; Distribution Power Grids

1. Introduction

A major advantage of the BPL networks is the fact that their development is simple and economically advantageous since their deployment is based on the already operating power grid infrastructure. As concerns the potential of the smart grid operation, BPL technology can act as either an autonomous communications system or a cooperative communications network that interoperates with other wired and wireless communications solutions in an integrated intelligent IP-based network environment. Anyway, the synergy of telecommunications solution under the aegis of the smart grid can support a myriad of smart grid applications [1]-[4].

In the first paper [5], the determination of the channel attenuation and reflection coefficient of overhead medium-voltage (OV MV) BPL networks have been achieved by extending the original TM2 method, which is the core part of the top-down approach of the well-established hybrid method [3], [6]-[22] during the normal operation of OV MV

*Corresponding author: AGLazaropoulos@gmail.com

BPL networks, to the extended TM2 method. In fact, extended TM2 method can give as output the reflection coefficients during the operation of OV MV BPL networks where a main distribution line fault occurs (fault operation). In the second paper [23], the role of measurement differences that occur during the determination of reflection coefficients due to the "real-life" conditions and during the identification of main distribution line faults has been analyzed. Actually, the destructive impact of measurement differences during the main distribution line identification has been significantly counteracted through the application of piecewise monotonic data approximations (PMAs), such as L1PMA. In the vast majority of the cases examined, the fault operation has been identified by applying the main distribution line fault identification percentage metric (MDLFI), which accompanies the main distribution fault identification methodology. In this paper, the detailed presentation of the main line localization methodology (MLFLM) is provided. It is obvious that the MLFLM commences to operate since the identification of a main distribution line fault is granted on the basis of the findings of the first and second paper. Initially, MLFLM supports the preparation of a detailed database of coupling reflection coefficients and respective MDLFIs for all the possible OV MV BPL topologies. Apart from the plethora of OV MV BPL topologies that may be supported, this database also takes into account the nature of the main distribution line fault (i.e., short- or open-circuit termination load, see [5]). Then, statistics regarding the database access as well as the exact procedure that is followed in order to parse the database and, finally, to exactly localize the main distribution line fault is provided. Here, it should be noted that the previous experience concerning the creation and management of databases, which has been obtained from the Topology Identification Methodology (TIM) of [22], [24] and Fault and Instability Identification Methodology (FIIM) of [25], [26], is exploited in MLFLM.

The rest of this paper is organized as follows: In Sec.II, the findings of [5], [23] that are used in this paper are briefly outlined. In Sec.III, the creation procedure of the MLFLM database is detailed as well as implementation details and characteristics concerning its access during the fault operation. Sec.IV discusses the simulations of various OV MV BPL topologies with random main distribution line faults intending to mark out the performance efficiency of the proposed MLFLM when measurement differences occur. Sec.V concludes this paper.

2. Brief Presentation of the OV MV BPL Topologies, Main Distribution Line Faults, Measurement Differences and MDLFI

In accordance with [5], [23], four indicative OV MV BPL topologies of average path length of 1000m, which are treated as the original topologies, are also examined in this paper, namely:

1. A typical urban topology (denoted as urban case) with N=3 branches (L_1=500m, L_2=200m, L_3=100m, L_4=200m, L_{b1}=8m, L_{b2}=13m, L_{b3}=10m).
2. A typical suburban topology (denoted as suburban case) with N=2 branches (L_1=500m, L_2=400m, L_3=100m, L_{b1}=50m, L_{b2}=10m).
3. A typical rural topology (denoted as rural case) with only N=1 branch (L_1=600m, L_2=400m, L_{b1}=300m).
4. The "LOS" transmission along the same end-to-end distance $L=L_1+\ldots+L_{N+1}$=1000m (denoted as "LOS" case) when no branches are

encountered. This topology corresponds to Line of Sight transmission in wireless channels.

Already been mentioned, critical problematic conditions, such as the main distribution line faults that are examined in these three papers, can occur across the distribution power grid during its operation. With reference to Fig. 1(b) of [5], let the main distribution line be broken at a specific location from the transmitting end. On the basis of the original OV MV BPL networks, new OV MV BPL topologies occur with path lengths equal or shorter than 1000m whose path lengths depend on the location of the main distribution line fault. Not only the path length but depending on the fault location, the new OV MV BPL topologies are characterized by different number of branches in comparison with the respective original ones. These new OV MV BPL topologies are denoted as modified OV MV BPL topologies. Except for their topological characteristics concerning the path length and the number of branches, modified OV MV BPL topologies differ from the respective original ones in the nature of the terminal load, which is situated at the location of the fault. While original OV MV BPL topologies are characterized by terminal loads that are matched to the characteristic impedances of the modes examined, the terminal loads of the respective modified OV MV BPL topologies are equal to either short- or open-circuit depending on the nature of the main distribution line fault (see [5] for further details). Hence, two sets of the four modified OV MV BPL topologies are examined in this subsection, each one corresponding to the two different values of the terminal load.

As been presented in [5], a main distribution line fault can be easily identified through the extended TM2 method and its coupling reflection coefficients. However, apart from the main distribution line fault, a set of practical reasons and "real-life" conditions create significant differences between experimental measurements and theoretical results. In accordance with [22], the causes of the measurement differences presented to the coupling reflection coefficients can be grouped into six categories, namely: (i) Isolation difficulties of specific MTL parameters in time- and frequency-domain; (ii) Low accuracy and sensitivity of the used equipment during measurements; (iii) Cross-talk and resonant phenomena due to the parasitic capacitances and inductances of lines; (iv) The weakness of including specific wiring and grounding practices; (v) Practical impedance deviations of lines, branches, terminations and transmitting/receiving ends; and (vi) The isolation lack of the noise effect during the transfer function computations.

The PMA experience, which has been acquired either in the case of coupling transfer functions [3], [22], [24]-[26] or in the case of coupling reflection coefficients [5], secures the identification of a main distribution line fault despite the measurement differences. On the basis of PMA piecewise monotonicity property, PMAs receive as inputs the measured coupling reflection coefficient data, the measurement frequencies and the number of monotonic sections and give as outputs the optimal primary extrema and the best fit of the measured OV MV BPL reflection coefficient data. In order to assess at the same time the mitigation performance against measurement differences and the main distribution line fault identification efficiency, the main distribution line fault identification percentage metric (MDLFI) has been proposed in [5]. MDLFI acts as the accompanying performance metric of the identification process of main distribution line faults and describes the relative error between L1PMA approximations of the measured and theoretical data. According to the results of [5], the main distribution line fault identification efficiency depends on the magnitude of the measurement differences,

critical thresholds of the MDLFI ($MDLFI_{thr}$) and the relative distance of main distribution line fault from the transmitting end. However, MLFLM achieves to exactly localize the main distribution line faults getting rid of the MDLFI dependencies, such as $MDLFI_{thr}$ and the relative fault distance from the transmitting end, by wisely: (i) applying MDLFI equation between coupling reflection coefficient measurements and theoretical coupling reflection coefficient data of MLFLM database; and (ii) using both the available coupling reflection coefficient measurement sites, which are the transmitting and receiving end of the examined original OV MV BPL topology (see more details in Sec.III).

3. OV MV BPL Topology Database with MDLFI and MLFLM

In accordance with [3], [22], the first step of MLFLM is the creation of the MLFLM database. In fact, MLFLM database consists of all possible modified OV MV BPL topologies that can occur due to main distribution line faults.

In [23], it has been identified that the identification efficiency of a main distribution line fault significantly depends on the location of the fault across the OV MV BPL topology. In fact, when the fault is located near to the transmitting end the identification becomes easier in comparison with the faults that are closer to the receiving end. In order to exploit this finding, the complimentary OV MV BPL topology to the original one from the side of the receiving end should also been considered in the database for given OV MV BPL topology. Hence, the computational load of MLFLM database becomes double in comparison with the respective one of TIM and FIIM since each database record now consists of a pair of two modified OV MV BPL topologies [3], [22], [25], [26]. Here, it should be noted that the nature of the termination load remains the same for given database record pair. Since the average transmission length is equal to 1000m and the length spacing L_s that defines the database accuracy is assumed equal to 50m in this paper, there are $\left(\frac{1000\text{m}}{50\text{m}}\right)+1=21$ pairs of OV MV BPL topologies for given original OV MV BPL topology.

Except for the database properties regarding the number of the considered OV MV BPL topologies, the second step for the creation of the detailed MLFLM database urges the database enrichment with information concerning coupling reflection coefficients. In order to simplify the procedure and apply the findings of [22], a set of database specifications is here given:

- $k_{sect,min}$ is the lower monotonic section bound, which is assumed to be equal to 1 in this paper, and $k_{sect,max}$ is the upper monotonic section bound, which is assumed to be equal to 20 in this paper
- The operation frequency range and the flat fading subchannel frequency spacing are assumed equal to 1-30MHz and 1MHz, respectively. Therefore, the number of subchannels u in the examined frequency range is equal to 30.
- Arbitrarily, the WtG^3 coupling scheme is applied during the following simulations. As it is usually done [9], [27], [28], [29], [18], [30], the selection of representative coupling schemes is a typical procedure for the sake of reducing manuscript size and simplicity.
- For each OV MV BPL topology that is considered in the database, the two cases of termination loads should be considered (either short- or open-circuit).

In accordance with the previous assumptions and eqs (5) and (6) of [23], there is a need for inserting 2×20=40 approximated theoretical OV MV BPL coupling reflection coefficient column vectors (say, $\overline{\overline{\mathbf{\Gamma}_{\text{theor,1}}^{\text{WtG}}}}$ and $\overline{\overline{\mathbf{\Gamma}_{\text{theor,2}}^{\text{WtG}}}}$) per each possible OV MV BPL topology pair of the database, which corresponds to the respective 20 monotonic sections. Each approximated theoretical OV MV BPL coupling reflection coefficient column vector $\overline{\overline{\mathbf{\Gamma}_{\text{theor},k}^{\text{WtG}}}}$, k=1…2 consists of 30 elements (say, $\overline{\overline{\Gamma_{\text{theor},k}^{\text{WtG}}}}(f_i)$, k=1…2, i=1,…,*30*), which corresponds to the respective 30 measurement frequencies f_i, i=1,…,*30*. Therefore, the detailed OV MV BPL topology database comprises 40×30=1200 elements for each OV MV BPL topology pair. Since main distribution line faults can be treated as either short- or open-circuit terminations, there are 2×600=1200 element insertions per pair or 50'400 insertions in total that should be added into the database concerning its enrichment with coupling reflection coefficient attributes.

Let assume that a main distribution line fault occurs and the measured coupling reflection coefficients from the side of the transmitting and receiving end of the original OV MV BPL topology are equal to $\overline{\Gamma_{\text{meas,1}}^{\text{WtG}}}$ and $\overline{\Gamma_{\text{meas,2}}^{\text{WtG}}}$, respectively. Note that $\overline{\Gamma_{\text{meas,1}}^{\text{WtG}}}$ and $\overline{\Gamma_{\text{meas.2}}^{\text{WtG}}}$ are the coupling reflection coefficients of the modified OV MV BPL topologies when the nature of the termination load is considered. For the 30 measurement frequencies f_i, i=1,…,*30*, the measured OV MV BPL reflection coefficient column vectors $\overline{\mathbf{\Gamma}_{\text{meas,1}}^{\text{WtG}}}$ and $\overline{\mathbf{\Gamma}_{\textit{meas},2}^{\text{WtG}}}$ consist of the respective measured coupling reflection coefficients from the transmitting end $\overline{\Gamma_{\text{meas,1}}^{\text{WtG}}}(f_i)$, i=1,…,*30* and receiving end $\overline{\Gamma_{\text{meas,2}}^{\text{WtG}}}(f_i)$, i=1,…,*30*. L1PMA software processes its inputs, which are the measured coupling reflection coefficient column vectors $\overline{\mathbf{\Gamma}_{\text{meas},k}^{\text{WtG}}}$, k=1…2, and gives as outputs the respective approximated measured OV MV BPL reflection coefficient column vectors $\overline{\overline{\mathbf{\Gamma}_{\text{meas},k}^{\text{WtG}}}}$, k=1…2.

The third and final step of MLFLM is the localization of the main distribution line faults through the computation of $\text{MDLFI}_{\text{par}}$ and MDLFI. Similarly to MDLFI of [23], MDLFI_k, k=1…2 of the respective two modified OV MV BPL topologies is given by

$$MDLFI_k = \frac{\sum_{k_{\text{sect}}=1}^{20} MDLFI_{\text{par},k}(k_{\text{sect}})}{600}, k=1\ldots2 \quad (1)$$

where

$$MDLFI_{\text{par},k}(k_{\text{sect}}) = \sum_{i=1}^{30} \frac{\left|\overline{\overline{\mathbf{\Gamma}_{\text{meas,k}}^{\text{WtG}}}}(f_i,k_{\text{sect}}) - \overline{\overline{\mathbf{\Gamma}_{\text{theor,k}}^{\text{WtG}}}}(f_i,k_{\text{sect}})\right|}{\left|\overline{\overline{\mathbf{\Gamma}_{\text{theor,k}}^{\text{WtG}}}}(f_i,k_{\text{sect}})\right|}, k=1\ldots2 \quad (2)$$

Observing eq. (1), several interesting remarks concerning the application of MDLFI to localize main distribution line faults can be pointed out:

- In order to exploit the efficiency of MDLFI to identify main distribution line faults that are closer to the measurement instrument, $MDLFI_1$ and $MDLFI_2$ offer a differential advantage through the two available measurement locations of coupling reflection coefficients (i.e., the side of the transmitting and receiving end of the original OV MV BPL topology). With reference to eq. (1), if the main distribution line fault is located near to the transmitting end then $MDLFI_1$ presents higher values than the respective ones of $MDLFI_2$. In the reverse case of a main distribution line fault located near to the receiving end, $MDLFI_2$ presents a more reliable identification behavior in comparison with $MDLFI_1$.
- According to [23], MDLFI describes the relative error between L1PMA approximations of the measured and theoretical data. The identification of the main distribution line faults has been achieved through the comparison of MDLFI with certain critical thresholds that mainly depends on the modified OV MV BPL topologies. Here, MLFLM exploits the differential reception of $MDLFI_1$ and $MDLFI_2$ by comparing the measured coupling reflection coefficients with the respective ones of all the available pairs of MLFLM database. The pairs of MLFLM database that present approximately the minimum $MDLFI_1$ and $MDLFI_2$ are the candidate modified OV MV BPL topologies while the location of the main distribution line fault and the nature of the terminal loads can straightforward been found from the insertion number of the MLFLM database.
- MLFLM performance is based on the detection of the MDLFI pair in the MLFLM database. Since MDLFI depends on: (i) the original OV MV BPL topology; (ii) the nature of the terminal load; (iii) the location of main distribution line faults; and (iv) the intensity of measurement differences, so do $MDLFI_1$ and $MDLFI_2$, the immunity performance of MLFLM against aforementioned MDLFI dependencies to localize the main distribution line faults through $MDLFI_1$ and $MDLFI_2$ is assessed in Sec.4.

4. Numerical Results and Discussion

4.1 Simulation Goals and Parameters

The four original OV MV BPL topologies of Sec.2 are simulated with the purpose of accurately localizing potential main distribution line faults by applying MLFLM. In this Section, the MLFLM efficiency is assessed when various factors such as the complicity of the original OV MV BPL topology, the nature of the terminal load and the location of main distribution line faults are assumed. Similarly to the identification of main distribution line faults, the localization of main distribution line faults becomes a challenging issue when real-life conditions are simulated through the application of measurement differences. For that reason, the measurement differences that occur in OV MV BPL networks during the determination of coupling reflection coefficients are typically described by continuous uniform distributions (CUD) with range from 0 to a maximum CUD value that is equal to α_{MD}. It is evident that the measurement difference CUD remains the same during the simultaneous coupling reflection coefficient measurements from the transmitting and receiving end of the original OV MV BPL topology.

The combined impact of measurement differences and main distribution line faults on the OV MV BPL coupling reflection coefficient is here investigated. First, three different measurement difference CUDs are assumed, namely:

(i) CUD with a_{MD}=0 (no measurement differences are assumed while this CUD case is denoted as CUD case A); (ii) CUD with a_{MD}=0.1 (denoted as CUD case B); and (iii) CUD with a_{MD}=0.2 (denoted as CUD case C). Second, three different locations of main distribution line faults are applied, namely: (a) fault location situated at 250m from the transmitting end (denoted as Fault case A); (b) fault location situated at 500m from the transmitting end (denoted as Fault case B); and (c) fault location situated at 750m from the transmitting end (denoted as Fault case C).

4.2 Fault Localization of Main Distribution Line Faults by Applying MLFLM (General Case)

Let assume that the fault case A has been identified in accordance with [23] during the operation of the urban case and the fault localization begins through the initiation of MLFLM procedures. Since the main distribution line fault occurs, $\overline{\mathbf{\Gamma}_{\text{meas,1}}^{\text{WtG}}}$ and $\overline{\mathbf{\Gamma}_{meas,2}^{\text{WtG}}}$ are available through the coupling reflection coefficient measurements from the transmitting and receiving end side, respectively. Since the MLFLM database has already been theoretically implemented for the urban case for all the available pairs of modified OV MV BPL topologies, MDLFIs (i.e., $MDLFI_1$ and $MDLFI_2$) are determined for each pair of the aforementioned modified OV MV BPL topologies. Therefore, in Fig. 1, MDLFIs (i.e., $MDLFI_1$ and $MDLFI_2$) are plotted versus the distance from the transmitting end of the original topology when CUD case A is adopted and the terminal load is assumed to be short-circuit during the main distribution line fault case A. For the sake of simplicity, only the pairs of the modified OV MV BPL topologies with short-circuit termination loads are retrieved from the MLFLM database. In Fig. 2, same plots are drawn with Fig. 1 but for the case of an open-circuit terminal load while the MLFLM database pairs of modified OV MV BPL topologies with open-circuit termination loads are only examined.

From Figs. 1 and 2, it is obvious that MDLFIs both receive their minimum values when the fault location from the transmitting end, which is related with the MLFLM database, is equal to the actual distance of the main distribution line fault from the transmitting end. Since fault case A mandates that the main distribution line fault is situated at 250m from the transmitting end, $MDLFI_1$ and $MDLFI_2$ are both equal to 0 in accordance with eqs. (1) and (2). This is due to the fact that $\overline{\overline{\mathbf{\Gamma}_{\text{theor},k}^{\text{WtG}}}}$ is equal to $\overline{\overline{\mathbf{\Gamma}_{\text{meas},k}^{\text{WtG}}}}$ for given k since no measurement differences are considered in the CUD case A. In all the other cases, MDLFIs receive values that are greater than zero. However, this ideal situation of localizing the main distribution line faults through the zeroing of MDLFIs stands only in the case of no measurement differences and, hence, the case of the inclusion of measurement differences requires further examination (see the following subsection).

4.3 The Impact of the Measurement Differences on the Fault Localization by Applying MLFLM

Although the fault localization through the simultaneous minimization of MDLFIs can be considered as an intuitive method to accurately localize main distribution

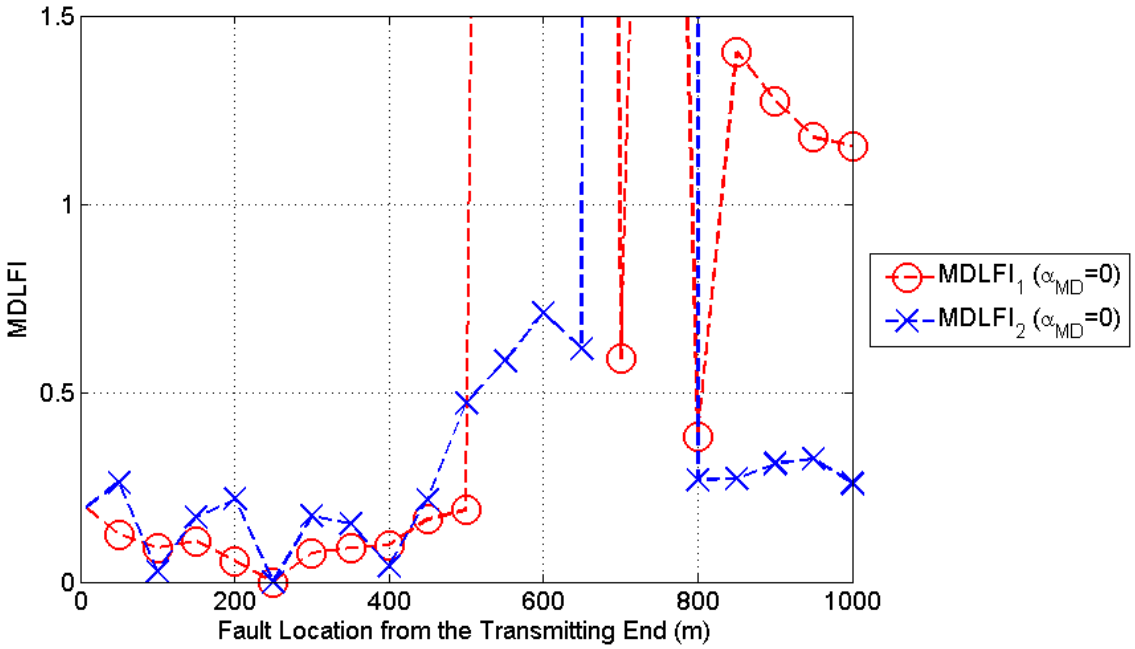

Figure 1. MDLFIs of the urban OV MV BPL topology versus the fault location from the transmitting end when fault case A (i.e., main distribution line fault situated at 250m from the transmitting end) and CUD case A (i.e., a_{MD}=0) are assumed (the terminal load is assumed to be a short-circuit termination load).

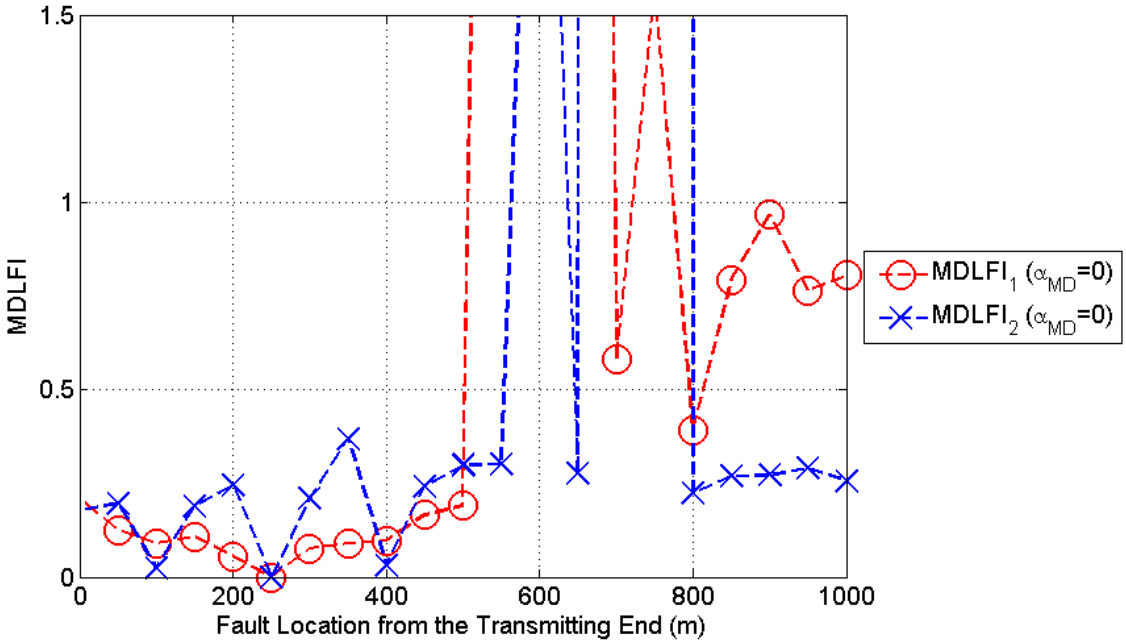

Figure 2. Same curves with Figure 1 but for the case of open-circuit terminal load.

line faults, this has verified until now only during the cases of no measurement differences. However, this finding needs to be validated during the fault localization by applying the simultaneous minimization of MDLFIs when measurement differences of various CUD magnitudes occur.

Similarly to the subsection 4.2, in Fig. 3, MDLFIs are plotted versus the distance from the transmitting end when the terminal load is assumed to be short-circuit during the main distribution line fault case A for CUD case A, B and C. In Fig. 4, same plots are drawn with Fig. 3 but for the case of an open-circuit terminal load.

Observing Figs. 3 and 4, it is again verified that MDLFIs can accurately localize the main distribution line faults through their simultaneous minimization even if measurement differences of various magnitudes occur. Actually, the localization of main distribution line faults becomes easier when measurement difference magnitudes remain low since then both MDLFIs tend to zero. When measurement difference magnitudes increase, MDLFIs start to differ from zero even at the location of the main distribution line fault but still maintaining lower values than ones of the other locations. However, MDLFI behavior strongly depends on the location of the main distribution line fault as verified in [5], [23]. Hence, the validity of the previous findings needs to be examined for various fault cases in the following subsection.

From the Figs. 3 and 4, it should also be noted that MDLFIs can efficiently localize main distribution line faults regardless of the nature of the terminal load (i.e., either short- or open-circuit termination). This is an interesting remark that allows the examination of only one case (say, the case of short-circuit terminal load) to be considered in the rest of this paper.

4.4 The Impact of the Main Distribution Line Fault Location on the Fault Localization by Applying MLFLM

As been presented in subsections 4.2 and 4.3, MDLFIs have very efficiently determined the location of the main distribution line fault during the fault case A. In fact, the location of the main distribution line fault has been retrieved by the simultaneous minimization of MDLFIs even if measurement differences occur during the presence of a main distribution line fault. In fact, MDLFI metric acts as a dissimilarity metric resembling with the metrics of relative and absolute error but in a more sophisticated manner since it exploits the inherent piecewise monotonic trend of coupling transfer functions and coupling reflection coefficients of OV MV BPL networks [25], [26], [24]. Since MDLFI acts as a dissimilarity metric between the coupling transfer functions of original and modified OV MV BPL topologies [5], [23], MDLFI achieves to more easily identify main distribution line faults that are located near to the transmitting end than to receiving end since the differences between theoretical coupling reflection coefficients of the original OV MV BPL topology and measured coupling reflection coefficients of the measured OV MV BPL topology remains significant. In order to cope with this finding of [23], coupling reflection coefficient measurements are received both from the transmitting and receiving end by applying $MDLFI_1$ and $MDLFI_2$, respectively, as determined in eqs. (1) and (2).

Indeed, in Fig. 5, MDLFIs are plotted versus the distance from the transmitting end when the terminal load is assumed to be short-circuit during the main distribution line fault for all the CUD cases examined so far. Note that the Fault case B is here assumed. In Fig. 6, same plots are drawn with Fig. 5 but for the Fault case C.

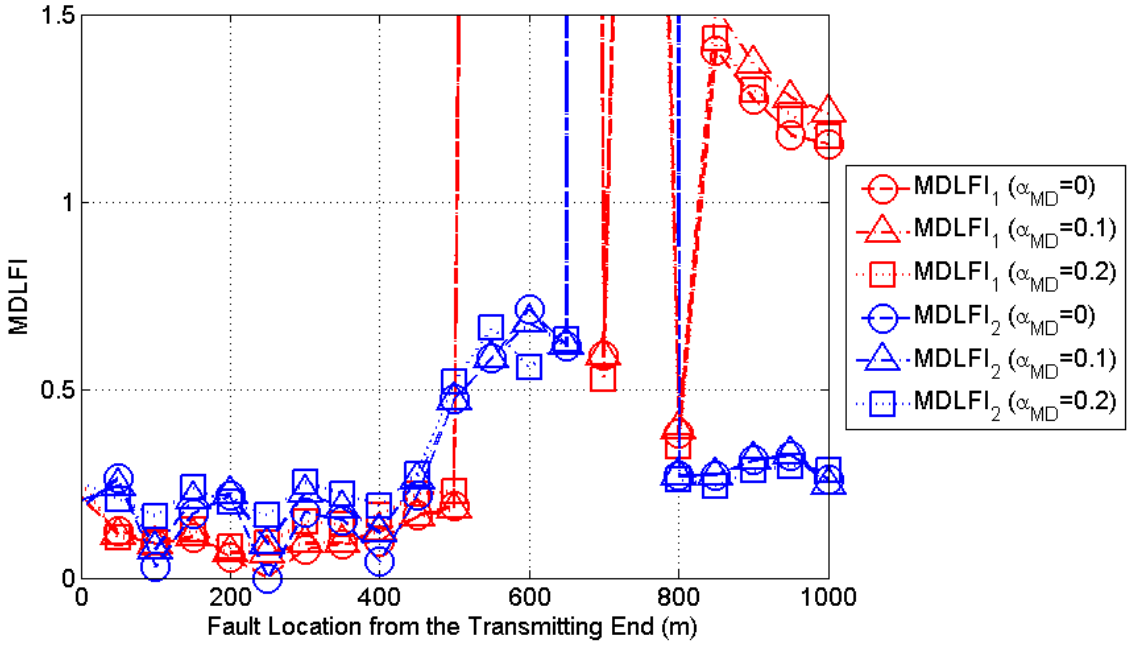

Figure 3. MDLFIs of the urban OV MV BPL topology versus the fault location from the transmitting end for various CUD magnitudes when fault case A is applied (the terminal load is assumed to be a short-circuit termination load).

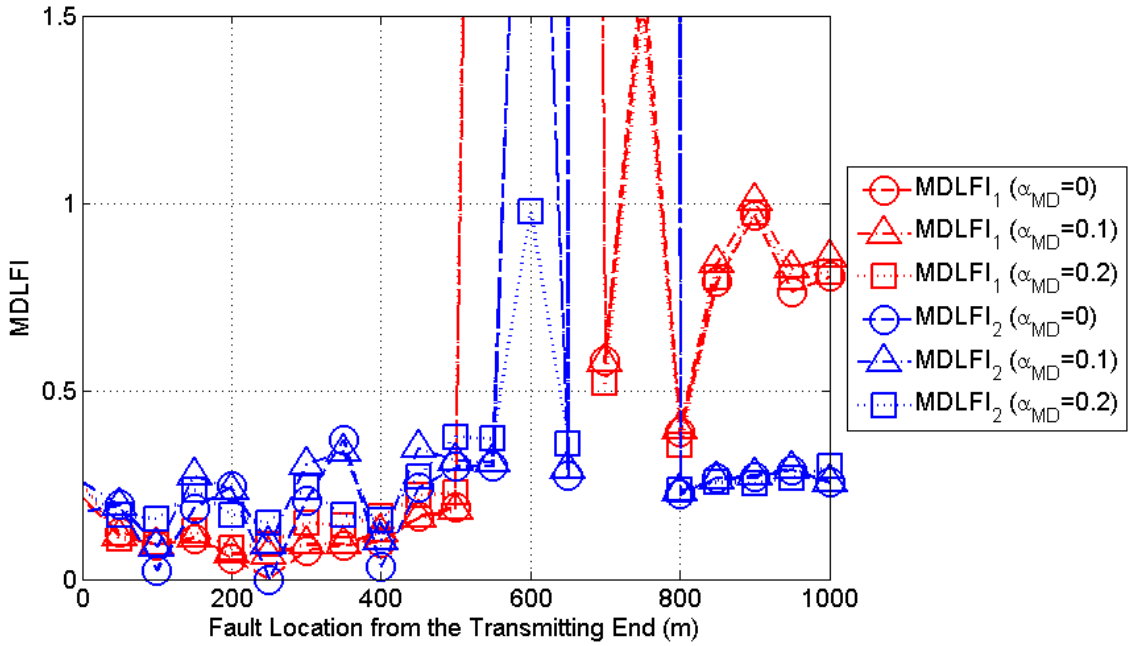

Figure 4. Same curves with Figure 3 but for the case of open-circuit terminal load.

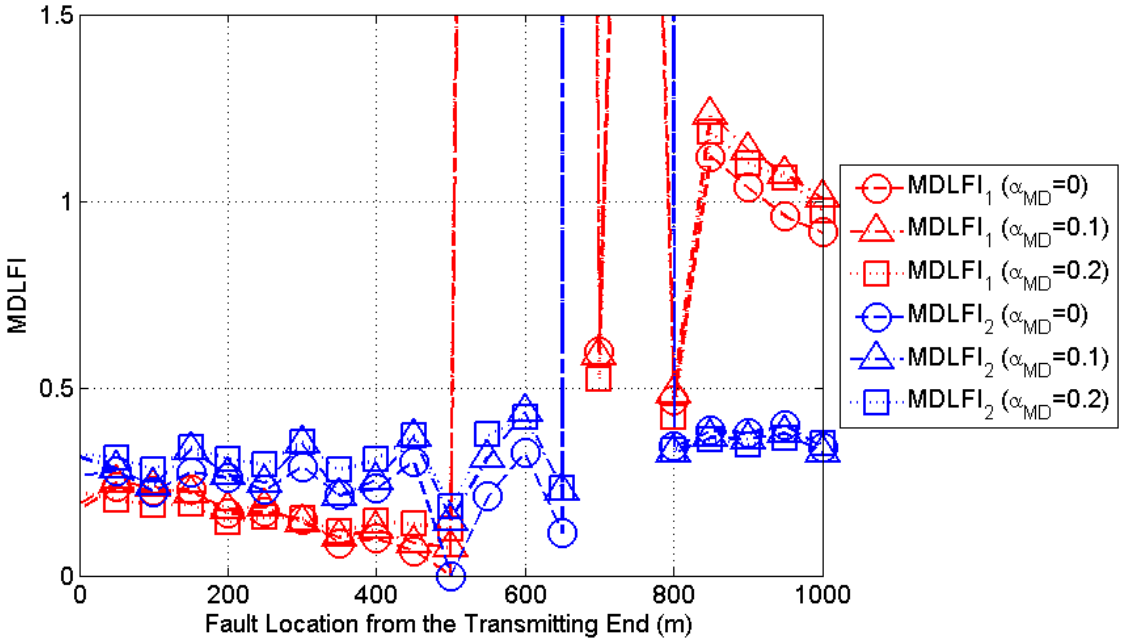

Figure 5. MDLFIs of the urban OV MV BPL topology versus the fault location from the transmitting end for various CUD cases when Fault case B occurs (the terminal load is assumed to be a short-circuit termination load).

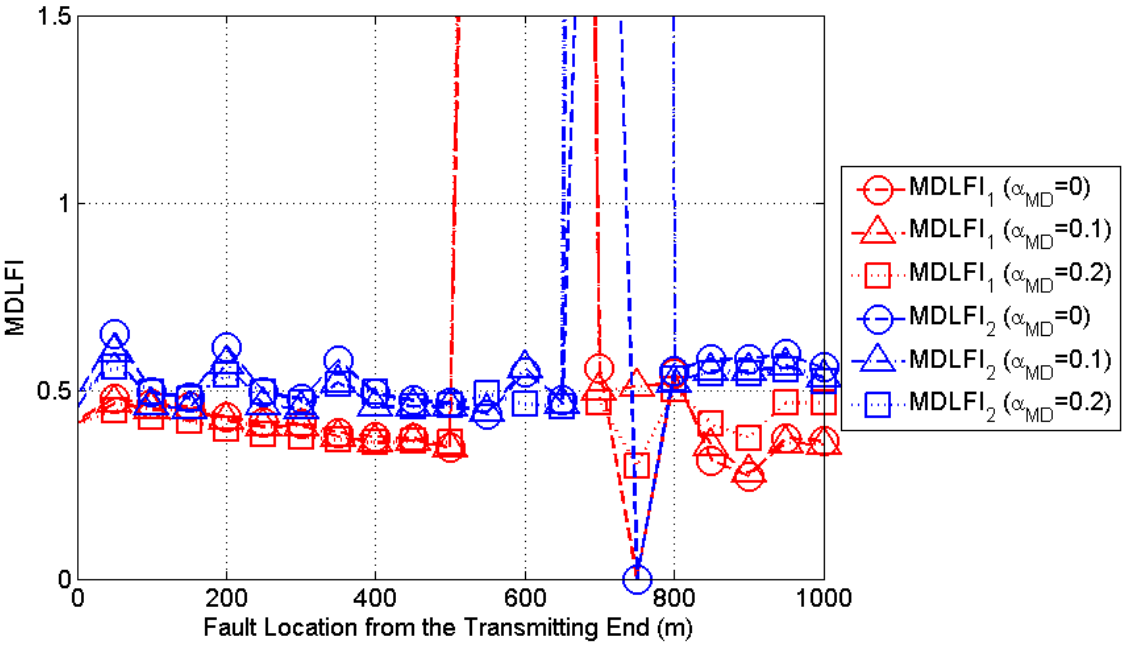

Figure 6. Same curves with Figure 5 but for the Fault case C.

Comparing Figs. 3, 5 and 6, the combined use of the available MDLFIs can allow the exact localization of main distribution line faults regardless of their location across the distribution grid. Also, the MLFLM localization of main distribution line faults remains robust even in the cases of normal measurement differences. In fact, the combined operation of $MDLFI_1$ and $MDLFI_2$ achieves to bypass the inherent difficulty of dissimilarity metrics, which is the easier identification of main distribution line faults

near to the end that are applied using the respective coupling reflection coefficient measurements. Thus, the combined minimization of MDLFIs that is the core assumption of MLFLM methodology successfully copes with the different locations of main distribution line faults.

However, until now, the performance of the localization of main distribution line faults by applying MLFLM has focused on the performance assessment of the localization in the urban OV MV BPL topology when various factors affecting the methodology performance has been taken into account. In the following subsection, the performance of MLFLM methodology is assessed for the other three indicative original OV MV BPL topologies described in Sec. 2 –say, suburban, rural and "LOS" OV MV BPL topologies–.

4.5 The Impact of the Original OV MV BPL Topologies on the Fault Localization by Applying MLFLM

Previously been mentioned, the presence of main distribution line faults across the original OV MV BPL topologies has as a result the definition of two new modified OV MV BPL topologies which have the termination load of the main distribution line fault as the only common point. Since there are two different measurement points, which are located at the transmitting and receiving end of the original OV MV BPL topology, these two modified OV MV BPL topologies operate as the complimentary topologies of the original OV MV BPL topology. Until now, only the urban OV MV BPL topology of Sec. 2, had been used as the original OV MV BPL topology where the main distribution line faults have been imposed. In this subsection, the MLFLM efficiency against different original OV MV BPL topologies is assessed.

Indeed, in Fig. 7, MDLFIs are plotted versus the distance from the transmitting end of the original suburban OV MV BPL topology when the terminal load is assumed to be short-circuit. Note here that the Fault case A and all the available CUD cases are assumed in Fig. 7. In Figs. 8 and 9, same plots are drawn with Fig. 7 but for the rural and "LOS" cases, respectively.

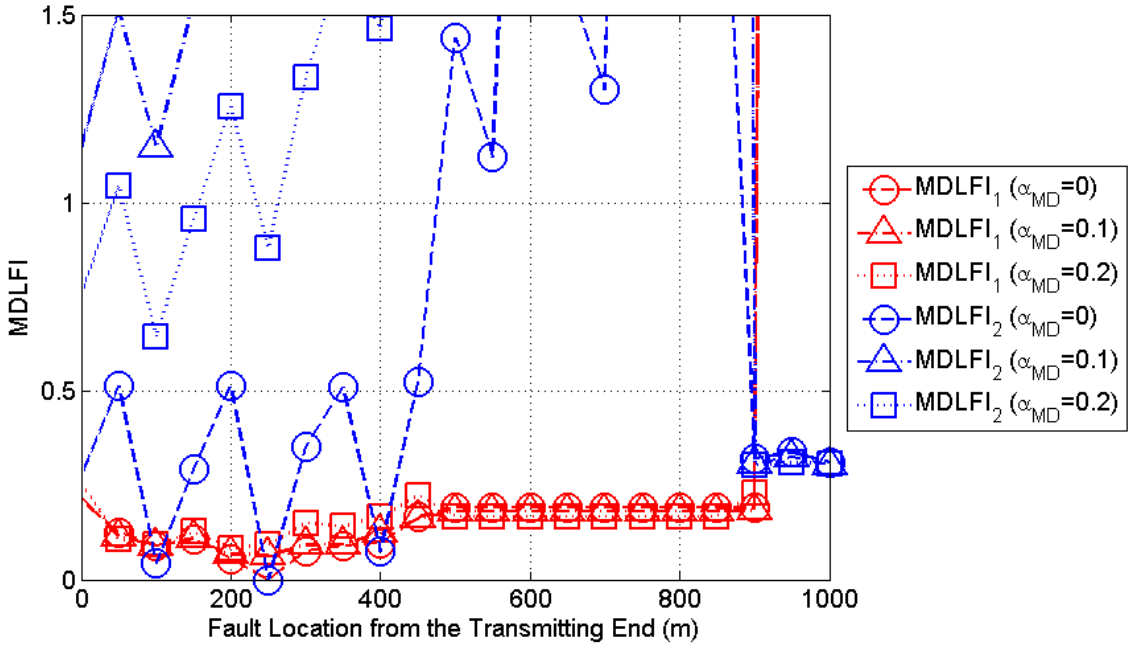

Figure 7. MDLFIs of the original suburban OV MV BPL topology versus the fault location from the transmitting end for various CUD cases when Fault case A occurs (the terminal load is assumed to be a short-circuit termination load).

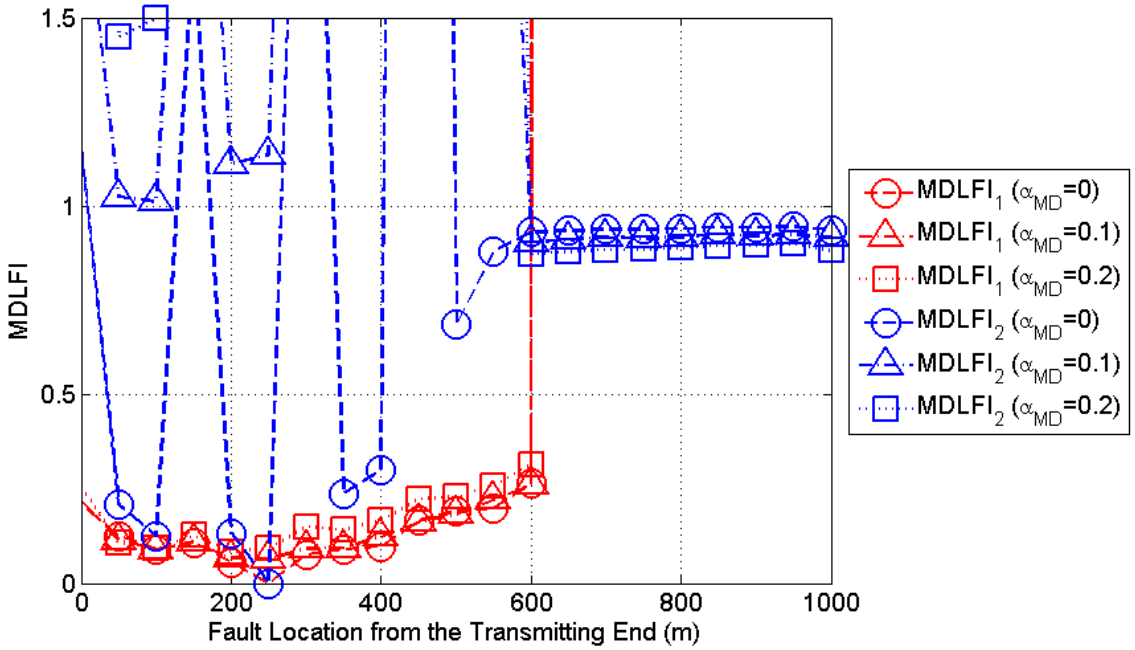

Figure 8. Same curves with Figure 7 but for the rural case.

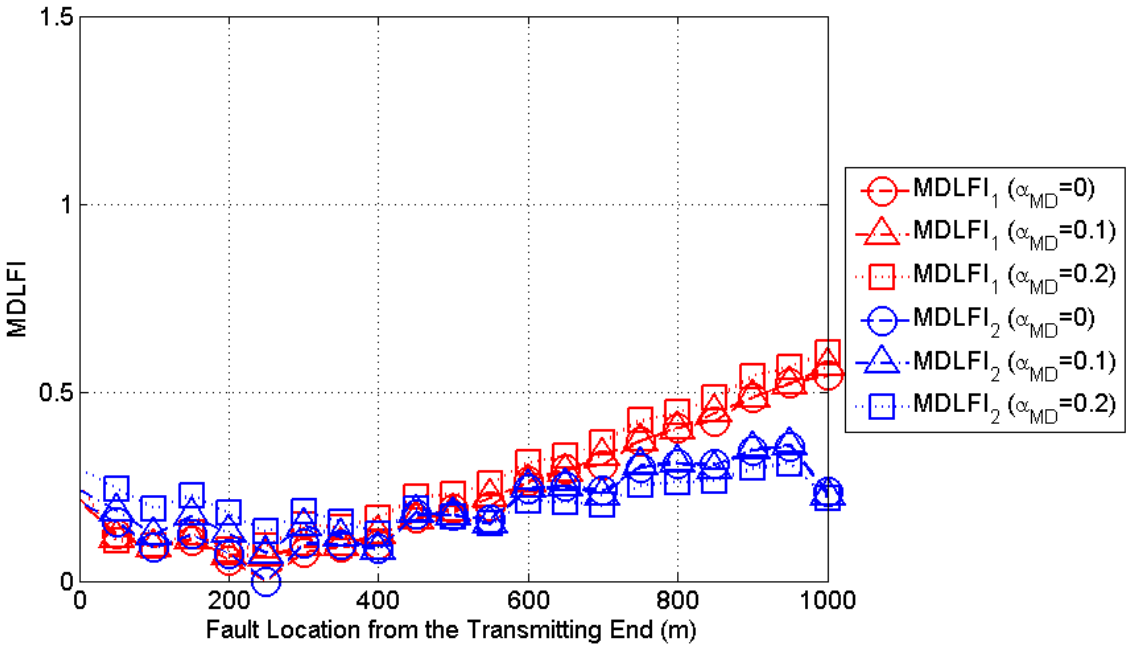

Figure 9. Same curves with Figure 7 but for the "LOS" case.

Comparing Figs. 3, 7, 8 and 9, MDLFIs can successfully localize main distribution line faults regardless of the intensity of the occurred measurement differences and the original OV MV BPL topology. More specifically, when the CUD magnitude of measurement differences is equal to zero MDLFIs are also equal to zero in all the examined original OV MV BPL topologies. When the CUD magnitude of measurement differences increases, MDLFIs take value greater than zero but their trend and their minima still imply the exact location of the examined main distribution line fault. Since the simultaneous minimization of MDLFIs is required in order to securely localize the main distribution line faults, this allows MLFLM to crosscheck the fault location even if the identification by applying one of MDLFIs remains low but does not take the minimum value. As presented, the latter case is rare and can stand only in the cases of intense measurement differences.

In this paper, the exact localization of main distribution line faults has been achieved by applying MLFLM when the identification of the presence of main distribution line faults is assured as described in [5], [23]. Actually, MLFLM is based on the application of MDLFIs by taking advantage of the double coupling reflection coefficient measurement sets (i.e., the first set from the transmitting end side and the other one from the receiving end side of the original OV MV BPL topology) and the MLFLM database. Then, the simultaneous minimization of MDLFIs offers the exact location of the main distribution line fault across the original OV MV BPL topology regardless of the CUD magnitude of measurement differences, the location of the main distribution line fault and the original OV MV BPL topology.

4.6 General Remarks Concerning the Identification and Localization of Faults and Instabilities across Distribution Power Grids

Already been identified in [3], [22], [24]-[26], various serious problematic conditions can occur across the distribution power grid such as faults and instabilities. More specifically, faults and instabilities can further be divided into two subcategories each. On the basis of a typical OV MV BPL topology, which is presented in Fig. 10(a), the subcategories of faults and instabilities are reported as follows:

- *Faults*: All the interruptions that can occur across the lines of a distribution power grid. The two fault subcategories of line interruptions are: (i) *Fault in main distribution line* –see Fig. 10(b)–; and (ii) *Fault in branch line* –see Fig. 10(c)–.
- *Instabilities*: All the failures that can occur in the equipment across the distribution power grid. There are two subcategories of equipment failures, namely: (iii) *Instability in branch interconnections* –see Fig. 10(d)–; and (iv) *Instability in branch terminations* –see Fig. 10(e)–.

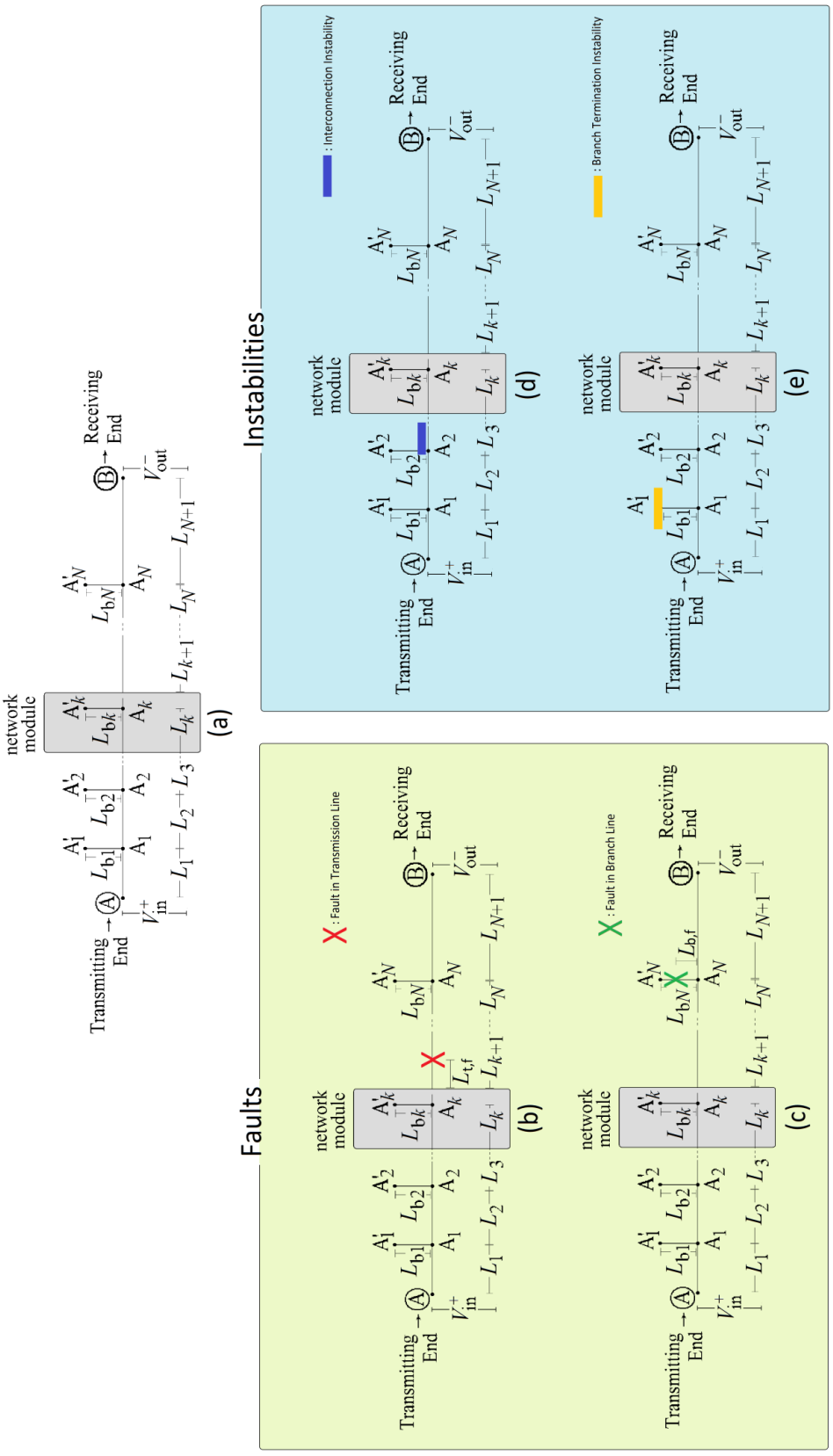

Figure 10. (a) General OV MV BPL topology [22], [24]. (b, c) Faults in OV MV BPL topologies. (d, e) Instabilities in OV MV BPL topologies [3].

Until now, the identification and localization methodology of the fault in branch line, the instability in branch interconnections and the instability in branch terminations have well defined and analyzed in [3], [22], [24]-[26]. However, the case of the identification and localization of the main distribution line faults had been treated till these three papers as a *reductio ad absurdum* case. This set of three papers has achieved to cover this identification / localization methodology gap through the proposal and application of MLFLM methodology by identifying and exactly localizing possible main distribution line faults [5], [23]. Therefore, a complete methodology of identifying and localizing possible faults and instabilities across distribution power grids is now available.

Conclusions

In this paper, which is the last part of a set of three manuscripts, the detailed presentation and the performance assessment of MLFLM have been demonstrated. In fact, MLFLM describes the identification and localization methodology of main distribution line faults across the distribution power grids. This paper concludes the study of faults and instabilities across transmission and distribution power grids revealing the strong potential of the BPL technology in order to identify and exactly localize potential failures across the grids.

This paper has first reported the required steps to create MLFLM database, which is the essential part of MLFLM. Second, MDLFIs, which are the accompanied metrics of MLFLM, and their application to the coupling reflection coefficient insertions of MLFLM database have been proposed. Third, the interaction procedure between MLFLM database and MDLFIs that finally leads to the localization of the main distribution line faults has been outlined.

After MLFLM theoretical analysis, various scenarios concerning the localization of main distribution line faults have been investigated by applying MLFLM. More specifically, MLFLM has successfully localized the occurred main distribution line faults regardless of the examined OV MV BPL topologies, the location of the main distribution line faults and the CUD magnitude of the measurement differences. Among the main conclusions of MLFLM application, some of them that deserve special attention are: (i) the same MLFLM efficiency of localizing main distribution line faults despite the complexity of the examined original OV MV BPL topology; (ii) through the combined measurement operation of coupling reflection coefficients from the transmitting and receiving end, MDLFIs have been simultaneously defined, thus rendering MLFLM immune against the location of main distribution line faults; and (iii) MLFLM can mitigate measurement differences since the combined minimization of MDLFIs secures MLFLM performance.

After this set of papers, apart from the identification and localization methodology of the fault in branch line, the instability in branch interconnections and the instability in branch terminations, the case of the identification and localization of the main distribution line faults has also been achieved. Now, a complete methodology of identifying and localizing possible faults and instabilities across transmission and distribution power grids, which is based on the signal transmission theory and signal processing techniques through informatics, is now available.

CONFLICTS OF INTEREST

The author declares that there is no conflict of interests regarding the publication of this paper.

References

[1] L. Lutz, A. M. Tonello, and T. G. Swart, *Power Line Communications: Principles, Standards and Applications from multimedia to smart grid*, John Wiley & Sons, 2016.

[2] G. Artale, A. Cataliotti, V. Cosentino, D. Di Cara, R. Fiorelli, S. Guaiana, and G. Tine, "A New Low Cost Coupling System for Power Line Communication on Medium Voltage Smart grids," *IEEE Trans. on Smart Grid*, to be published, 2017.

[3] A. G. Lazaropoulos, "Measurement Differences, Faults and Instabilities in Intelligent Energy Systems – Part 2: Fault and Instability Prediction in Overhead High-Voltage Broadband over Power Lines Networks by Applying Fault and Instability Identification Methodology (FIIM)," *Trends in Renewable Energy*, vol. 2, no. 3, pp. 113 – 142, Oct. 2016. [Online]. Available: http://futureenergysp.com/index.php/tre/article/view/27/33

[4] A. G. Lazaropoulos, A. Sarafi, and P. G. Cottis, "The emerging smart grid — A pilot MV/BPL network installed at Lavrion, Greece," in *Proc. Workshop on Applications for Powerline Communications WSPLC 2008*, Thessaloniki, Greece, Oct. 2008. [Online]. Available: http://newton.ee.auth.gr/WSPLC08/Abstracts%5CSG_3.pdf

[5] A. G. Lazaropoulos, "Main Line Fault Localization Methodology in Smart Grid – Part 1: Extended TM2 Method for the Overhead Medium-Voltage Broadband over Power Lines Networks Case," *Trends in Renewable Energy*, vol. 3, no. 3, pp. 2-25, 2017.

[6] A. G. Lazaropoulos, "Factors Influencing Broadband Transmission Characteristics of Underground Low-Voltage Distribution Networks," *IET Commun.*, vol. 6, no. 17, pp. 2886-2893, Nov. 2012.

[7] A. G. Lazaropoulos and P. G. Cottis, "Transmission characteristics of overhead medium voltage power line communication channels," *IEEE Trans. Power Del.*, vol. 24, no. 3, pp. 1164-1173, Jul. 2009.

[8] A. G. Lazaropoulos and P. G. Cottis, "Capacity of overhead medium voltage power line communication channels," *IEEE Trans. Power Del.*, vol. 25, no. 2, pp. 723-733, Apr. 2010.

[9] A. G. Lazaropoulos and P. G. Cottis, "Broadband transmission via underground medium-voltage power lines-Part I: transmission characteristics," *IEEE Trans. Power Del.*, vol. 25, no. 4, pp. 2414-2424, Oct. 2010.

[10] A. G. Lazaropoulos and P. G. Cottis, "Broadband transmission via underground medium-voltage power lines-Part II: capacity," *IEEE Trans. Power Del.*, vol. 25, no. 4, pp. 2425-2434, Oct. 2010.

[11] A. G. Lazaropoulos, "Broadband transmission characteristics of overhead high-voltage power line communication channels," *Progress in Electromagnetics Research B*, vol. 36, pp. 373-398, 2012. [Online]. Available: http://www.jpier.org/PIERB/pierb36/19.11091408.pdf

[12] A. G. Lazaropoulos, "Towards broadband over power lines systems integration: Transmission characteristics of underground low-voltage distribution power lines," *Progress in Electromagnetics Research B*, 39, pp. 89-114, 2012. [Online]. Available: http://www.jpier.org/PIERB/pierb39/05.12012409.pdf

[13] A. G. Lazaropoulos, "Broadband transmission and statistical performance properties of overhead high-voltage transmission networks,"*Hindawi Journal of Computer Networks and Commun.*, 2012, article ID 875632, 2012. [Online]. Available: http://www.hindawi.com/journals/jcnc/aip/875632/

[14] A. G. Lazaropoulos, "Towards modal integration of overhead and underground low-voltage and medium-voltage power line communication channels in the smart grid landscape: model expansion, broadband signal transmission characteristics, and statistical performance metrics (Invited Paper)," *ISRN Signal Processing*, vol. 2012, Article ID 121628, 17 pages, 2012. [Online]. Available: http://www.isrn.com/journals/sp/aip/121628/

[15] A. G. Lazaropoulos, "Review and Progress towards the Common Broadband Management of High-Voltage Transmission Grids: Model Expansion and Comparative Modal Analysis," *ISRN Electronics*, vol. 2012, Article ID 935286, pp. 1-18, 2012. [Online]. Available: http://www.hindawi.com/isrn/electronics/2012/935286/

[16] A. G. Lazaropoulos, "Review and Progress towards the Capacity Boost of Overhead and Underground Medium-Voltage and Low-Voltage Broadband over Power Lines Networks: Cooperative Communications through Two- and Three-Hop Repeater Systems," *ISRN Electronics*, vol. 2013, Article ID 472190, pp. 1-19, 2013. [Online]. Available: http://www.hindawi.com/isrn/electronics/aip/472190/

[17] A. G. Lazaropoulos, "Green Overhead and Underground Multiple-Input Multiple-Output Medium Voltage Broadband over Power Lines Networks: Energy-Efficient Power Control," *Springer Journal of Global Optimization*, vol. 2012 / Print ISSN 0925-5001, pp. 1-28, Oct. 2012.

[18] P. Amirshahi and M. Kavehrad, "High-frequency characteristics of overhead multiconductor power lines for broadband communications," *IEEE J. Sel. Areas Commun.*, vol. 24, no. 7, pp. 1292-1303, Jul. 2006.

[19] T. Sartenaer, "Multiuser communications over frequency selective wired channels and applications to the powerline access network" Ph.D. dissertation, Univ. Catholique Louvain, Louvain-la-Neuve, Belgium, Sep. 2004. [Online} Available: https://dial.uclouvain.be/pr/boreal/en/object/boreal%3A5010/datastream/PDF_12/view

[20] T. Calliacoudas and F. Issa, ""Multiconductor transmission lines and cables solver," An efficient simulation tool for plc channel networks development," presented at the *IEEE Int. Conf. Power Line Communications and Its Applications*, Athens, Greece, Mar. 2002.

[21] A. G. Lazaropoulos, "Best L1 Piecewise Monotonic Data Approximation in Overhead and Underground Medium-Voltage and Low-Voltage Broadband over Power Lines Networks: Theoretical and Practical Transfer Function Determination," *Hindawi Journal of Computational Engineering*, vol. 2016, Article ID 6762390, 24 pages, 2016. doi:10.1155/2016/6762390. [Online]. Available: https://www.hindawi.com/journals/jcengi/2016/6762390/cta/

[22] A. G. Lazaropoulos, "Measurement Differences, Faults and Instabilities in Intelligent Energy Systems – Part 1: Identification of Overhead High-Voltage

Broadband over Power Lines Network Topologies by Applying Topology Identification Methodology (TIM)," *Trends in Renewable Energy*, vol. 2, no. 3, pp. 85 – 112, Oct. 2016.

[23] A. G. Lazaropoulos, "Main Line Fault Localization Methodology in Smart Grid – Part 2: Extended TM2 Method, Measurement Differences and L1 Piecewise Monotonic Data Approximation for the Overhead Medium-Voltage Broadband over Power Lines Networks Case," *Trends in Renewable Energy*, vol. 3, no. 3, pp. 26-61, 2017.

[24] A. G. Lazaropoulos, "Improvement of Power Systems Stability by Applying Topology Identification Methodology (TIM) and Fault and Instability Identification Methodology (FIIM) – Study of the Overhead Medium-Voltage Broadband over Power Lines (OV MV BPL) Networks Case," *Trends in Renewable Energy*, vol. 3, no. 2, pp. 102 – 128, Apr. 2017. [Online]. Available: http://futureenergysp.com/index.php/tre/article/view/34/pdf

[25] A. G. Lazaropoulos, "Power Systems Stability through Piecewise Monotonic Data Approximations – Part 1: Comparative Benchmarking of L1PMA, L2WPMA and L2CXCV in Overhead Medium-Voltage Broadband over Power Lines Networks," *Trends in Renewable Energy*, vol. 3, no. 1, pp. 2 – 32, Jan. 2017. [Online]. Available: http://futureenergysp.com/index.php/tre/article/view/29/34

[26] A. G. Lazaropoulos, "Power Systems Stability through Piecewise Monotonic Data Approximations – Part 2: Adaptive Number of Monotonic Sections and Performance of L1PMA, L2WPMA and L2CXCV in Overhead Medium-Voltage Broadband over Power Lines Networks," *Trends in Renewable Energy*, vol. 3, no. 1, pp. 33 – 60, Jan. 2017. [Online]. Available: http://futureenergysp.com/index.php/tre/article/view/30/35

[27] A. Canova, N. Benvenuto, and P. Bisaglia, "Receivers for MIMO-PLC channels: Throughput comparison," in *Proc. IEEE Int. Symp. Power Line Communications and Its Applications*, Rio de Janeiro, Brazil, Mar. 2010, pp. 114–119.

[28] D. Schneider, J. Speidel, L. Stadelmeier, and D. Schill, "Precoded spatial multiplexing MIMO for inhome power line communications," in *Proc. IEEE Global Telecommunications Conference*, New Orleans, LA, USA, Nov./Dec. 2008, pp. 1–5.

[29] M. Zimmermann and K. Dostert, "Analysis and modeling of impulsive noise in broad-band powerline communications," *IEEE Trans. Electromagn. Compat.*, vol. 44, no. 1, pp. 249-258, Feb. 2002.

[30] T. Esmailian, F. R. Kschischang, and P. G. Gulak, "In-building power lines as high-speed communication channels: Channel characterization and a test channel ensemble," *Int. J. Commun. Syst.*, vol. 16, pp. 381–400, May 2003.

CALL FOR PAPERS

Trends in Renewable Energy

ISSN Print: 2376-2136 ISSN online: 2376-2144

http://futureenergysp.com/index.php/tre/

Trends in Renewable Energy (TRE) is an open accessed, peer-reviewed semi-annual journal publishing reviews and research papers in the field of renewable energy technology and science. The aim of this journal is to provide a communication platform that is run exclusively by scientists. This journal publishes original papers including but not limited to the following fields:

- ✧ Renewable energy technologies
- ✧ Catalysis for energy generation, Green chemistry, Green energy
- ✧ Bioenergy: Biofuel, Biomass, Biorefinery, Bioprocessing, Feedstock utilization, Biological waste treatment,
- ✧ Energy issues: Energy conservation, Energy delivery, Energy resources, Energy storage, Energy transformation, Smart Grid
- ✧ Environmental issues: Environmental impacts, Pollution
- ✧ Bioproducts
- ✧ Policy, etc.

We publish the following article types: peer-reviewed reviews, mini-reviews, technical notes, short-form research papers, and original research papers.

The article processing charge (APC), also known as a publication fee, is fully waived for the Trends in Renewable Energy.

Call for Editorial Board Members

We are seeking scholars active in a field of renewable energy interested in serving as volunteer Editorial Board Members.

Qualifications

Ph.D. degree in related areas, or Master's degree with a minimum of 5 years of experience. All members must have a strong record of publications or other proofs to show activities in the energy related field.

If you are interested in serving on the editorial board, please email CV to editor@futureenergysp.com.